Multi-Echo fMRI

Javier Gonzalez-Castillo

Senior Associate Scientist,

National Institute of Mental Health, NIH, Bethesda, MD

September 17th , 2024 | Madison, WI

Agenda

- ❑ Why should we consider Multi-Echo acquisitions when doing fMRI experiments?

- ❑ Proposed analytical approaches for Multi-Echo fMRI Data? (timeline)

  - ❑ T2* Fit
  - ❑ Dual Echo
  - ❑ Weighted Combination of Echoes
  - ❑ Multi-Echo ICA-based Denoising
  - ❑ Multi-Echo Deconvolution

- ❑ Success stories

- ❑ Status of Multi-Echo fMRI Adoption

- ❑ What can faster gradients do for ME-fMRI?

- ❑ Conclusions

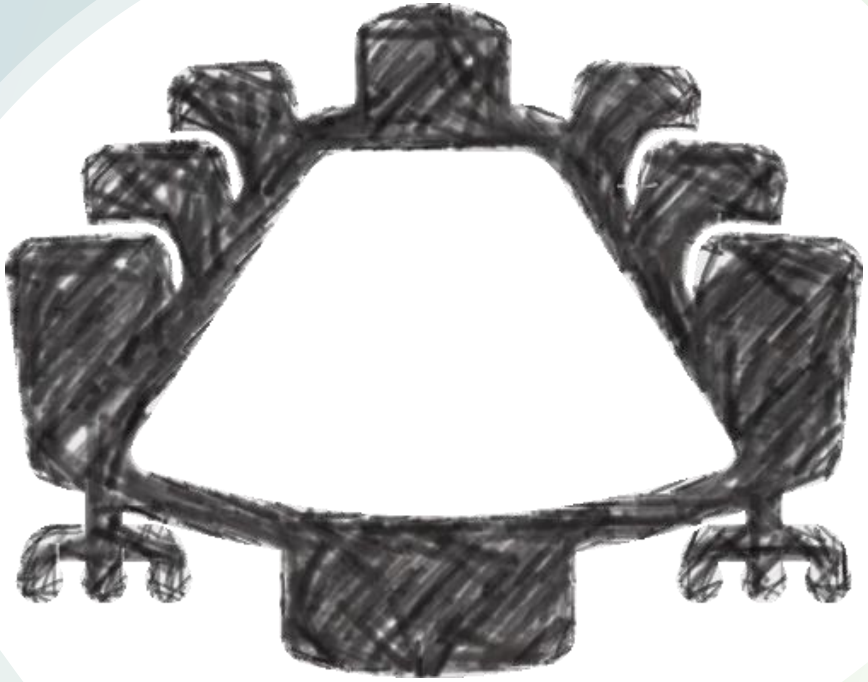

Single Echo fMRI

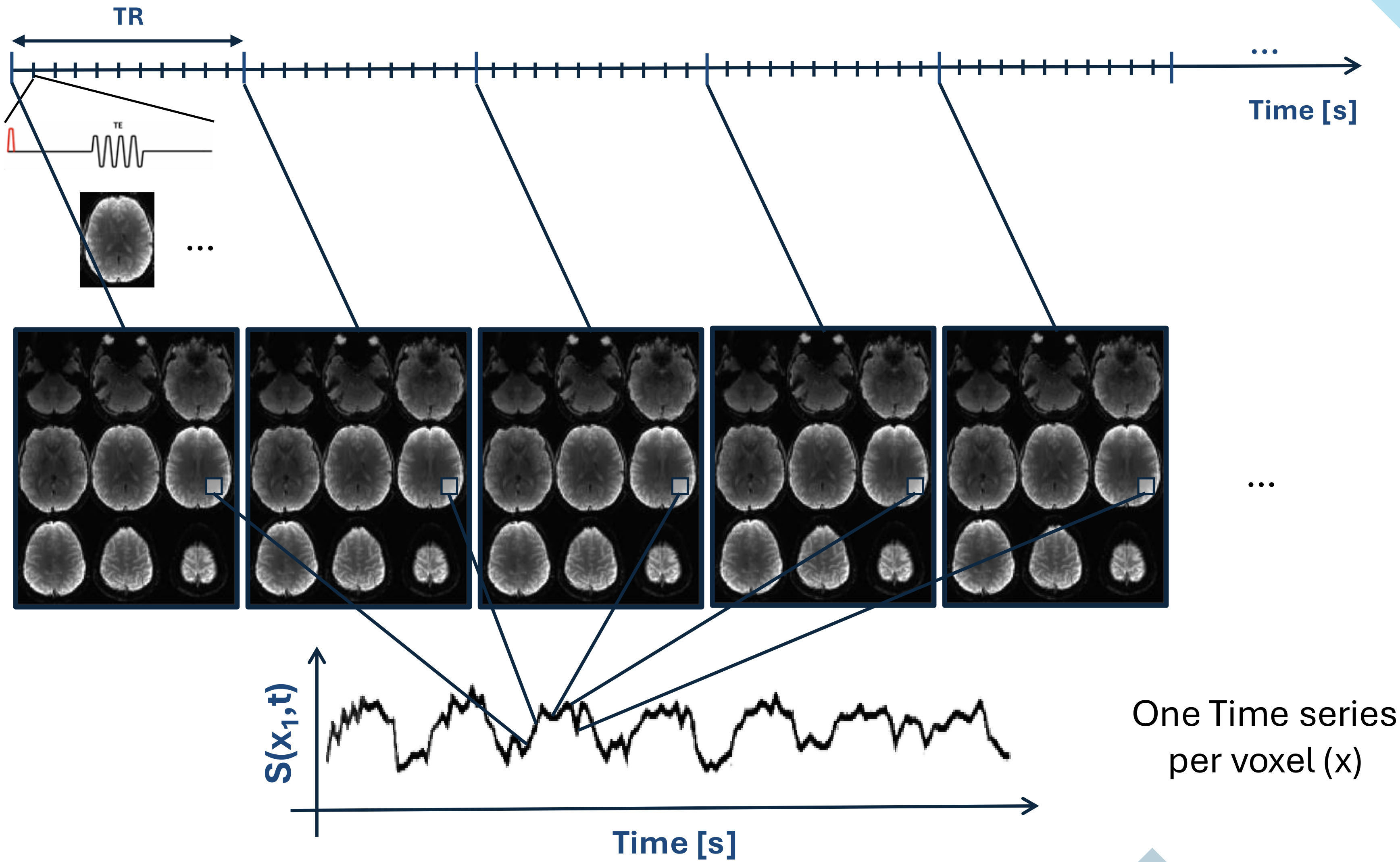

BOLD Contrast Sensitivity is Echo Time Dependent

4 Tesla Gradient Recalled Echo Characteristics of Photic Stimulation-Induced Signal Changes in the Human Primary Visual Cortex

Ravi S. Menon, Seiji Ogawa, David W. Tank, Kâmil Uğurbil

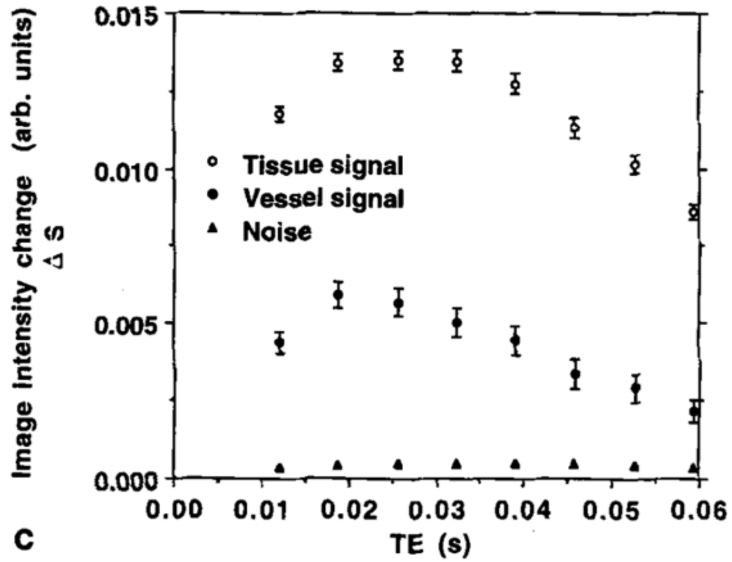

MRM (1993)

Experimental Determination of the BOLD Field Strength Dependence in Vessels and Tissue

Joseph S. Gati, Ravi S. Menon, Kâmil Uğurbil, Brian K. Rutt

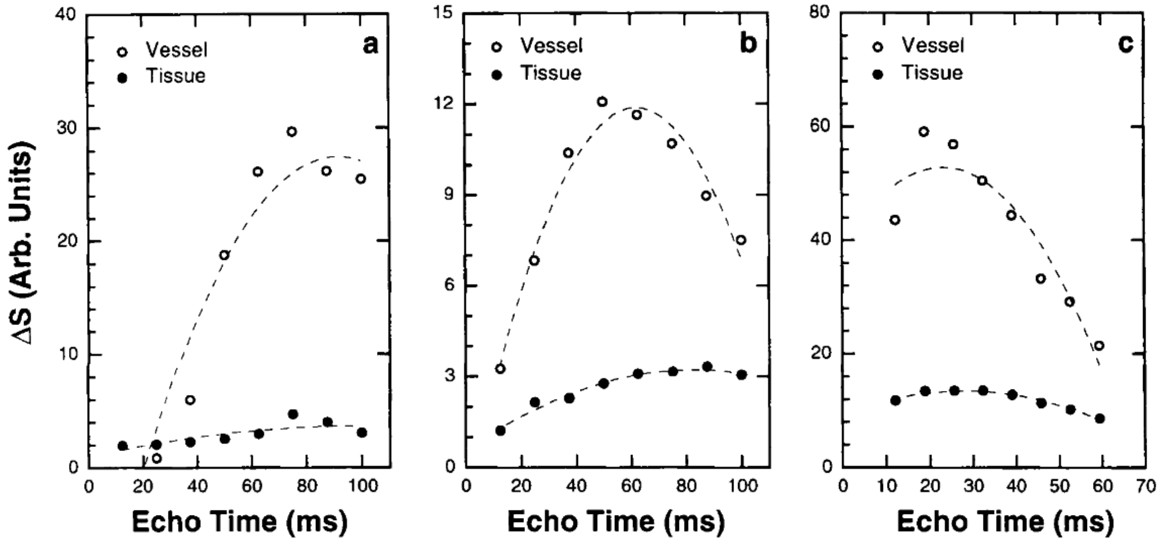

MRM (1997)

Best BOLD contrast happens for TE = T_2^* of Target Tissue

BOLD Contrast Sensitivity is Echo Time Dependent

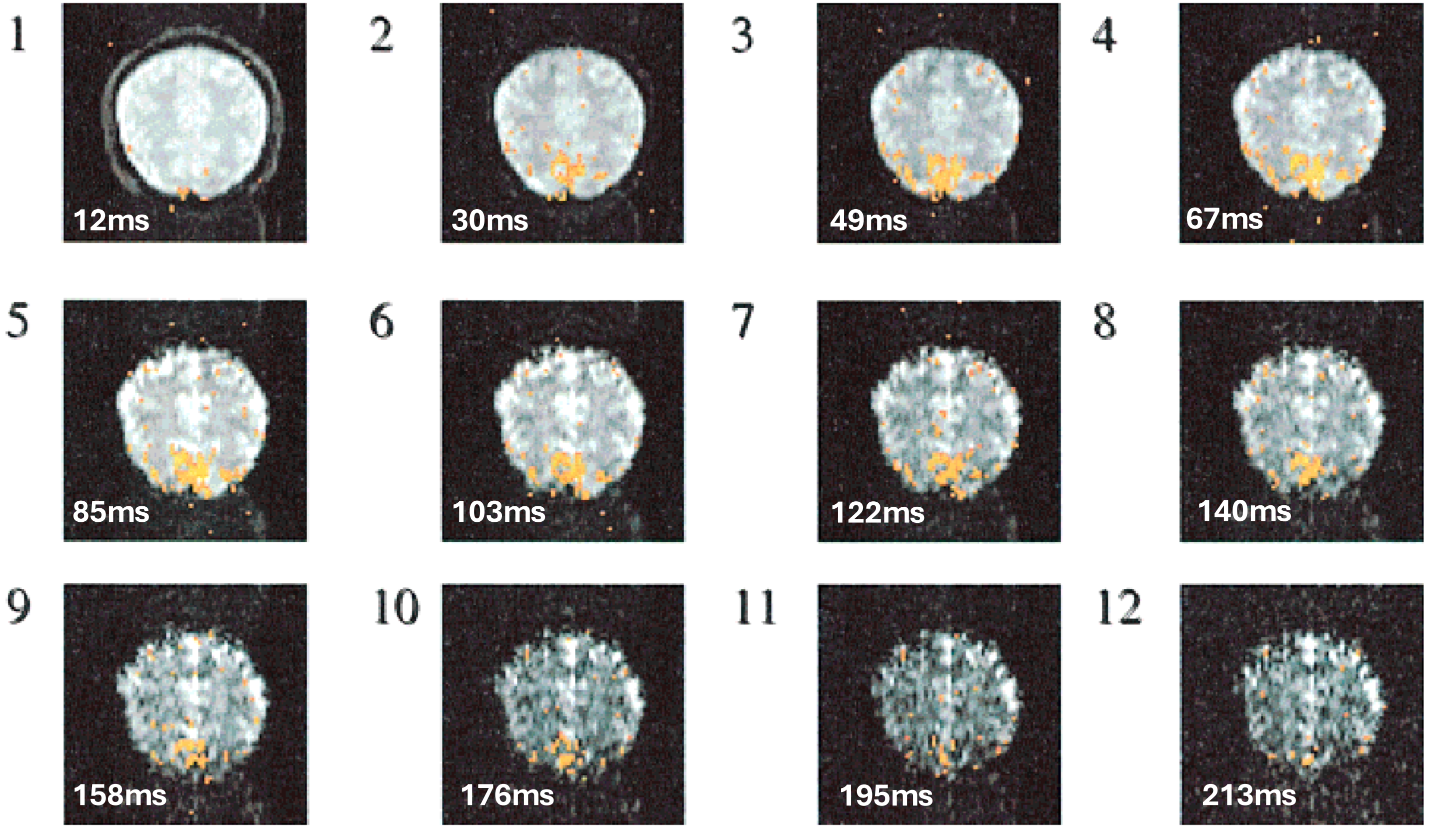

1.5 T Scanner

Posse S et al. NMR (1999)

Best BOLD contrast happens for TE = T_2^* of Target Tissue

T2* Varies substantially across subjects and regions

ADULTS

Table 1. Mean corrected T_2* values for all regions and field strengths

Field strength (T)	Grey matter (ms)	White matter (ms)	Caudate (ms)	Putamen (ms)
1.5	84.0±0.8	66.2±1.9	58.8±2.4	55.5±2.3
3	66.0±1.4	53.2±1.2	41.3±2.3	31.5±2.5
7	33.2±1.3	26.8±1.2	19.9±2.0	16.1±1.6

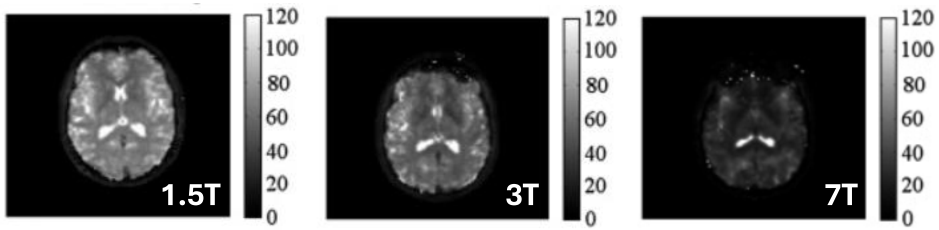

Peters et al. MRM (2007)

Table 3
Average T_2^* in Brain at 3.0 T (N = 7 males)

ROI	T_2^* ± std. error (ms) (msec, ±SE)
Frontal white matter	44.7 ± 1.2
Frontal gray matter	51.8 ± 3.3
Occipital white matter	48.4 ± 4.5
Occipital gray matter	41.6 ± 2.0

Wansapura et al. JMRI (1999)

T2* CHANGES WITH AGE

Table 3
Average T_2^* Within the Whole Brain and Four Regions of Interest

Region of Interest	Mean T_2^* ± SD	Range of Mean Values Across Participants
Whole brain	99 ± 8	91–115
Anterior cingulate cortex	113 ± 18	96–150
Insula	131 ± 11	116–149
Postcentral gyrus	87 ± 6	78–96
Thalamus	106 ± 8	98–122

Mean T_2^* values calculated across the whole brain and in four different ROIs from infant T_2^* maps (n = 7).
ROI, region of interest; SD, standard deviation.
Review article carefully. As needed, abbreviations deleted at only mention and expanded at first mention.

Hagberg et al. MRM (2012)

Table 3: Pearson correlation coefficients and corresponding *P* values for each ROI localization and the age dependence of T2*, T2′, and T2 values

T2 Values, ROI Localization	Pearson Correlation Coefficient	*P* Value
T2*_caudGM	−0.34	.001*
T2*_lentGM	−0.67	.001*
T2*_thalGM	0.10	.336
T2*_frontalWM	−0.01	.933
T2*_opWM	0.41	.001*
T2*_sWM	0.45	.001*

Siemonsen et al. AJNR (2008)

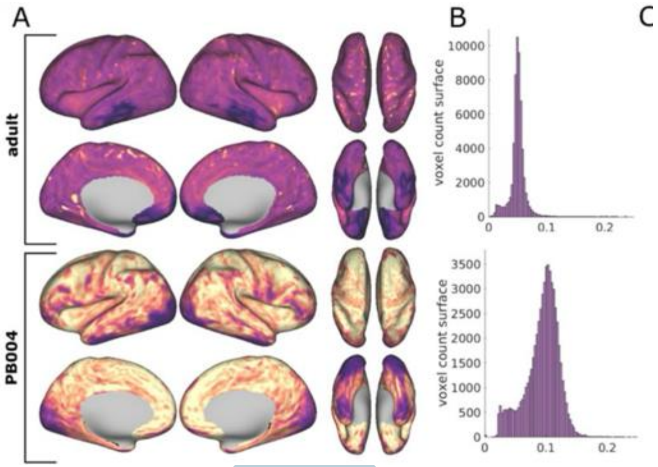

Moser et al. BioRxiv (2024)

Alternative: Acquire data at multiple echo times

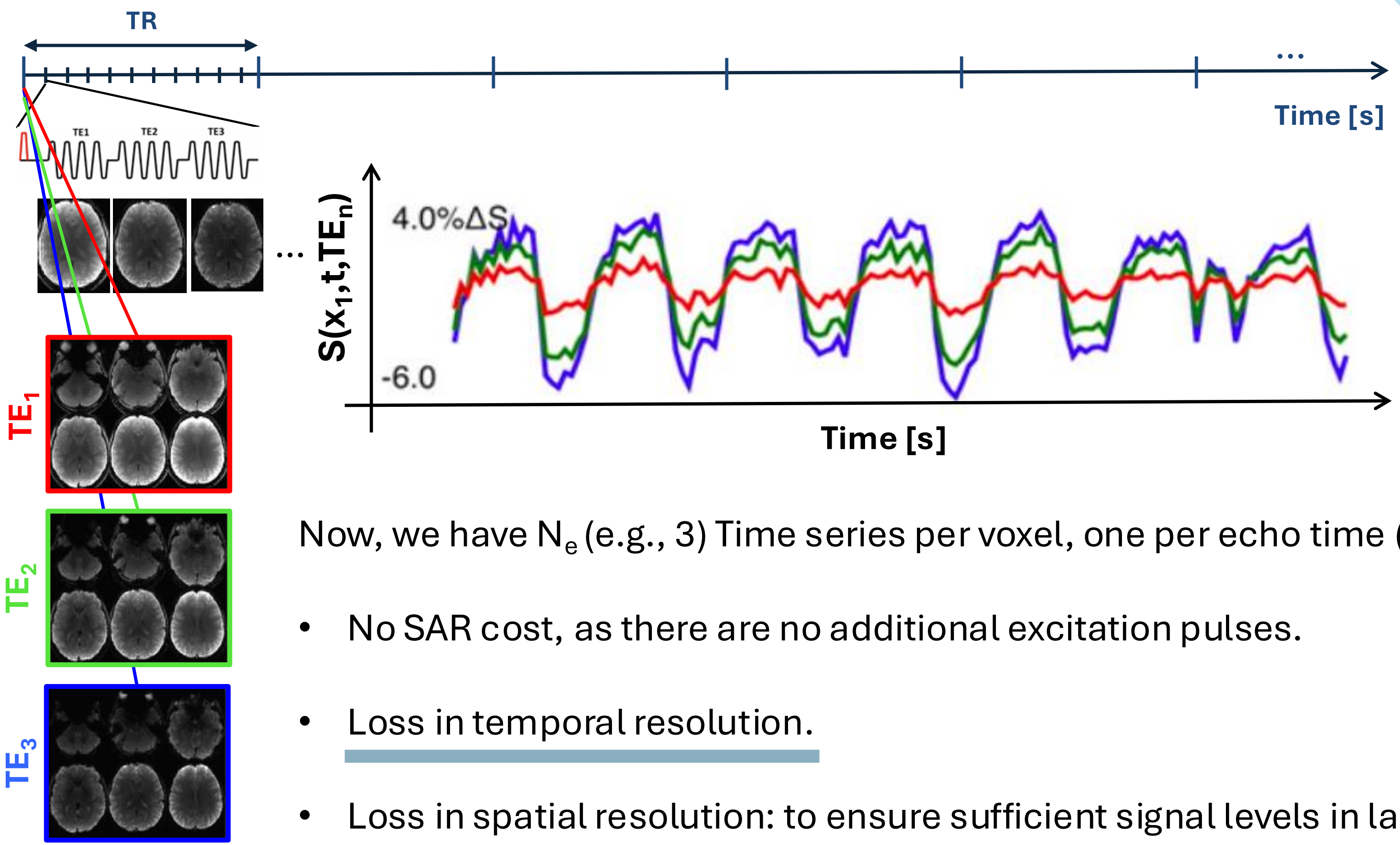

Now, we have N_e (e.g., 3) Time series per voxel, one per echo time (TE_n):

- No SAR cost, as there are no additional excitation pulses.
- Loss in temporal resolution.
- Loss in spatial resolution: to ensure sufficient signal levels in last echo.

Multi-Echo fMRI Timeline

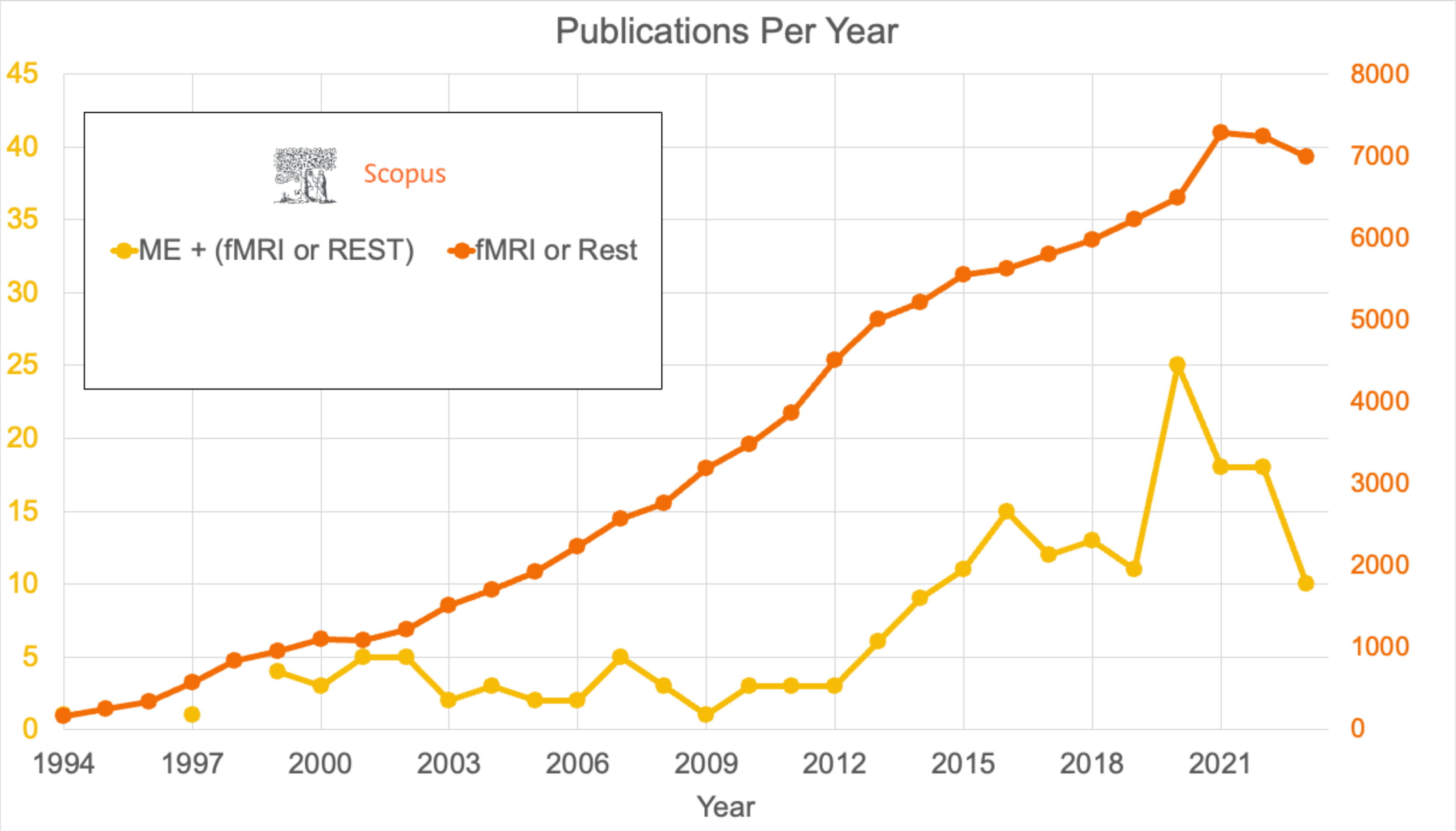

Dual Echo for separating inflow and BOLD

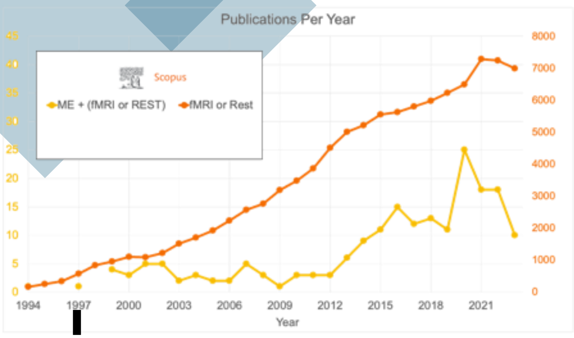

Decomposition of Inflow and Blood Oxygen Level-Dependent (BOLD) Effects with Dual-Echo Spiral Gradient-Recalled Echo (GRE) fMRI

Gary H. Glover, Susan K. Lemieux, Maria Drangova, John M. Pauly

First Acquisition

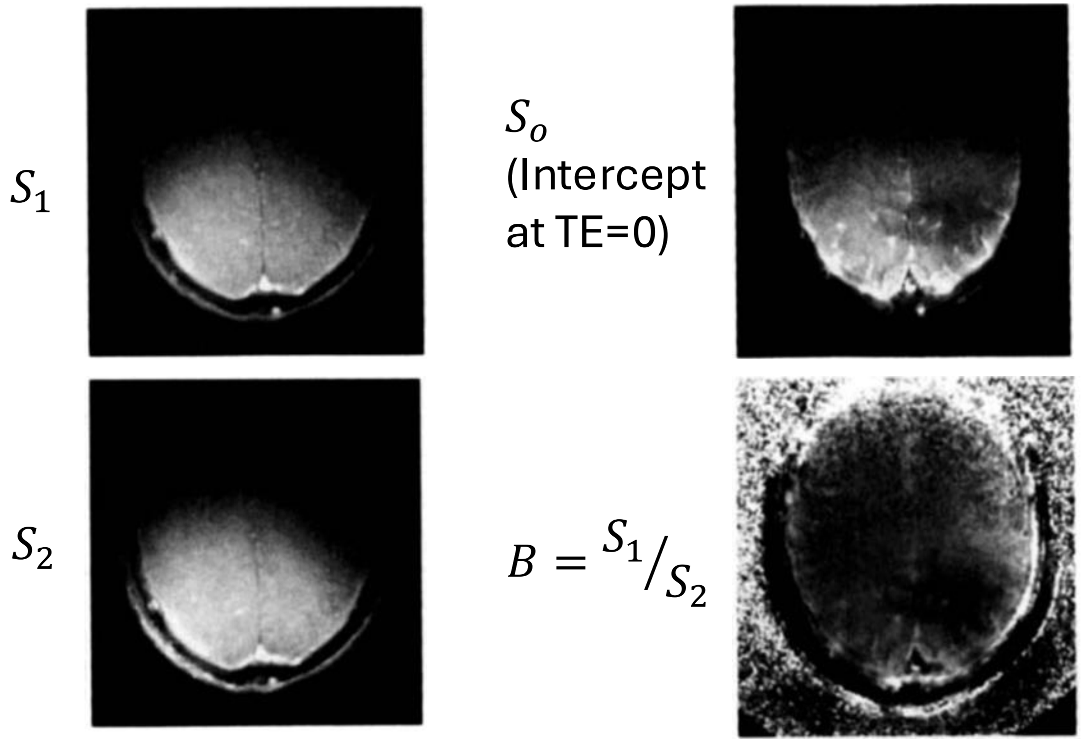

T-score Maps

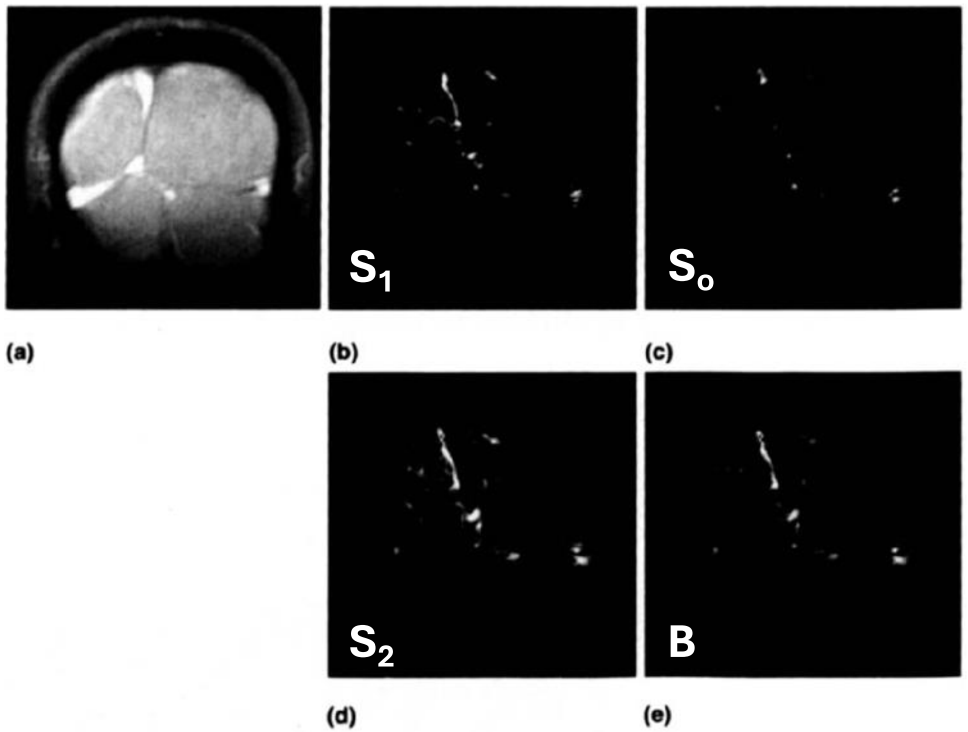

1.5T | 1 Slice | TE = 6.7, 47.7 | TR = 100ms

Dual Echo for denoising BOLD data

3T | 18 Slices | TR = 2s | 3.4x3.4x5 mm | TE_1 = 3.3ms, TE_2 = 35ms

Motion: FWD

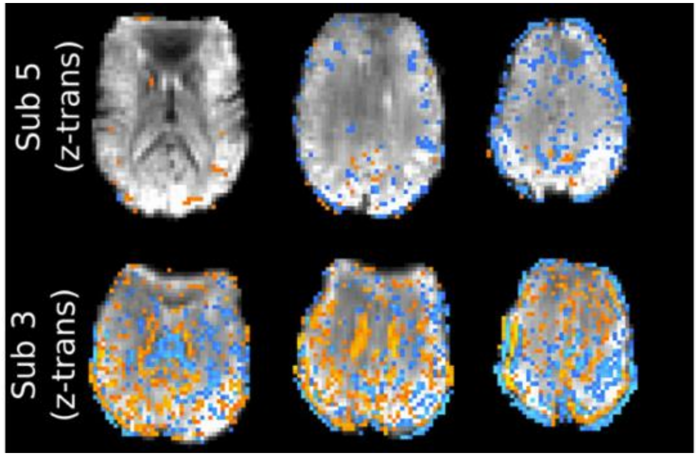

RETROICOR: respiration

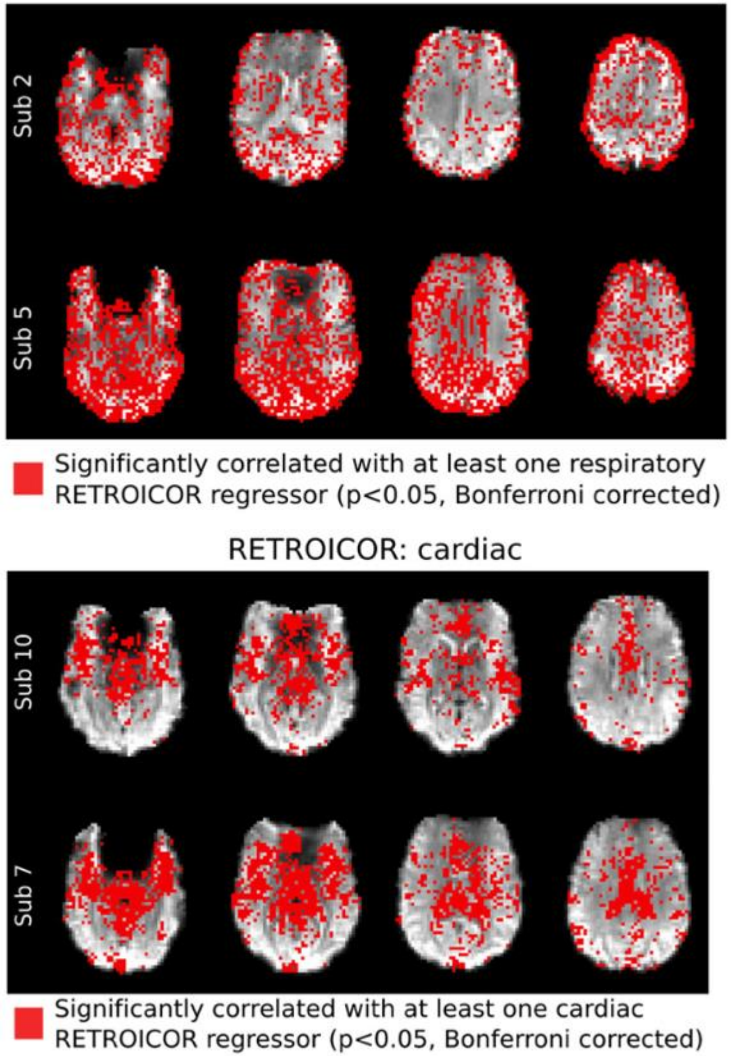

RVT

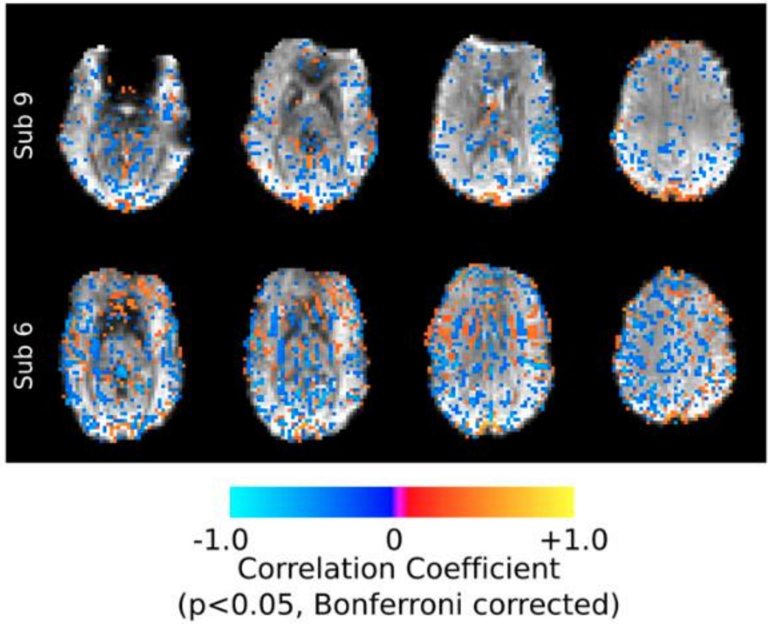

Bright & Murphy "Removing motion and physiological artifacts from intrinsic BOLD fluctuations using short echo data" NeuroImage (2013)

Dual Echo for denoising BOLD data

3T | 18 Slices | TR = 2s | 3.4x3.4x5 mm | TE_1 = 3.3ms, TE_2 = 35ms

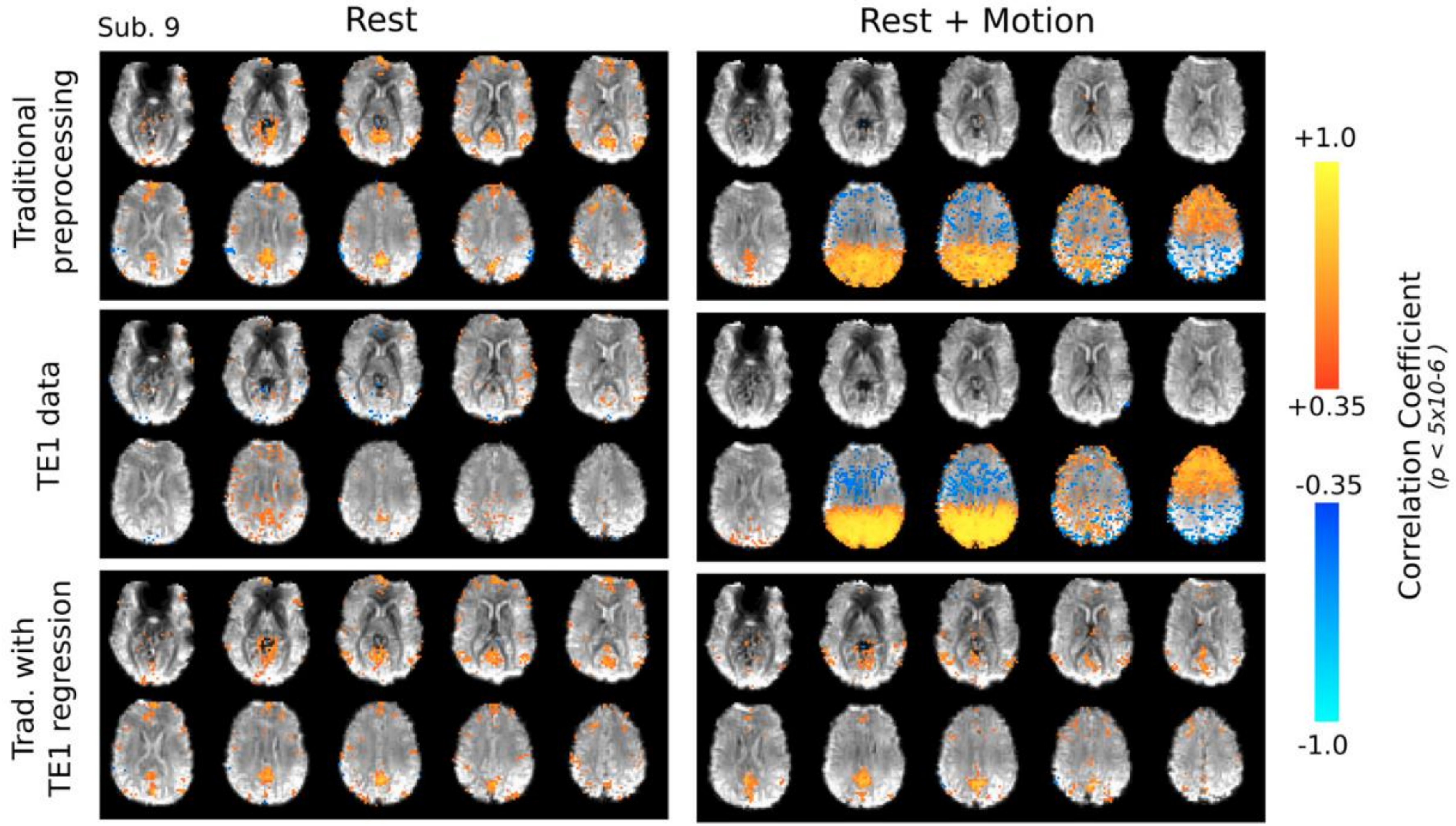

Bright & Murphy "Removing motion and physiological artifacts from intrinsic BOLD fluctuations using short echo data" NeuroImage (2013)

Dual Echo for denoising BOLD data

Subject	TE1 = 3.3 ms			TE1 = 10 ms		
	Traditional preprocessing	TE1 regression	% Change	Traditional preprocessing	TE1 regression	% Change
No. of activated voxels						
1	1103	882	−20.0%	988	566	−42.7%
2	1187	1002	−15.6%	1366	900	−34.1%
4	1181	1051	−11.0%	987	731	−25.9%
5	1031	851	−17.5%	1970	1293	−34.4%
6	1568	1354	−13.6%	2108	1563	−25.9%
8	1535	1167	−24.0%	2646	1813	−31.5%
9	1697	1360	−19.9%	2288	1629	−28.8%
10	2439	2193	−10.1%	2228	1438	−35.5%
Average	1468	1233	−16.5%	1823	1242	−32.3%*
Mean t-statistic						
1	15.2	13.5	−11.0%	16.4	11.8	−28.1%
2	16.2	14.4	−11.1%	21.9	14.9	−31.9%
4	25.4	21.7	−14.7%	18.2	14.4	−20.6%
5	15.5	13.7	−11.2%	31.9	18.2	−43.0%
6	20.6	16.6	−19.5%	28.3	18.6	−34.2%
8	18.8	15.0	−20.1%	35.2	19.9	−43.4%
9	16.0	13.7	−14.0%	25.3	16.3	−35.6%
10	24.9	19.9	−19.9%	19.4	13.2	−32.2%
Average:	19.1	16.1	−15.2%	24.6	15.9	−33.6% *

Bright & Murphy "Removing motion and physiological artifacts from intrinsic BOLD fluctuations using short echo data" NeuroImage (2013)

Voxel/Time-wise Fit of Exponential Decay

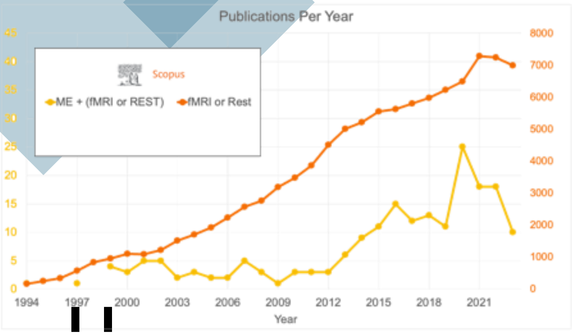

Functional Imaging by I_0- and T_2*-Parameter Mapping Using Multi-Image EPI

Oliver Speck, Jürgen Hennig

Magnetic Resonance in Medicine 40:243-248 (1999)

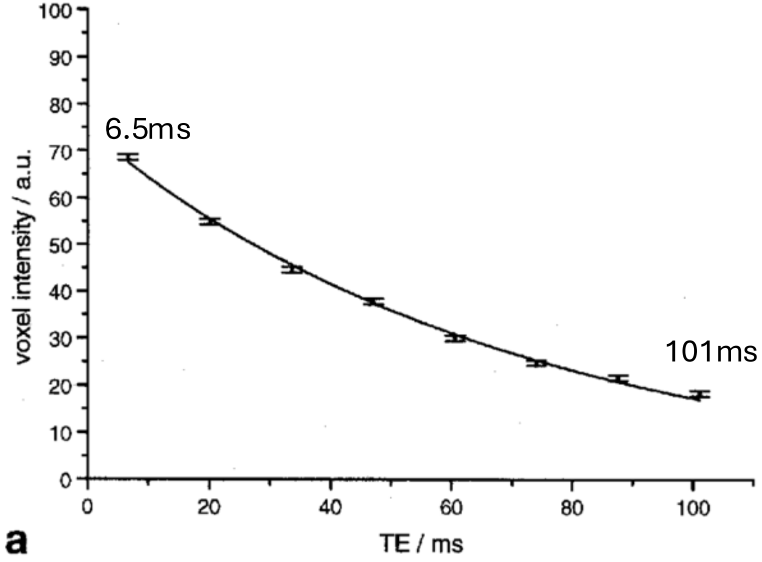

2T Magnet | 3 Slices | TR = 3s

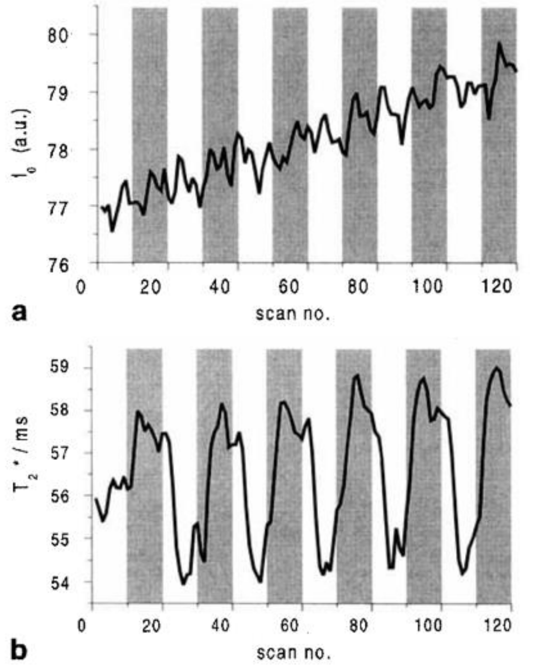

FIG. 5. Time course of I_0 (top) and T_2* (bottom). Values within the areas with a correlation coefficient >0.3 were averaged for a single subject. The gray shaded areas correspond to the time the visual stimulus was turned on. It is clearly visible that the signal drift in the data is due to an I_0 drift only.

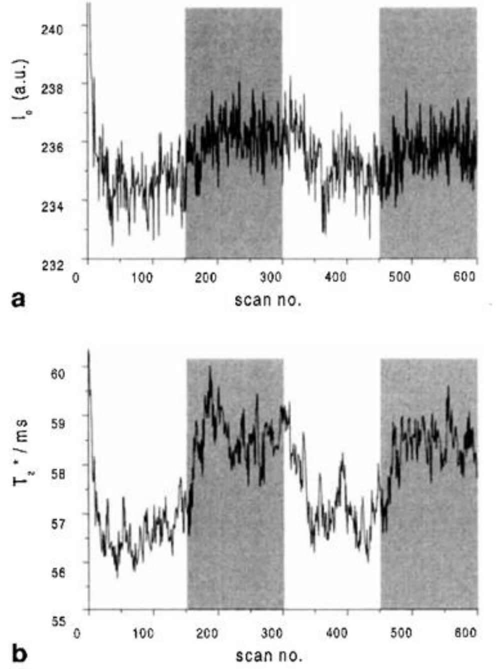

FIG. 7. Results of a first experiment to demonstrate the possibility to separate T_2* (bottom) from I_0 (top) effects. Only one slice has been measured with a TR of 200 ms and eight echo images per excitation. The shaded areas represent the time periods of visual stimulation. The increase not only in T_2* (BOLD) but also in I_0 (inflow) is clearly visible.

2T Magnet | 1 Slice | TR = 200ms

Combination of Echoes

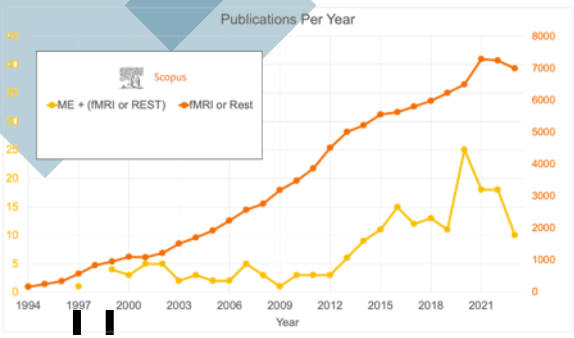

Magnetic Resonance in Medicine 42:87–97 (1999)

Enhancement of BOLD-Contrast Sensitivity by Single-Shot Multi-Echo Functional MR Imaging

Stefan Posse,[1]* Stefan Wiese,[1] Daniel Gembris,[1] Klaus Mathiak,[1] Christoph Kessler,[2] Maria-Liisa Grosse-Ruyken,[1] Barbara Elghahwagi,[1] Todd Richards,[3] Stephen R. Dager,[3] and Valerij G. Kiselev[1]

Exponential Fitting

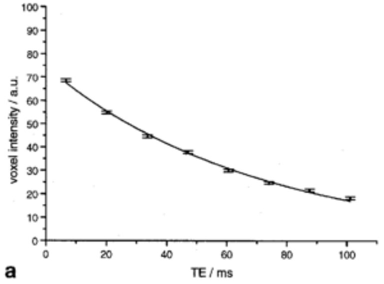

- Computationally expensive
- Noisy at voxel-level

Simple Echo Summation

$$\hat{S}(t_r) = \sum_{n=1}^{N} S(t_r, TE_n)$$

- Computationally inexpensive
- Later long echoes might degrade the average

Weighted Echo Summation

$$\hat{S}(t_r) = \sum_{n=1}^{N} S(t_r, TE_n) w(TE_n)$$

$$w(TE_n) = \frac{TE_n}{\tau} \exp\left(-\frac{TE_n}{\tau}\right)$$

- Computationally inexpensive
- Requires T2* estimates

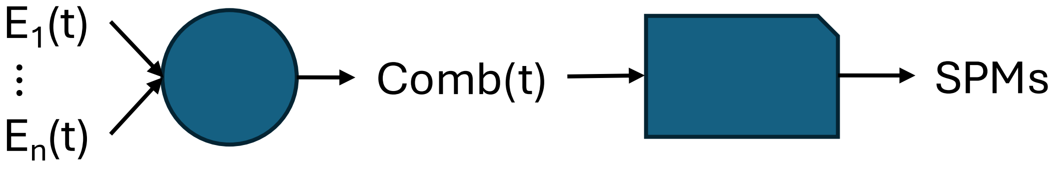

Combine Statistical Maps generated separately for each echo

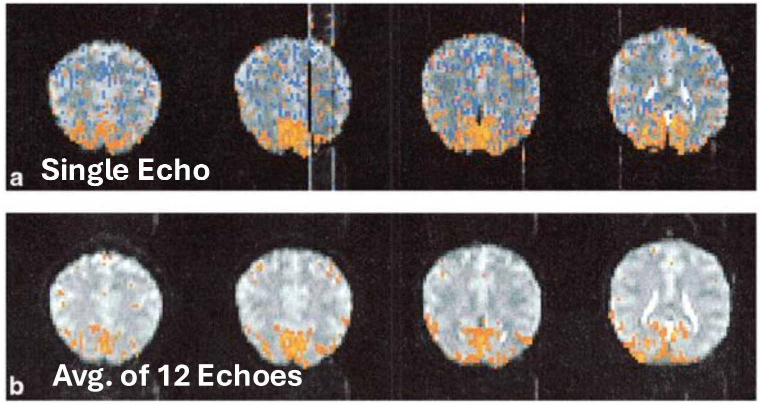

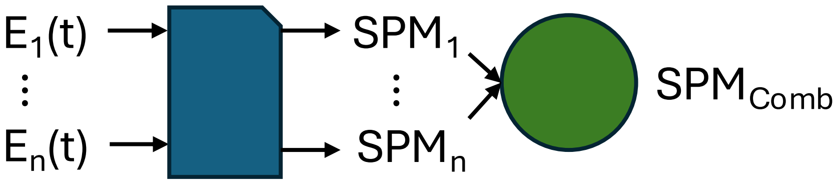

Combination of Echoes

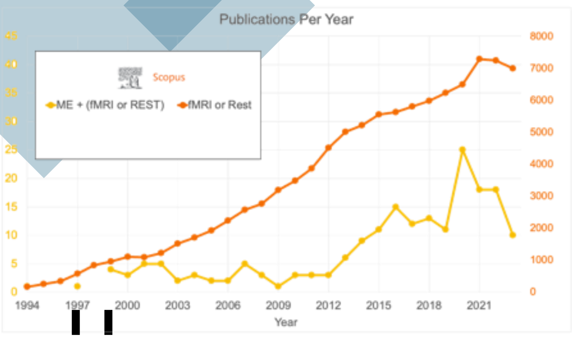

Magnetic Resonance in Medicine 42:87–97 (1999)

Enhancement of BOLD-Contrast Sensitivity by Single-Shot Multi-Echo Functional MR Imaging

Stefan Posse,[1]* Stefan Wiese,[1] Daniel Gembris,[1] Klaus Mathiak,[1] Christoph Kessler,[2] Maria-Liisa Grosse-Ruyken,[1] Barbara Elghahwagi,[1] Todd Richards,[3] Stephen R. Dager,[3] and Valerij G. Kiselev[1]

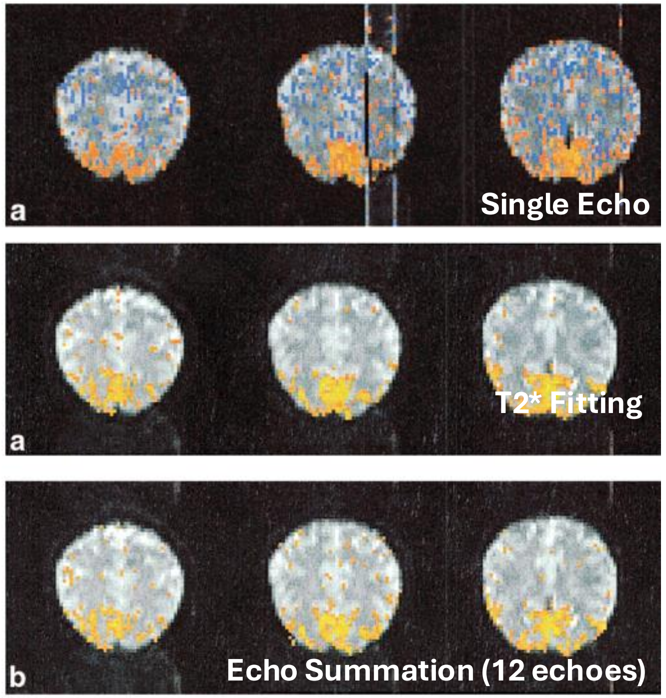

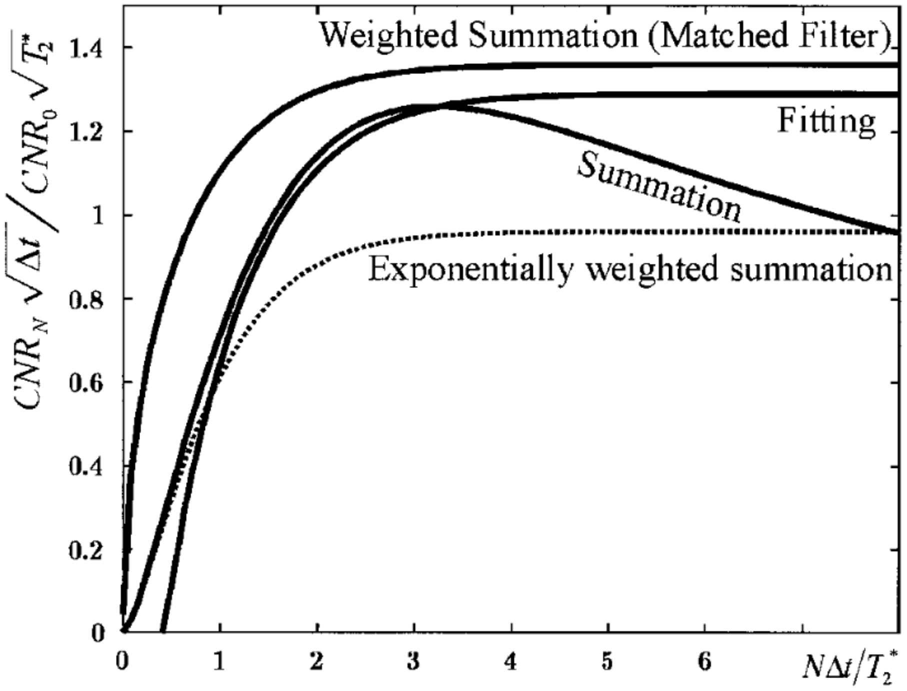

- ❑ Multi-echo outperforms single echo.
- ❑ Sensitivity gain depends on #echoes.
- ❑ Considering excessively long echoes can be detrimental.
- ❑ Despite limited sensitivity, T_2^*-Fit can be advantageous if interested in quantification of ΔT_2^*

Combination of Echoes

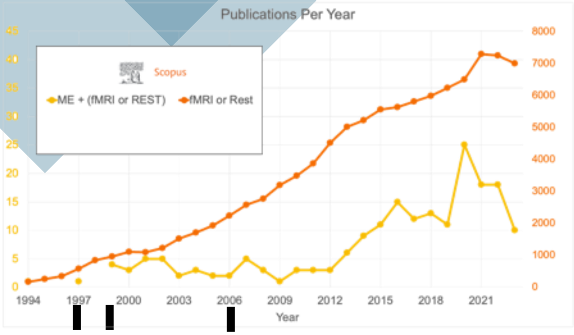

Magnetic Resonance in Medicine 55:1227–1235 (2006)

BOLD Contrast Sensitivity Enhancement and Artifact Reduction With Multiecho EPI: Parallel-Acquired Inhomogeneity-Desensitized fMRI

Benedikt A. Poser,[1*] Maarten J. Versluis,[2] Johannes M. Hoogduin,[2] and David G. Norris[1]

Simple Sum	$w_n = 1/N$
T_2^* Weighted	$w_n = \dfrac{TE_n \cdot e^{-TE_n/T_2^*}}{\sum_{i=1}^{N} TE_i \cdot e^{-TE_i/T_2^*}}$
CNR Weighted	$w_n = \dfrac{tSNR_n \cdot TE_n}{\sum_{i=1}^{N} tSNR_i \cdot TE_i}$

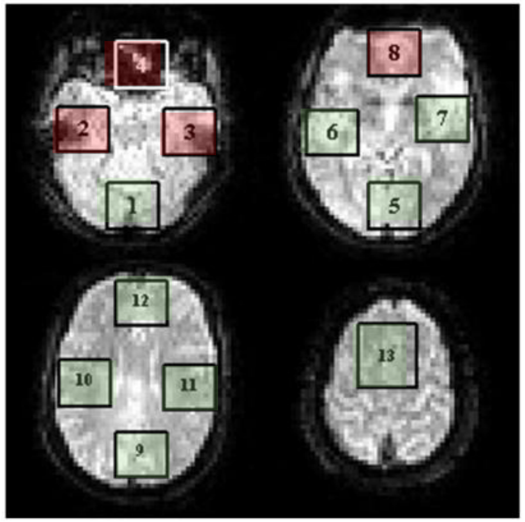

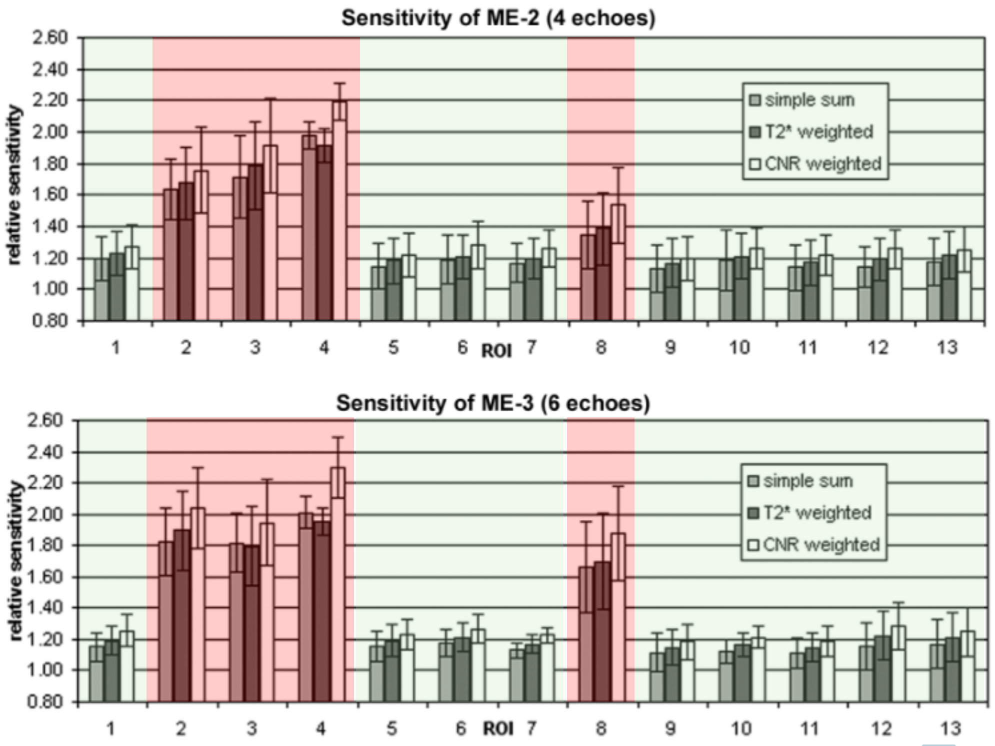

Gains relative to Single Echo

Simple Sum T2* Weighted

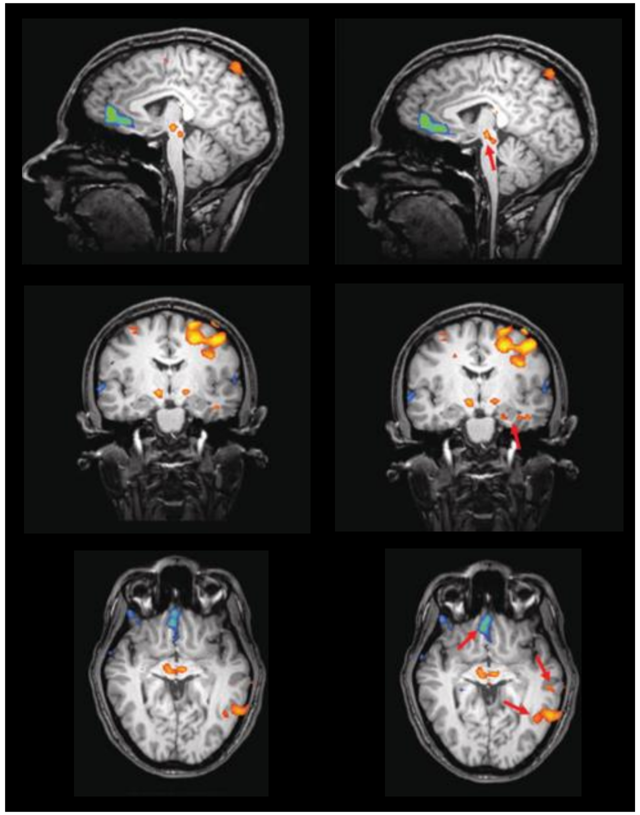

Combination of Echoes

Method	Weights	Requires T2* estimates	Weights vary by voxel	Weights vary with time
Simple Summation (Posse 1999)	$w_n = 1/N$	No	No	No
TE-Combined	$w_n = \frac{TE_n}{\sum_{i=1}^{N} TE_i}$	No	No	No
T_2^*-Combined (OC✢/BOLD✢✢) (Posse 1999)	$w_n = \frac{TE_n \cdot e^{-TE_n / T_2^*}}{\sum_{i=1}^{N} TE_i \cdot e^{-TE_i / T_2^*}}$	Yes	Yes	No
tSNR-Combined (Poser 2006)	$w_n = \frac{tSNR_n \cdot TE_n}{\sum_{i=1}^{N} tSNR_i \cdot TE_i}$	No	Yes	No
T_2^*-FIT Combined (Heunis 2021)	$w_n(t) = \frac{TE_n \cdot e^{-TE_n / T_2^*-FIT(t)}}{\sum_{i=1}^{N} TE_i \cdot e^{-TE_i / T_2^*-FIT(t)}}$	Yes	Yes	Yes

✢ a.k.a. Optimally Combined (OC) in Kundu et al. 2012
✢✢ a.k.a. BOLD weighting in Poser et al. 2006

Heunis et al. "The effects of multi-echo fMRI combination and rapid T2* mapping on offline and realtime BOLD sensitivity" NeuroImage (2021)

Combination of Echoes

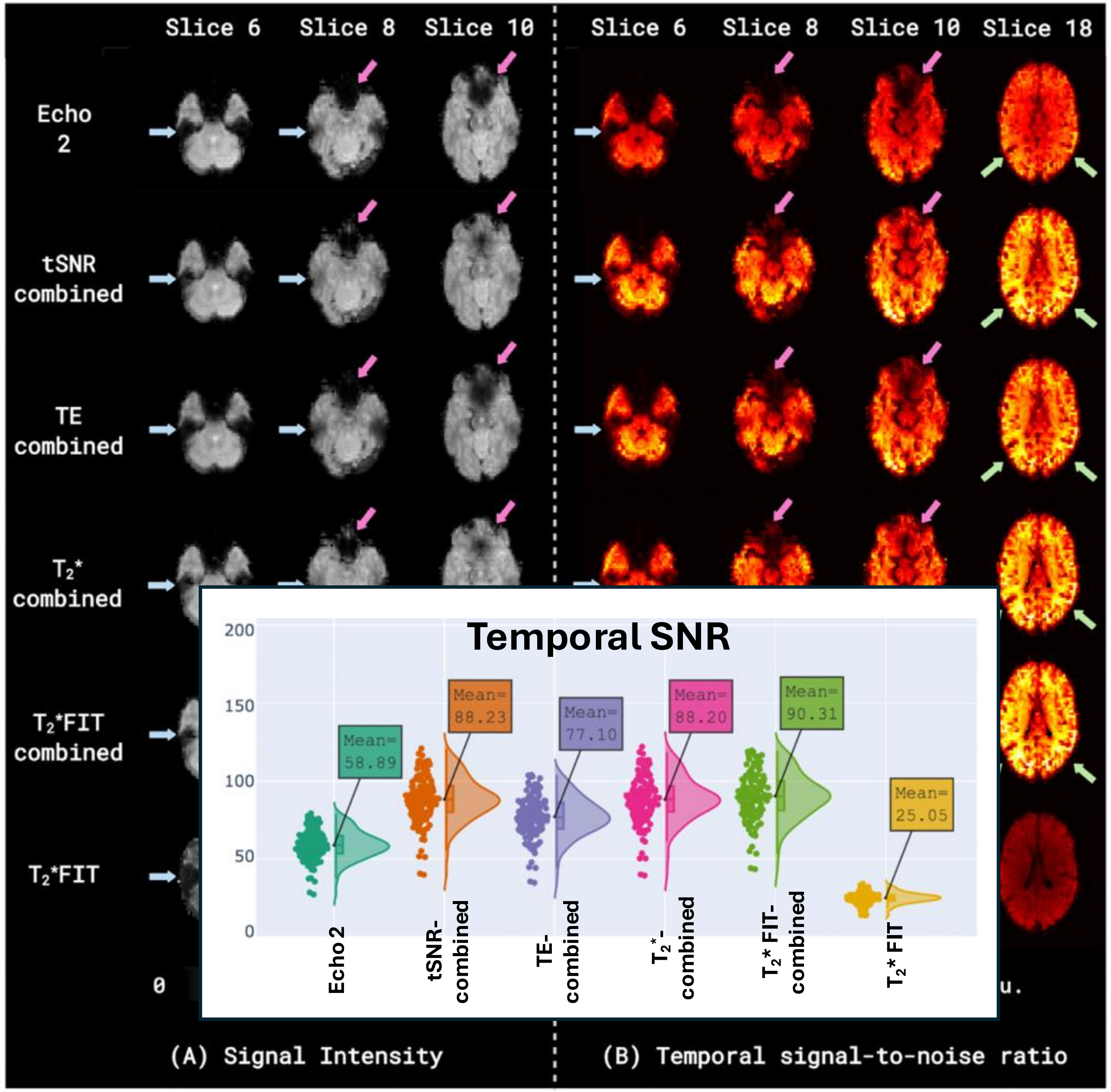

28 Participants | 3T | TR=2s | TE=14/28/42ms | 3.5iso | 34 Slices

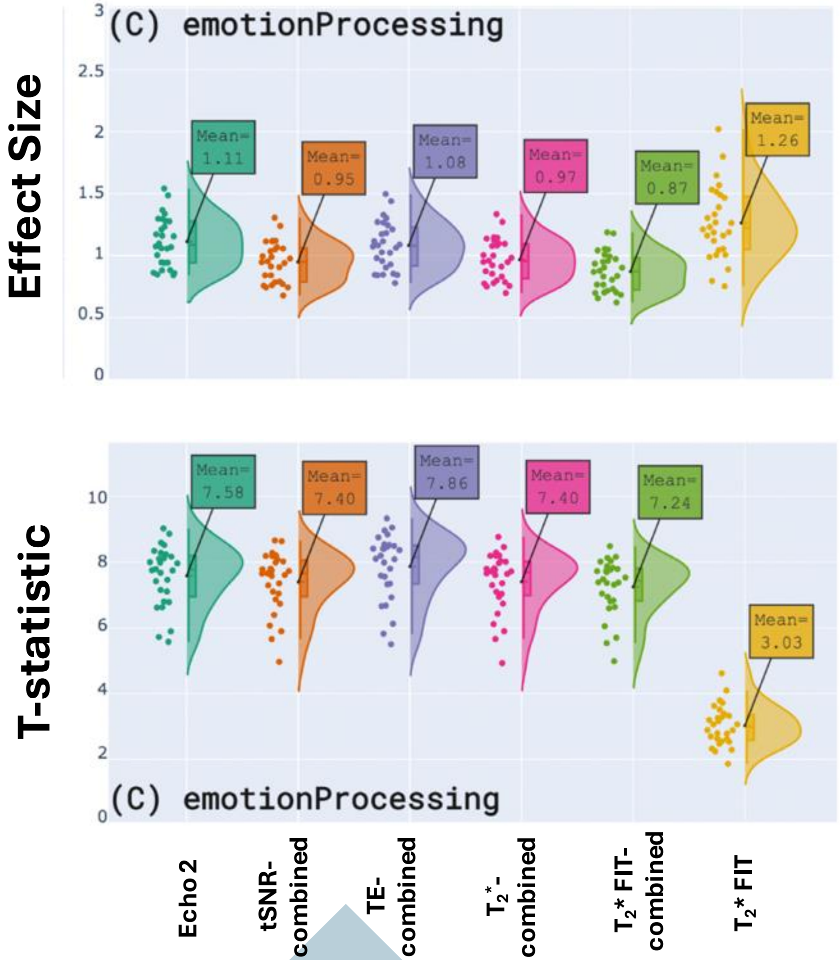

Heunis et al. "The effects of multi-echo fMRI combination and rapid T2* mapping on offline and realtime BOLD sensitivity" NeuroImage (2021)

Source Extraction Methods

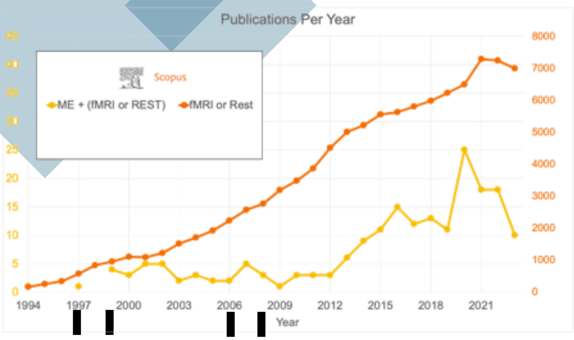

IEEE JOURNAL OF SELECTED TOPICS IN SIGNAL PROCESSING, VOL. 2, NO. 6, DECEMBER 2008

Extraction of Task-Related Activation From Multi-Echo BOLD fMRI

Pieter F. Buur, David G. Norris, and Christian W. Hesse, *Member, IEEE*

Multi-channel Signal Framework

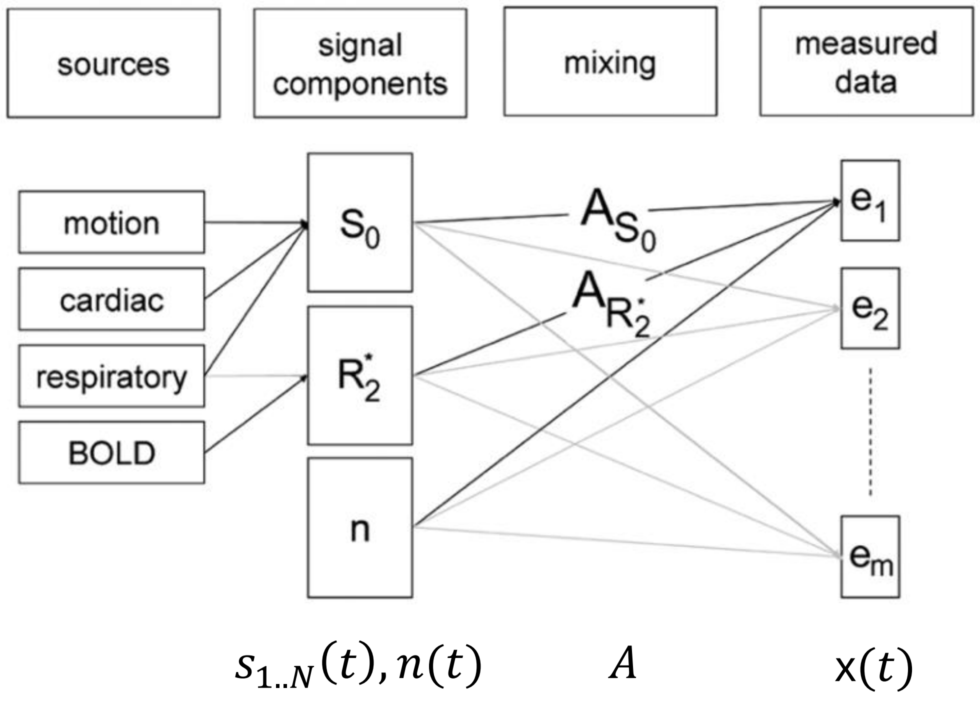

$$x(t) = As(t) + n(t) \mid N, s(t) \,\&\, A \ unknown$$

$$x(t) = S_o(t) \cdot e^{-TE \cdot R_2^*(t)} + n(t)$$

$$x(t) = As(t) + n(t)$$

<u>(1) Data must be linearized:</u>

$$\log(x(t)) = \log(S_o(t)) - TE \cdot R_2^*(t)$$

$$\mathrm{SPC}(t) = \Delta S_o(t)/\overline{S_o} - TE \cdot \Delta R_2^*(t)$$

<u>(2) Choose Source Extraction Model/ Priors:</u>

- Statistical Decomposition: PCA, ICA
- Echo-time Dependence: PINV, a-Beamformer, spICA
- Design Matrix based: Wiener Filter

Source Extraction Methods

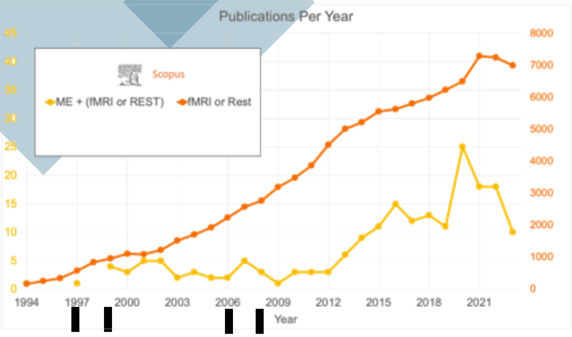

IEEE JOURNAL OF SELECTED TOPICS IN SIGNAL PROCESSING, VOL. 2, NO. 6, DECEMBER 2008

Extraction of Task-Related Activation From Multi-Echo BOLD fMRI

Pieter F. Buur, David G. Norris, and Christian W. Hesse, *Member, IEEE*

No Transform

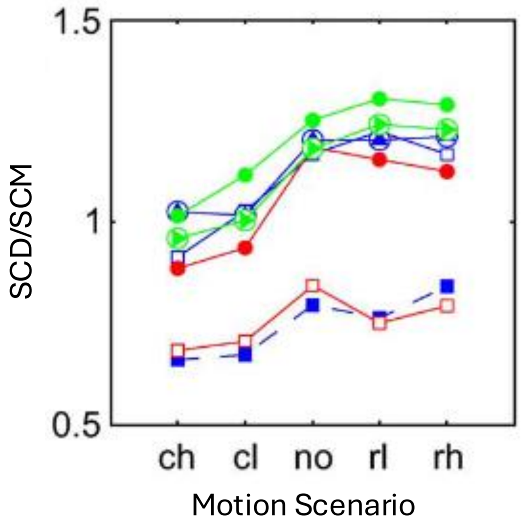

Linearization: Log

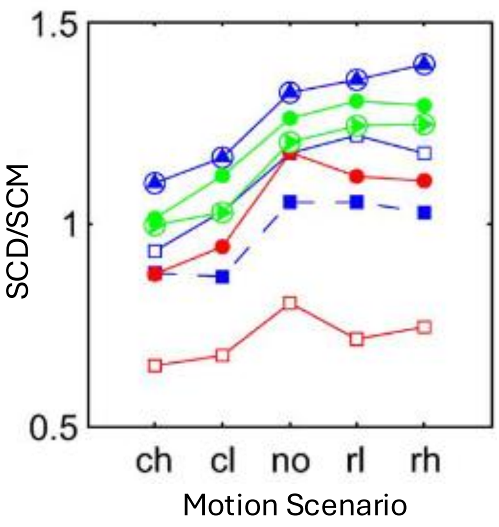

Linearization: SPC

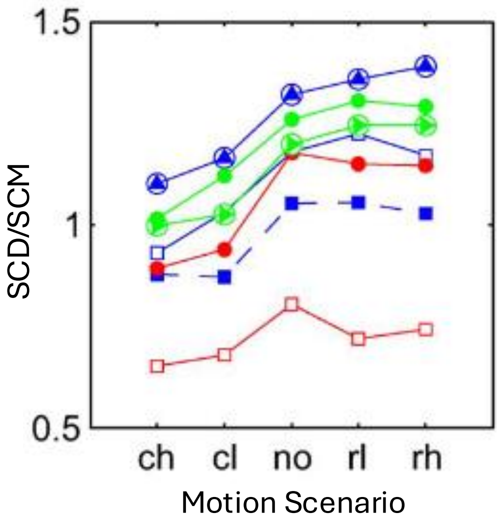

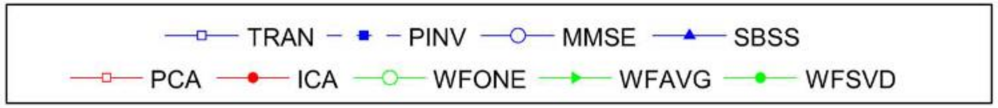

6 Participants | 3T | TE=9.3,21.1,33,45,56ms | TR=2s | Stroop Task | Artificially-induced motion: task-correlated (c), random (r) & normal (no)

Quality measured in terms of correlation to task (SCD) / correlation to motion (SCM)

TE-ICA Denoising (ME-ICA/tedana)

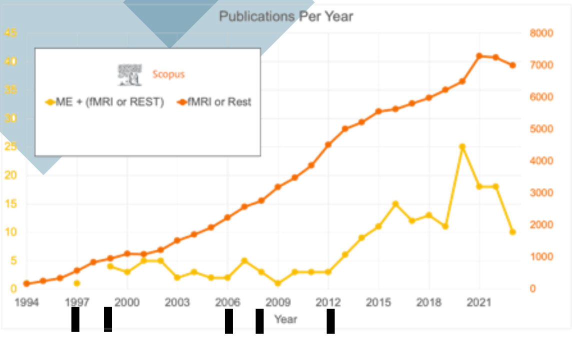

Multiplexed Echo Planar Imaging for Sub-Second Whole Brain FMRI and Fast Diffusion Imaging

David A. Feinberg[1,2,3]*, Steen Moeller[4], Stephen M. Smith[5], Edward Auerbach[4], Sudhir Ramanna[1], Matt F. Glasser[6], Karla L. Miller[5], Kamil Ugurbil[4], Essa Yacoub[4]

1 Advanced MRI Technologies, Sebastopol, California, United States of America, **2** Helen Wills Institute for Neuroscience, University of California, Berkeley, California, United States of America, **3** Department of Radiology, University of California San Francisco, San Francisco, California, United States of America, **4** Department of Radiology, Center for Magnetic Resonance Research, University of Minnesota Medical School, Minneapolis, Minnesota, United States of America, **5** Oxford Centre for Functional MRI of the Brain, University of Oxford, John Radcliffe Hospital, Oxford, United Kingdom, **6** Anatomy and Neurobiology, Washington University School of Medicine, Washington University, St. Louis, Missouri, United States of America

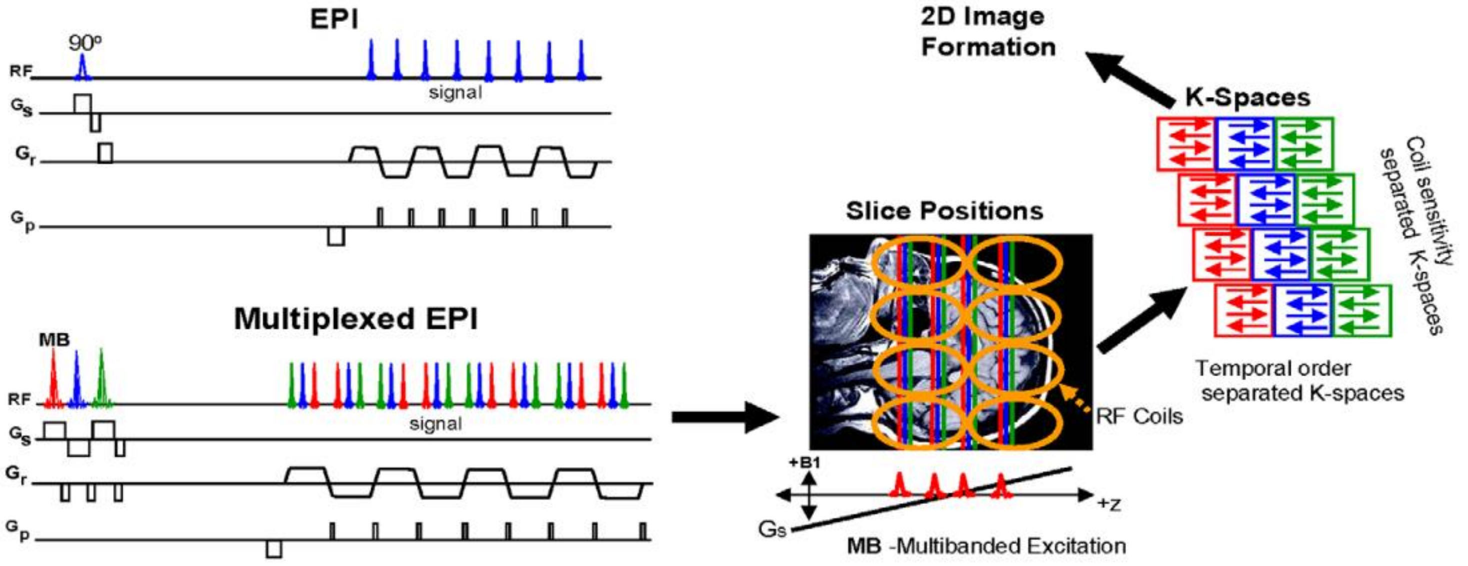

TE-ICA Denoising (ME-ICA/tedana)

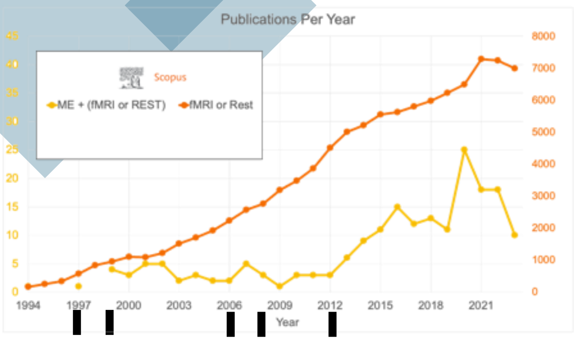

Contents lists available at ScienceDirect
NeuroImage
journal homepage: www.elsevier.com/locate/neuroimage

Multi-echo fMRI: A review of applications in fMRI denoising and analysis of BOLD signals

Prantik Kundu[a,*], Valerie Voon[b], Priti Balchandani[a], Michael V. Lombardo[c], Benedikt A. Poser[d], Peter A. Bandettini[e]

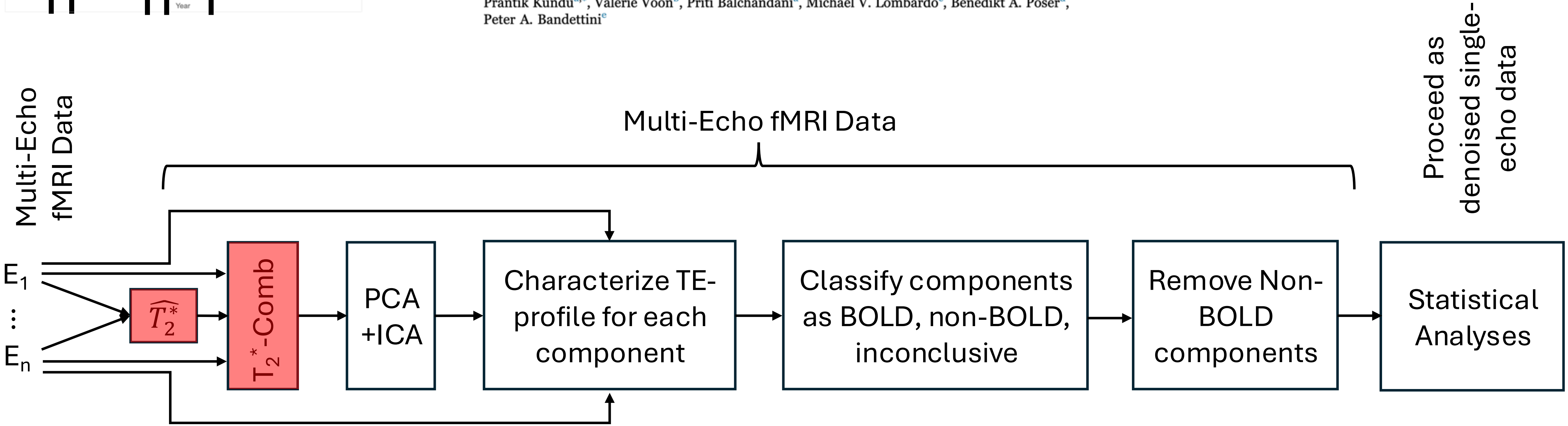

ME-ICA/tedana

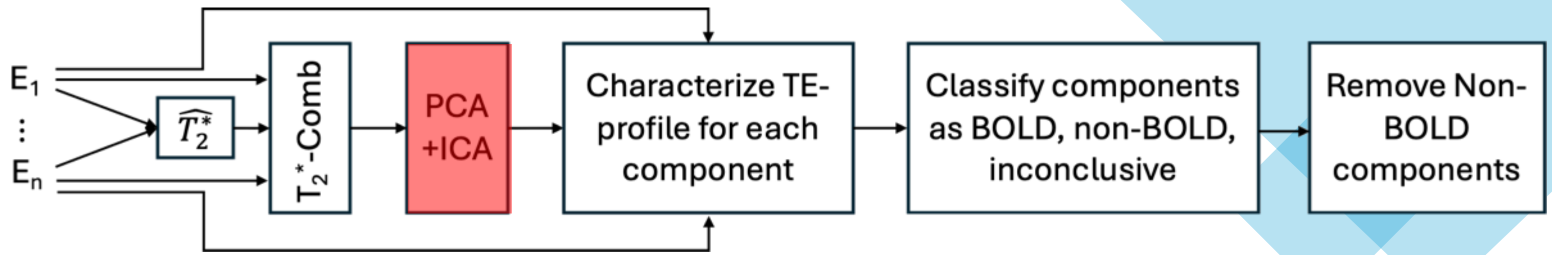

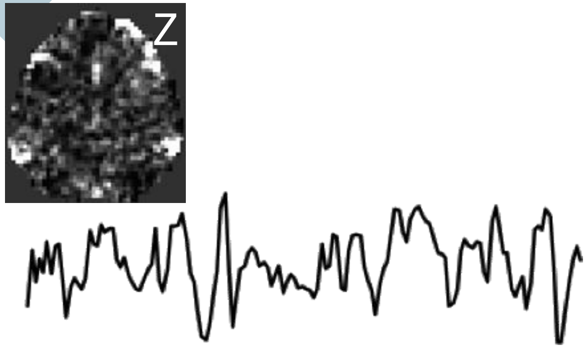

ICA_1

⋮

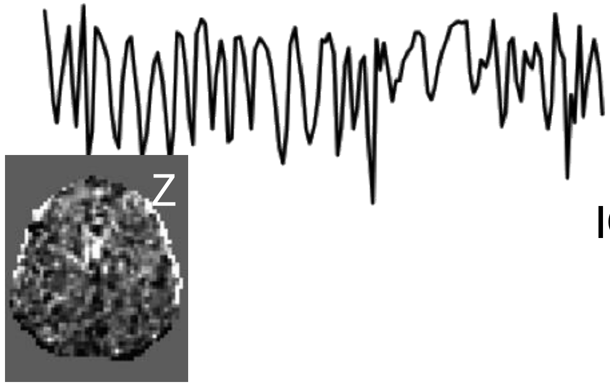

ICA_n

Kundu et al., NeuroImage 2012

ME-ICA/tedana

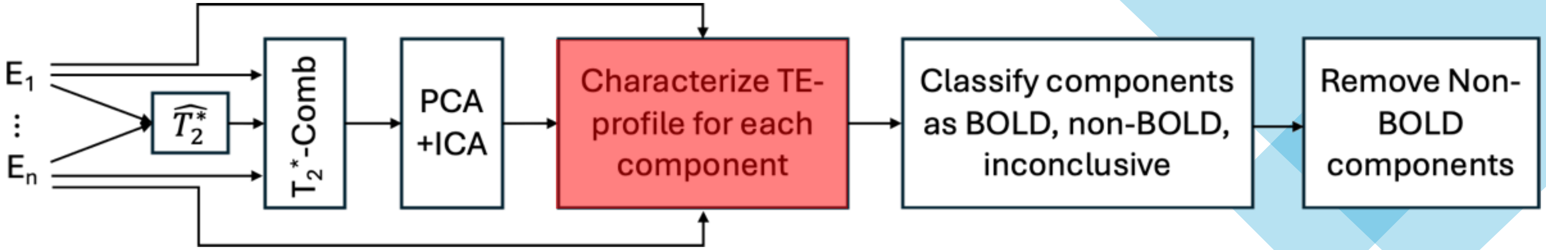

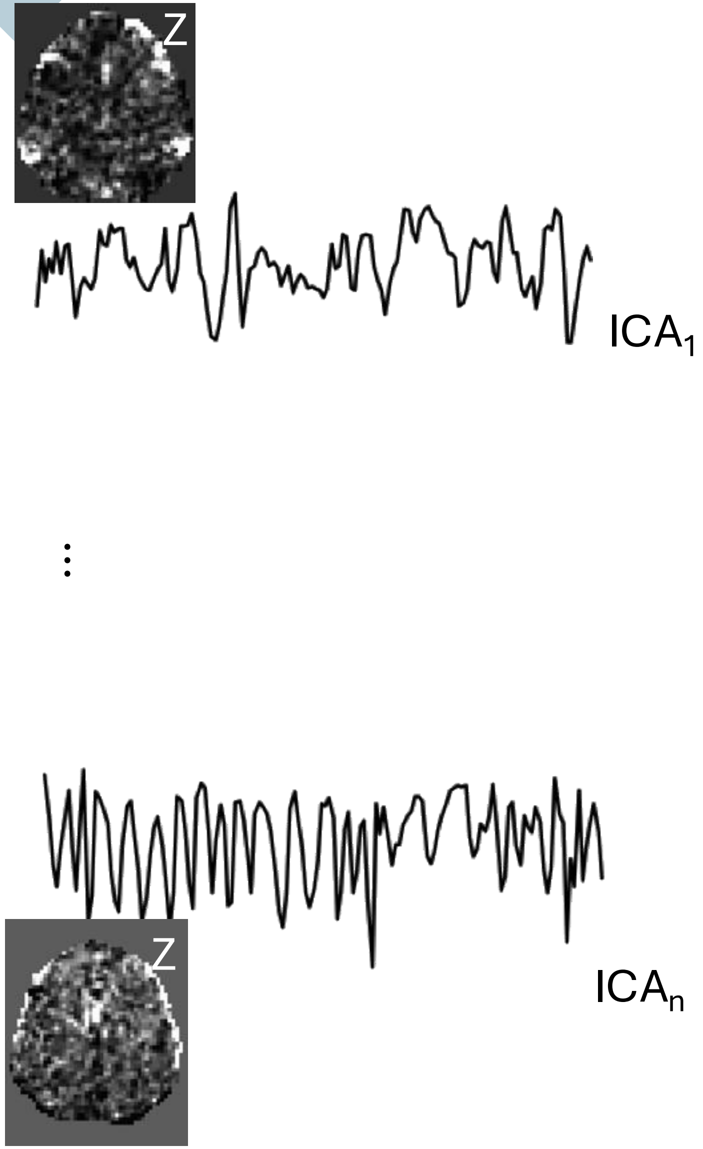

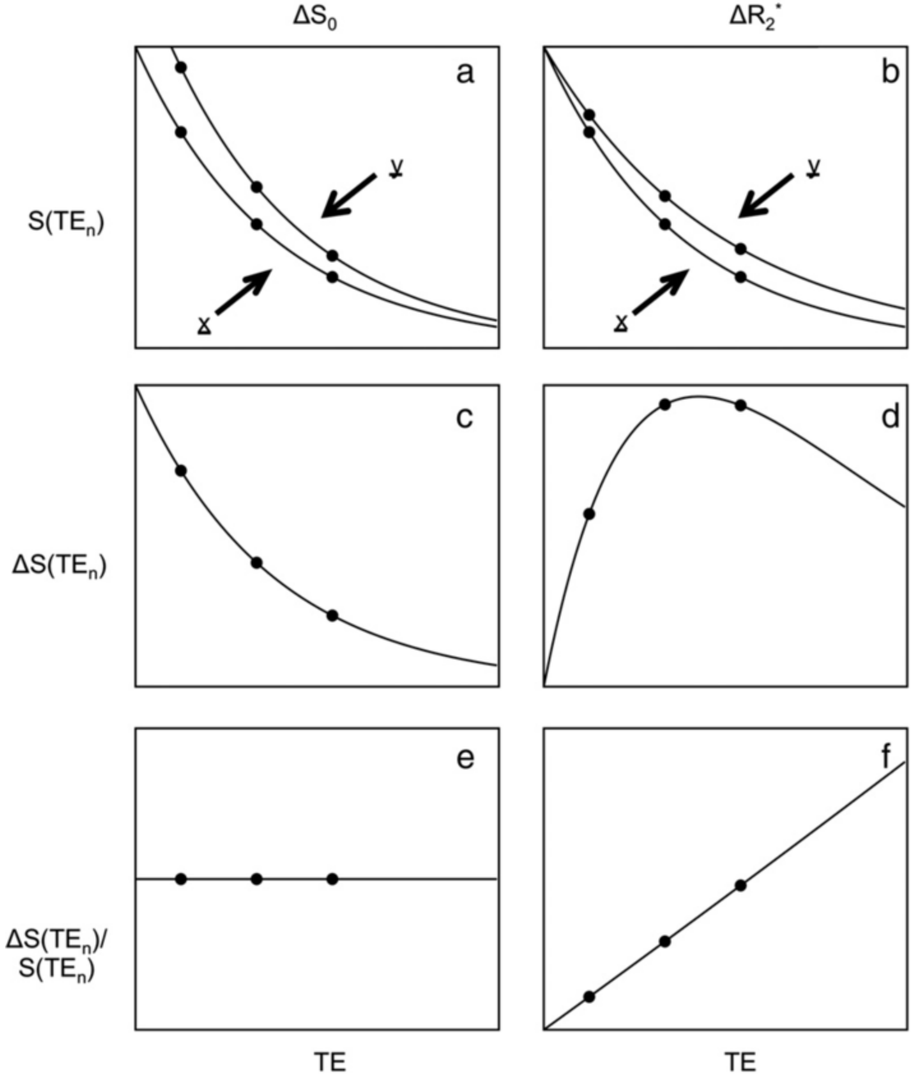

Kundu et al., NeuroImage 2012

ME-ICA/tedana

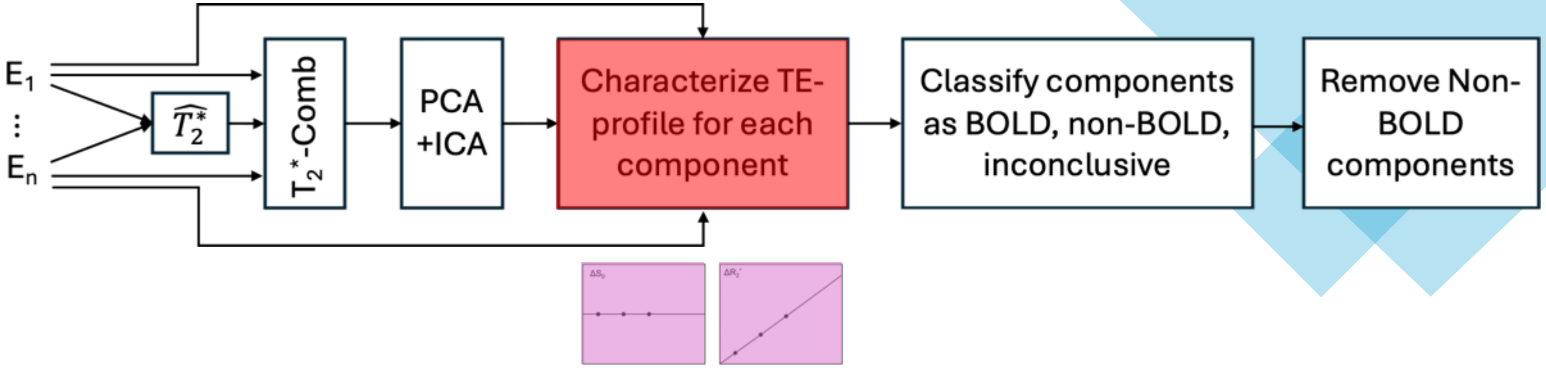

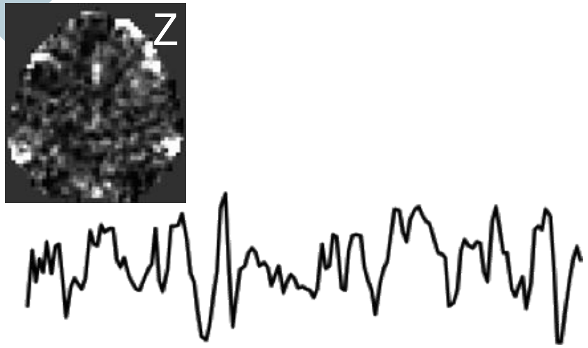

ICA$_1$

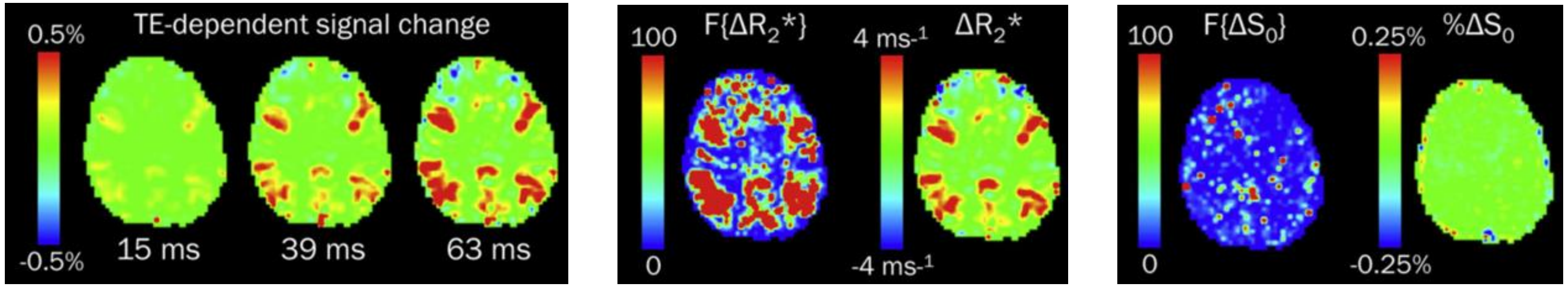

$\kappa = 210$

$\rho = 10$

$$\kappa = \sum_{All\,Voxels} Z^2\, F_{R_2^*} \qquad \rho = \sum_{All\,Voxels} Z^2\, F_{S_0}$$

⋮

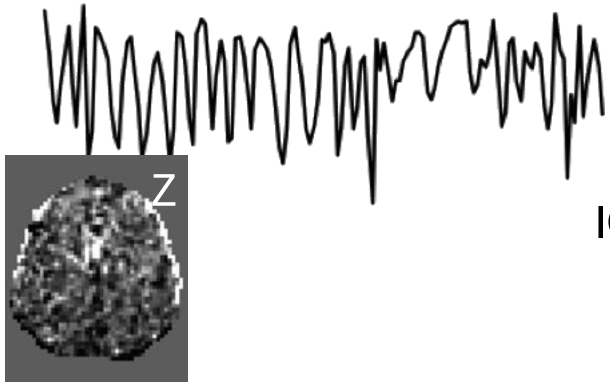

ICA$_n$

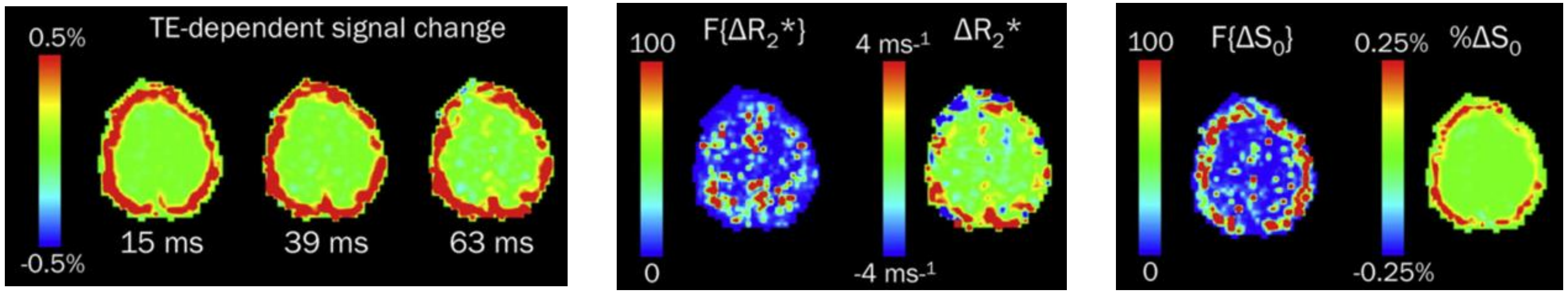

$\kappa = 32$

$\rho = 81$

Kundu et al., NeuroImage 2012

ME-ICA/tedana

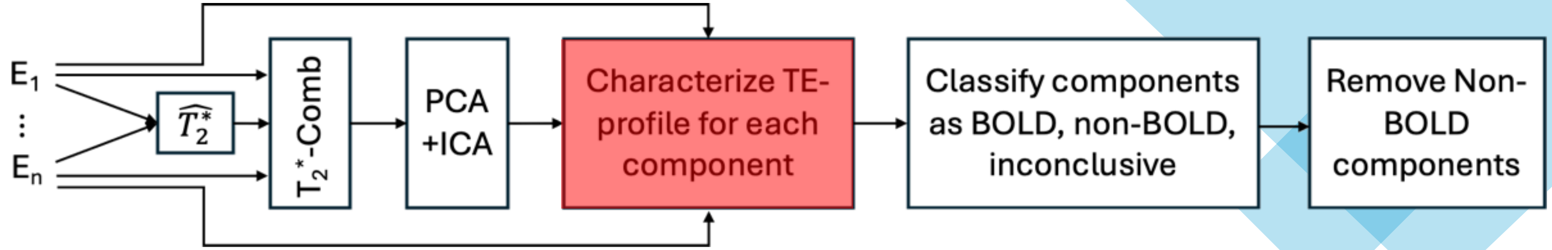

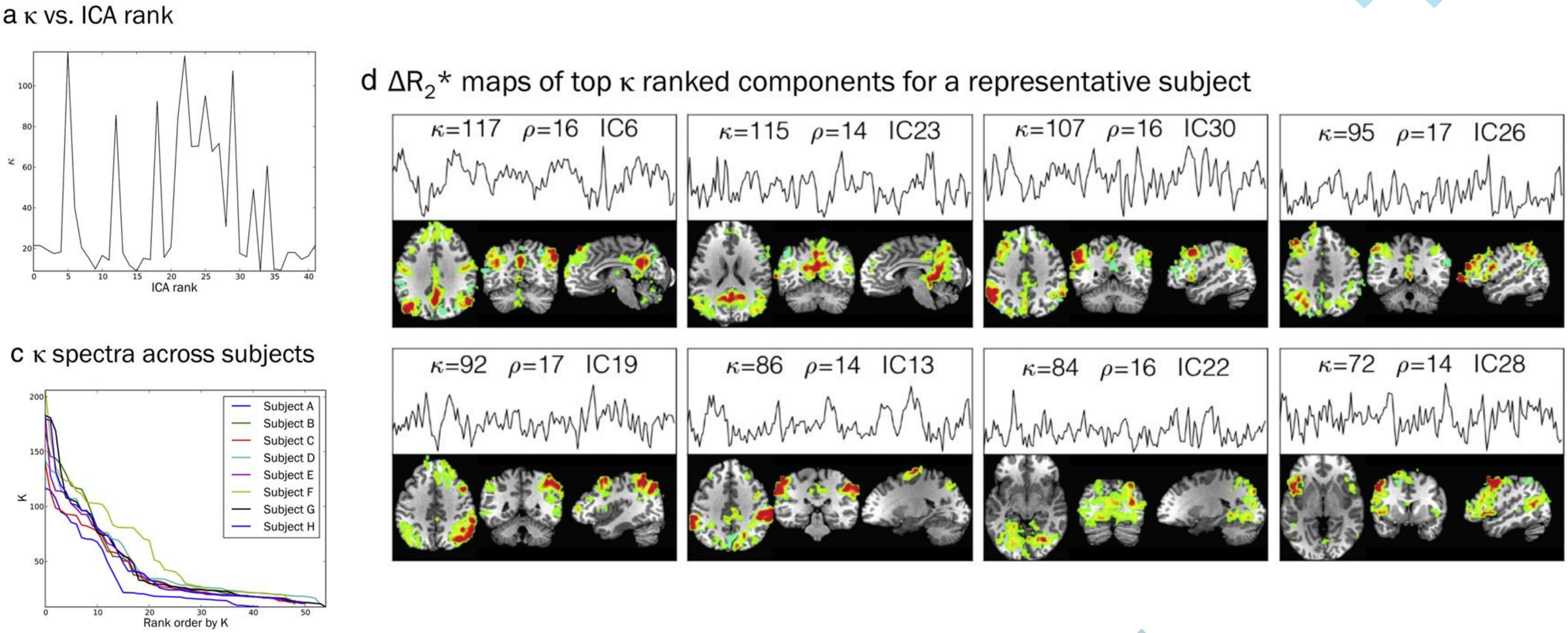

Kundu et al., NeuroImage 2012

ME-ICA/tedana

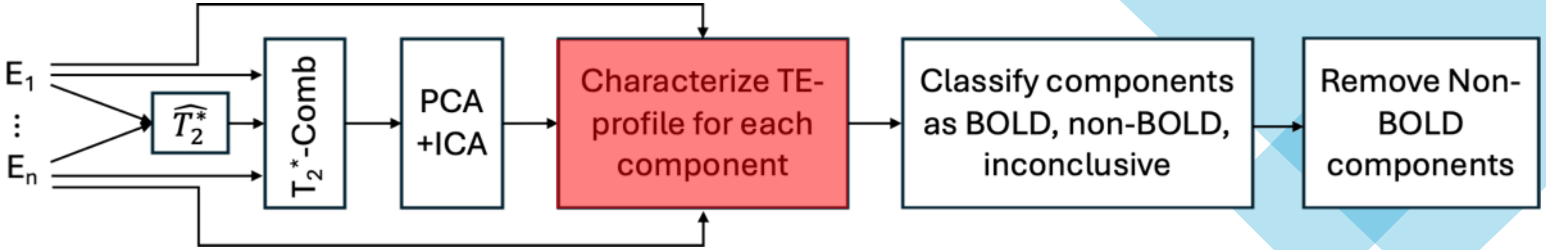

a ρ vs. ICA rank

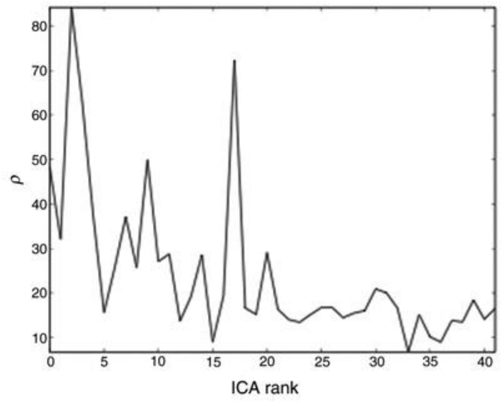

c ρ-spectrum across subjects

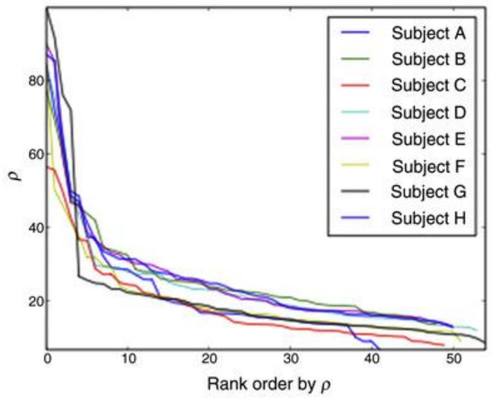

d ΔS_0 maps of top ρ-ranked components for a representative subject

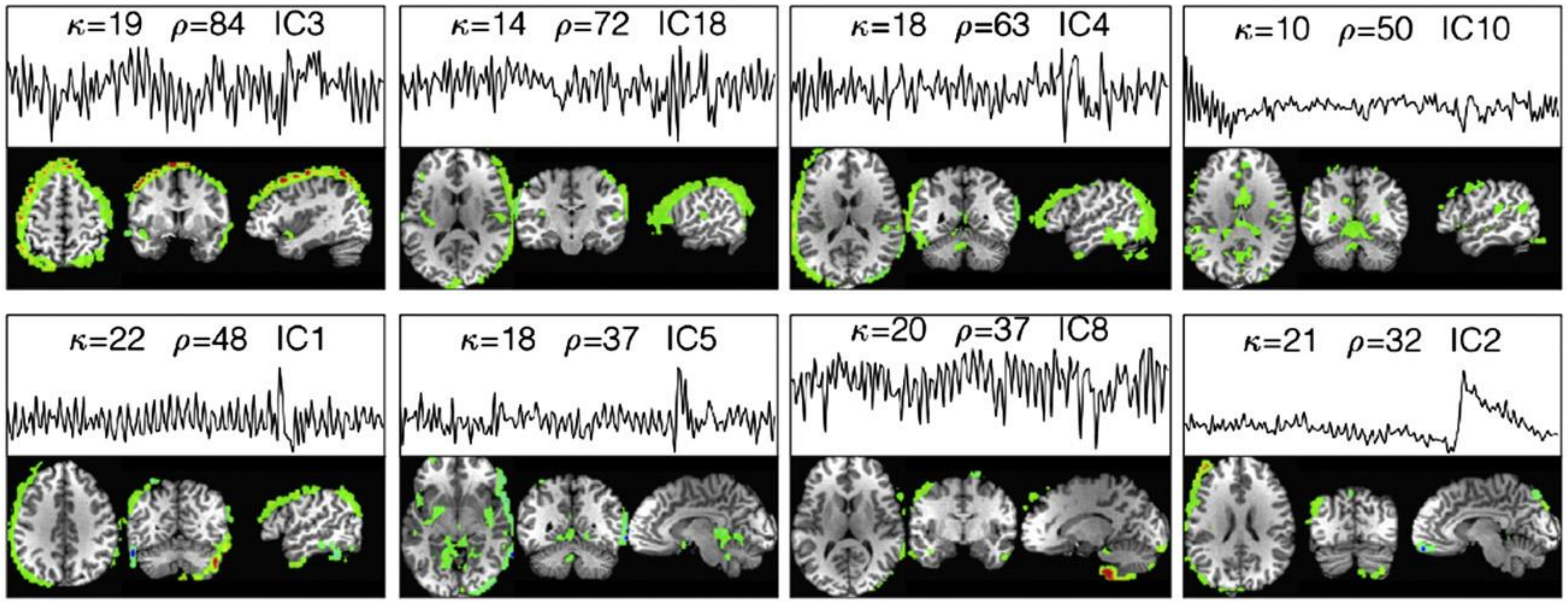

Kundu et al., NeuroImage 2012

ME-ICA/tedana

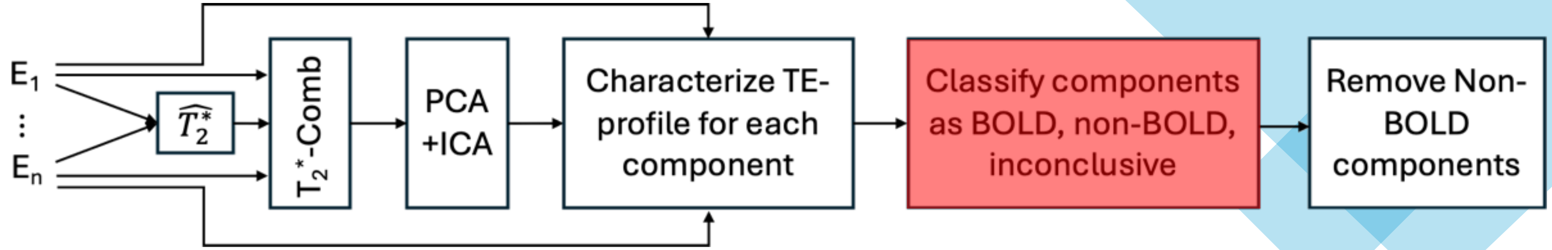

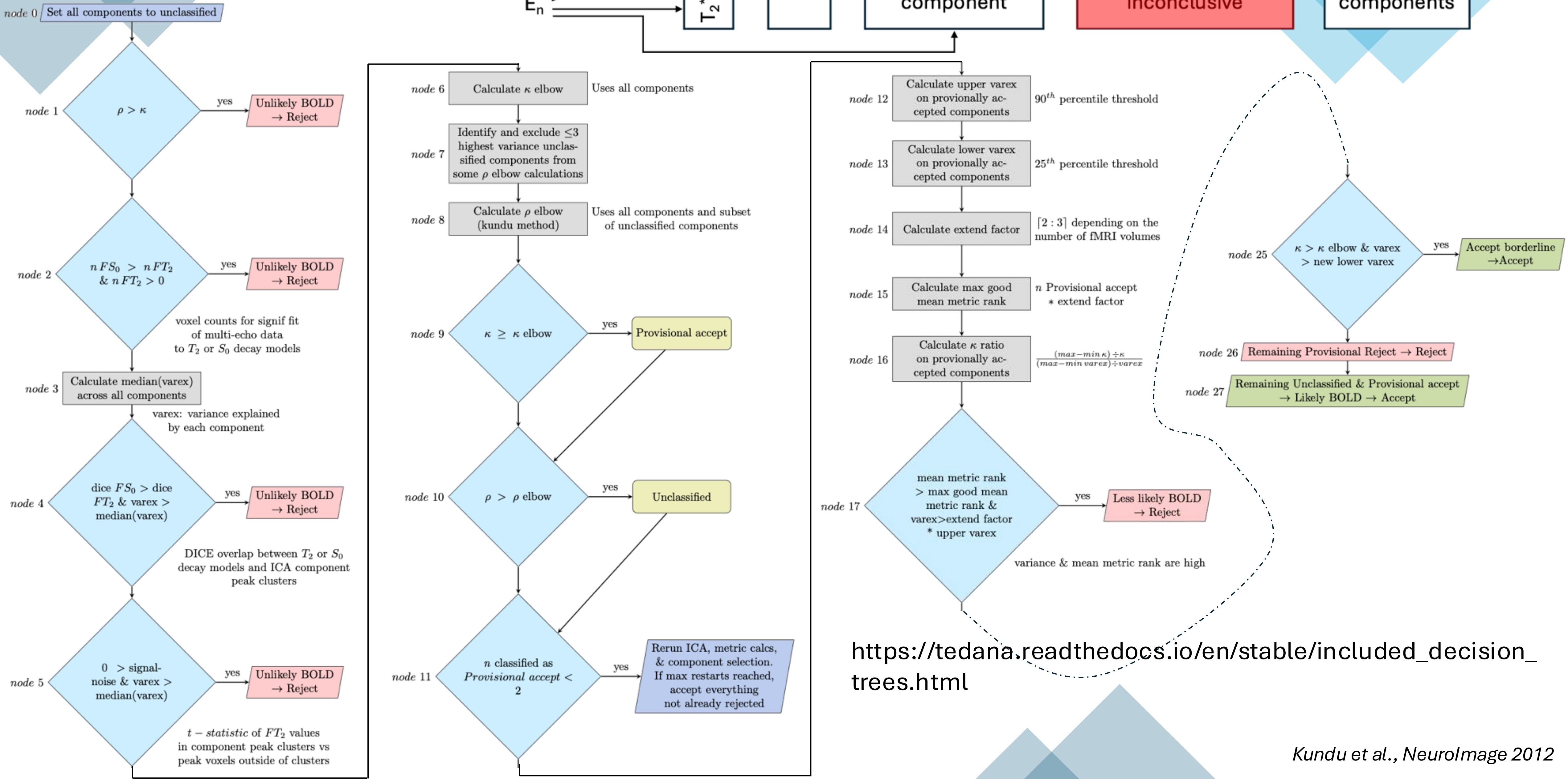

https://tedana.readthedocs.io/en/stable/included_decision_trees.html

Kundu et al., NeuroImage 2012

ME-ICA/tedana

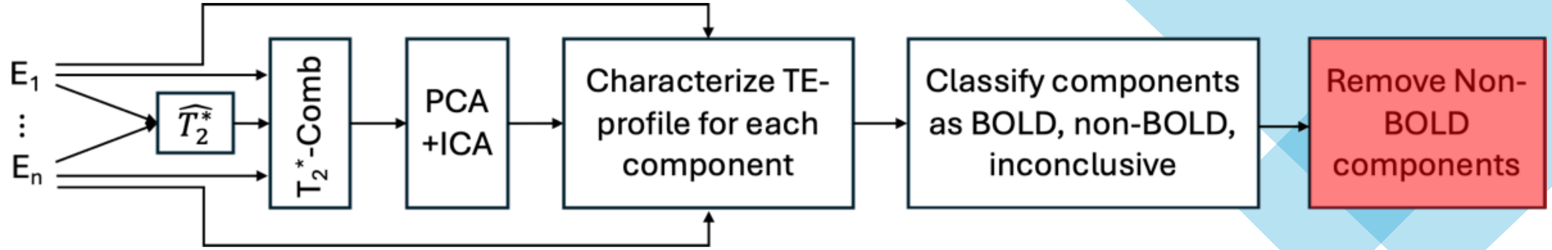

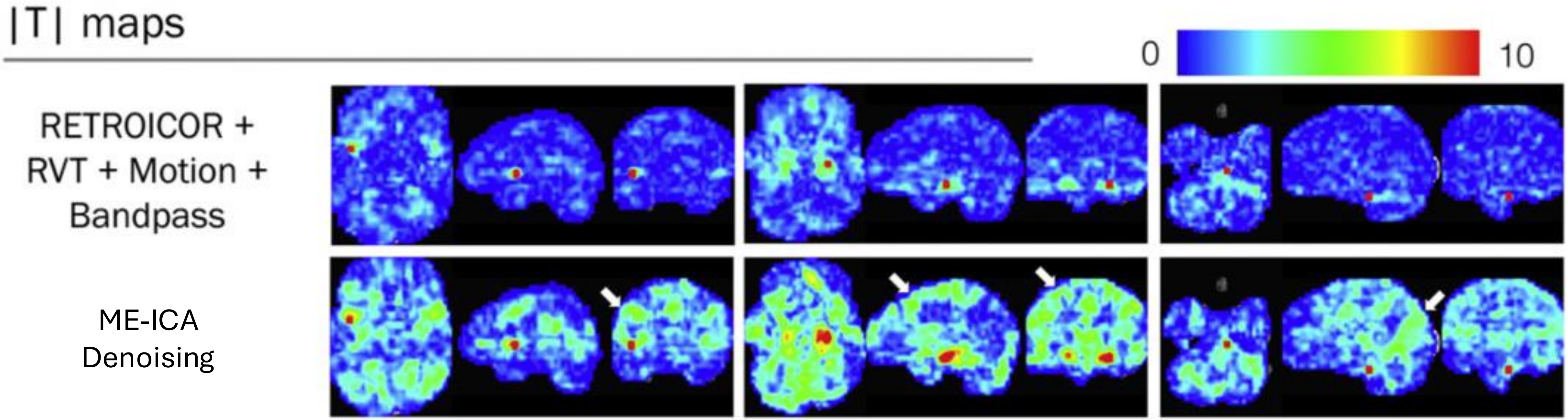

Kundu et al., NeuroImage 2012

ME-ICA vs. tedana

Contents lists available at ScienceDirect

NeuroImage

journal homepage: www.elsevier.com/locate/neuroimage

Multi-echo fMRI: A review of applications in fMRI denoising and analysis of BOLD signals

Prantik Kundu[a,*], Valerie Voon[b], Priti Balchandani[a], Michael V. Lombardo[c], Benedikt A. Poser[d], Peter A. Bandettini[e]

- ICA + TE-Dependence Analysis for denoising
- Full Pre-processing Pipeline
- Complex Decision Tree
- Relied on FSL/Melodic for ICA
- Hard to modify / extent

JOSS The Journal of Open Source Software

TE-dependent analysis of multi-echo fMRI with *tedana*

Elizabeth DuPre[*1], Taylor Salo[†2], Zaki Ahmed[3], Peter A. Bandettini[4], Katherine L. Bottenhorn[2], César Caballero-Gaudes[5], Logan T. Dowdle[6], Javier Gonzalez-Castillo[4], Stephan Heunis[7], Prantik Kundu[8], Angela R. Laird[2], Ross Markello[1], Christopher J. Markiewicz[9], Stefano Moia[5], Isla Staden[10], Joshua B. Teves[4], Eneko Uruñuela[5], Maryam Vaziri-Pashkam[4], Kirstie Whitaker[11], and Daniel A. Handwerker[‡4]

1 McGill University 2 Florida International University 3 Mayo Clinic 4 National Institutes of Health 5 Basque Center on Cognition, Brain and Language 6 Center for Magnetic Resonance Research, University of Minnesota 7 Eindhoven University of Technology 8 Mount Sinai Hospital 9 Stanford University 10 Thought Machine 11 Alan Turing Institute

tedana

- Started as an effort to improve ME-ICA (without preprocessing)
- Python library for denoising of multi-echo fMRI data
- Dual Interface: Command Line / Python API
- Dynamic Reporting Tools
- Includes different workflows / pipelines
- Integration with AFNI_proc.py and fMRIprep
- Open Science Project with extensive documentation

tedana

Full Documentation

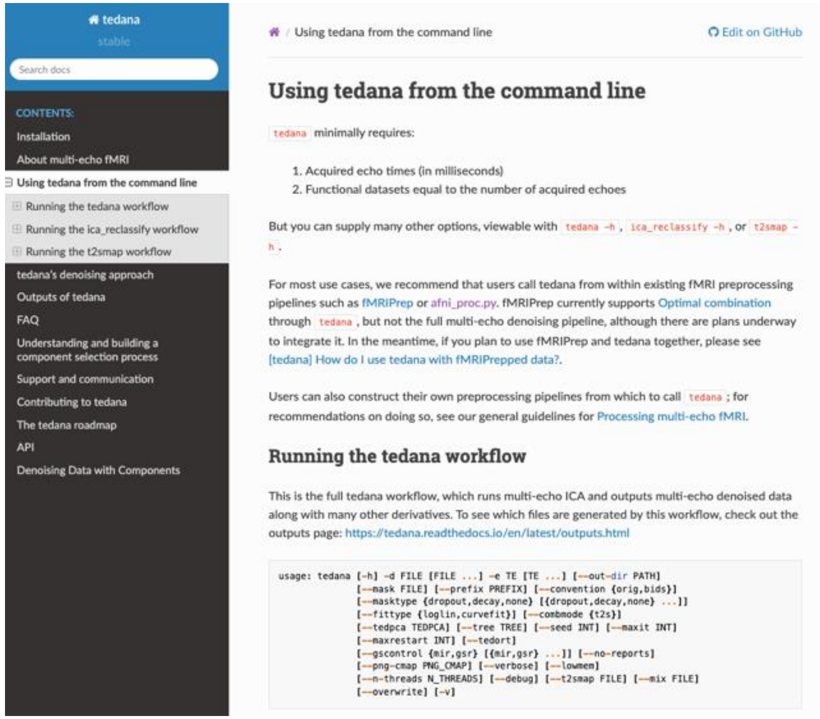

E-BOOK

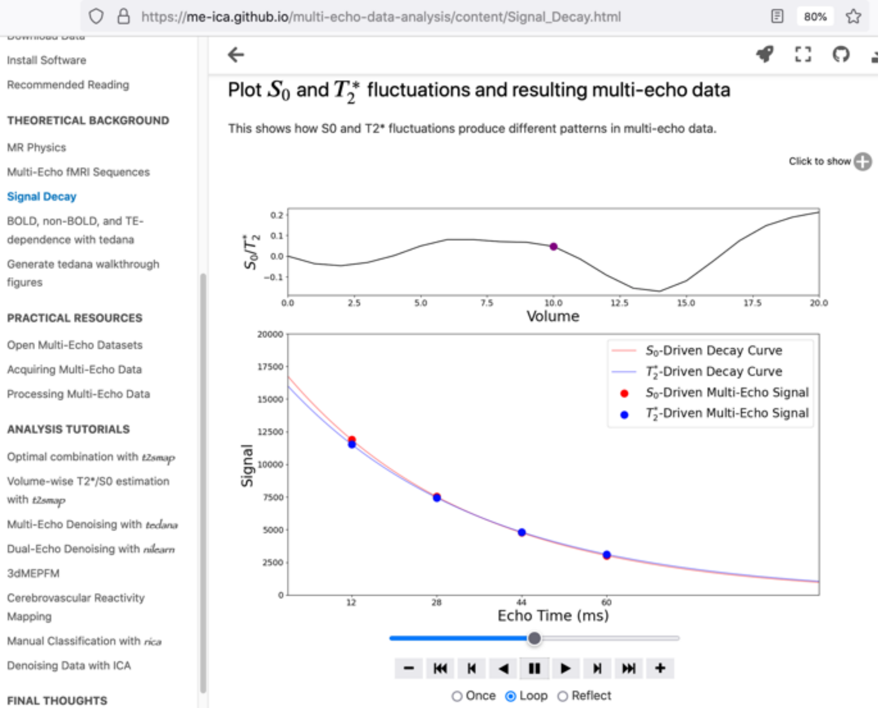

Active Discussion Board

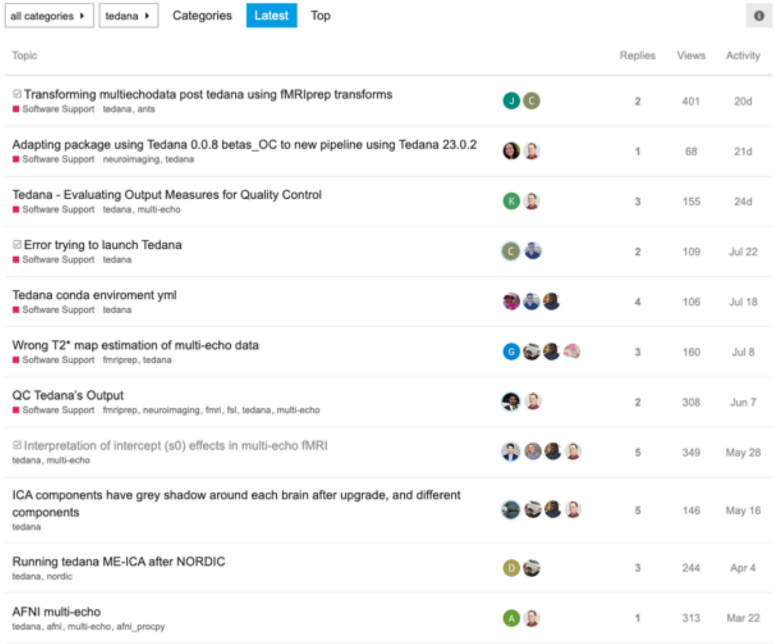

ME-ICA Decision Tree

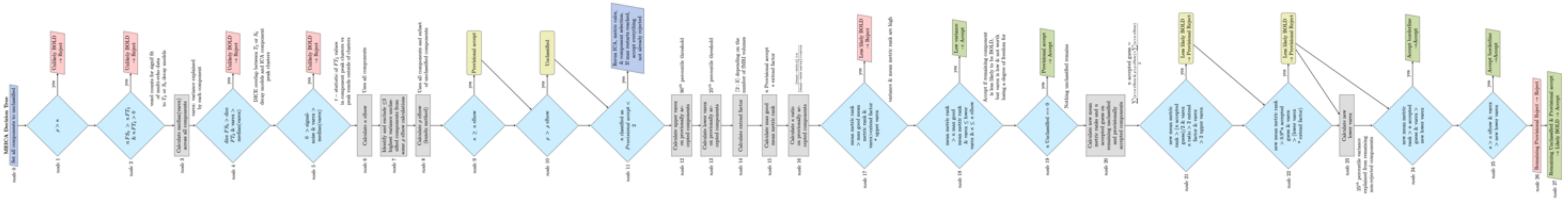

tedana Decision Tree

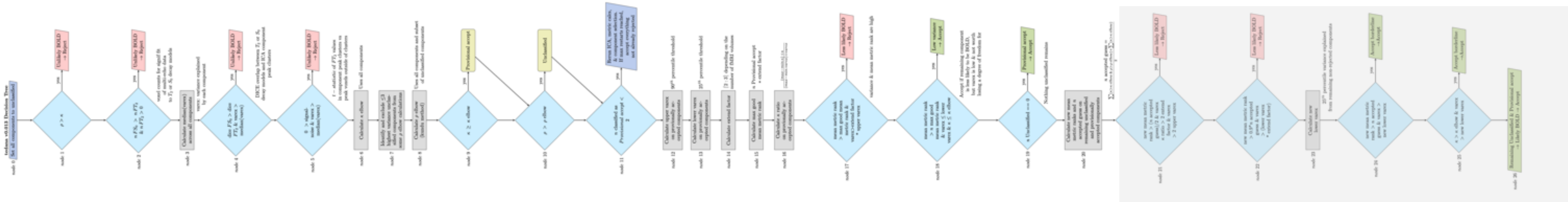

Minimal Decision Tree

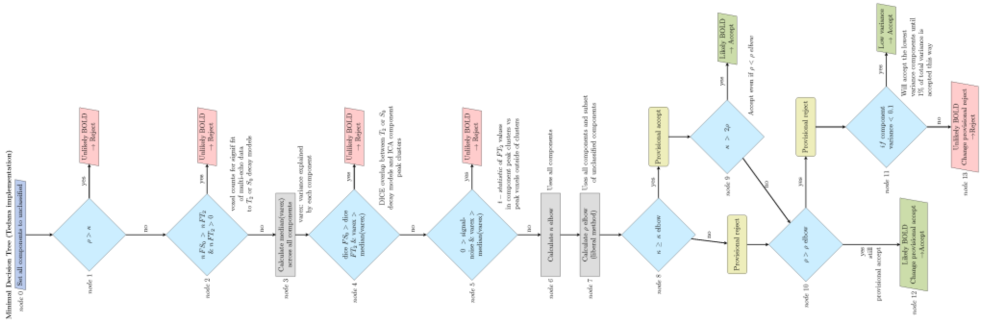

Built your own decision tree

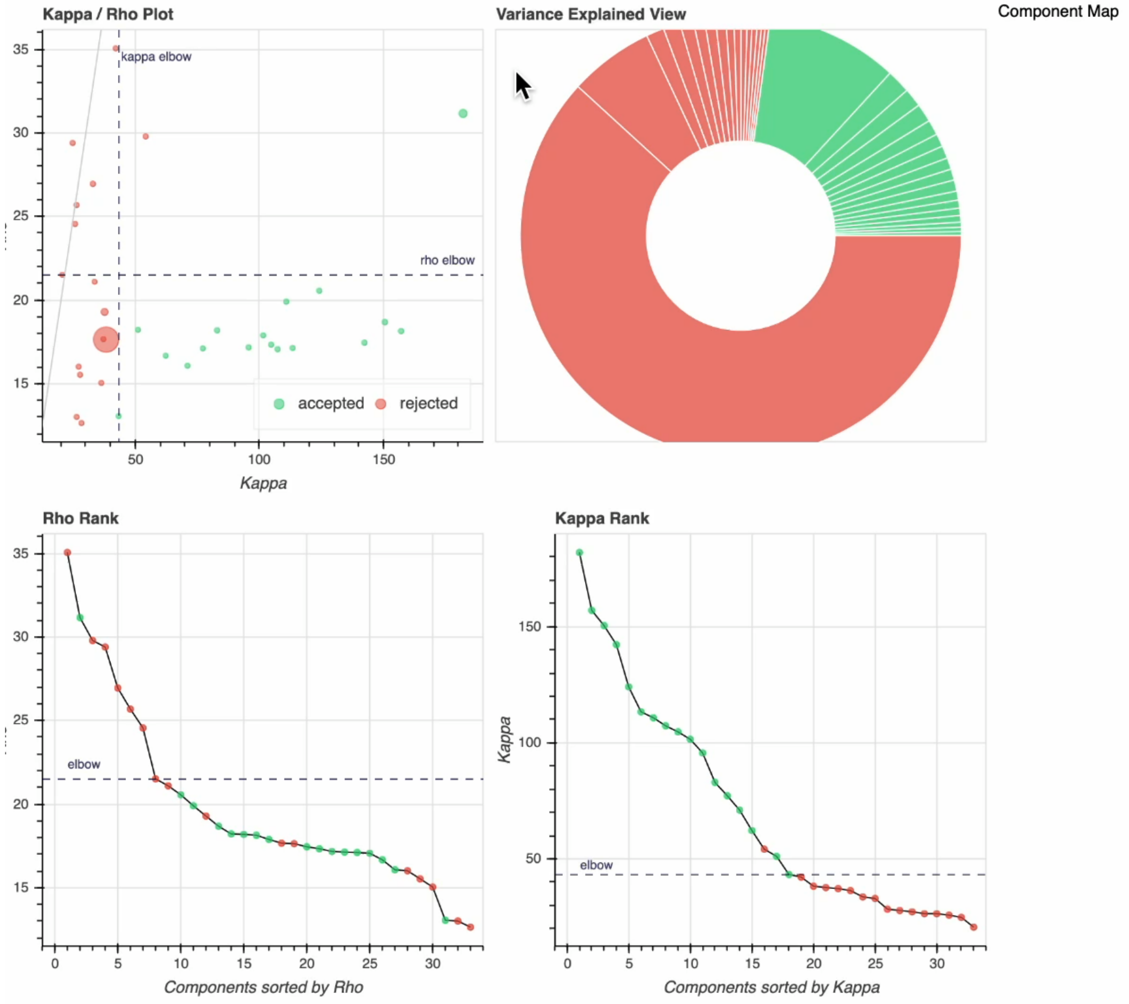
Kappa / Rho Plot
kappa elbow
rho elbow
accepted
rejected
Kappa
Variance Explained View
Component Map
Rho Rank
elbow
Components sorted by Rho
Kappa Rank
Kappa
elbow
Components sorted by Kappa

ME-based Hemodynamic Deconvolution

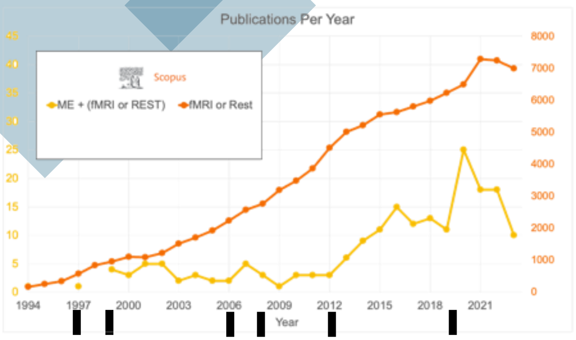

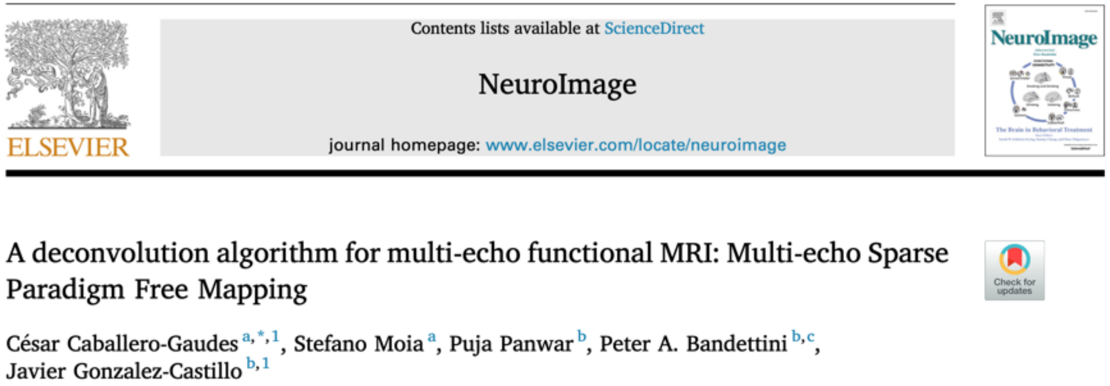

Contents lists available at ScienceDirect
NeuroImage
journal homepage: www.elsevier.com/locate/neuroimage

A deconvolution algorithm for multi-echo functional MRI: Multi-echo Sparse Paradigm Free Mapping

César Caballero-Gaudes [a,*,1], Stefano Moia [a], Puja Panwar [b], Peter A. Bandettini [b,c], Javier Gonzalez-Castillo [b,1]

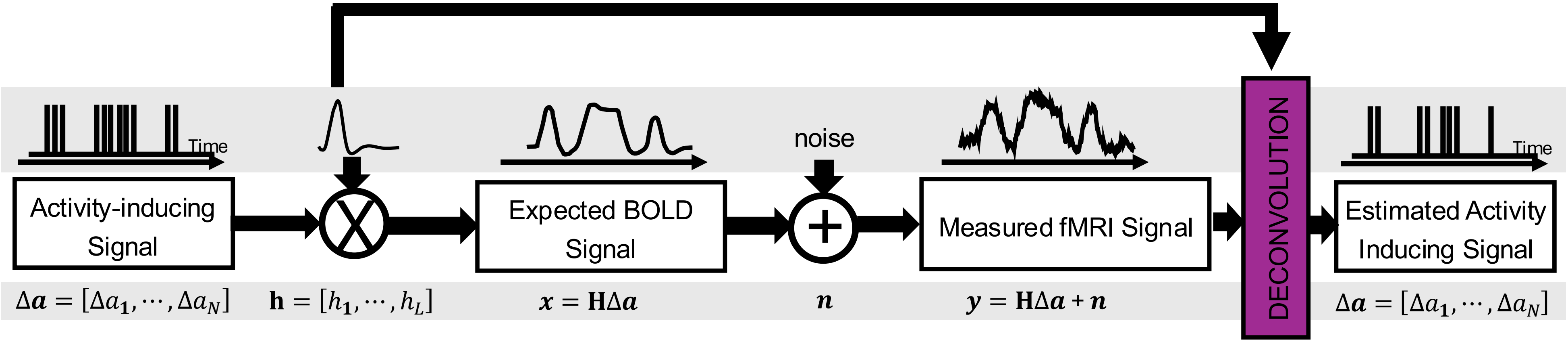

If one assumes the underlying activity-inducing signal to consist of brief, sparse events, then the formulated deconvolution problem can be solved using LASSO regularization:

$$\Delta\hat{\boldsymbol{a}} = \arg\min_{\Delta\boldsymbol{a}} \overbrace{\frac{1}{2}\|\boldsymbol{y} - \mathbf{H}\Delta\boldsymbol{a}\|_2^2}^{\text{Error Minimization Term}} + \underbrace{\lambda\|\Delta\boldsymbol{a}\|_1}_{\text{L1-Norm Regularization (Sparseness)}}$$

Single Echo Sparse Free Paradigm Mapping Algorithm

3dPFM

ME-based Hemodynamic Deconvolution

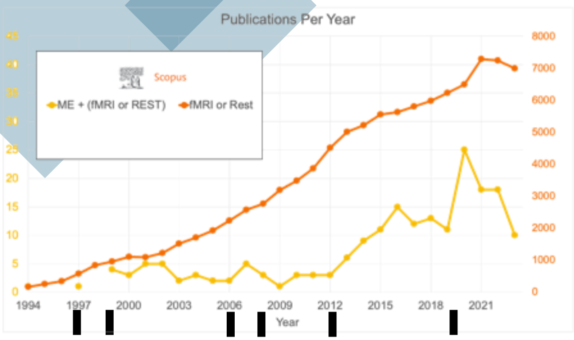

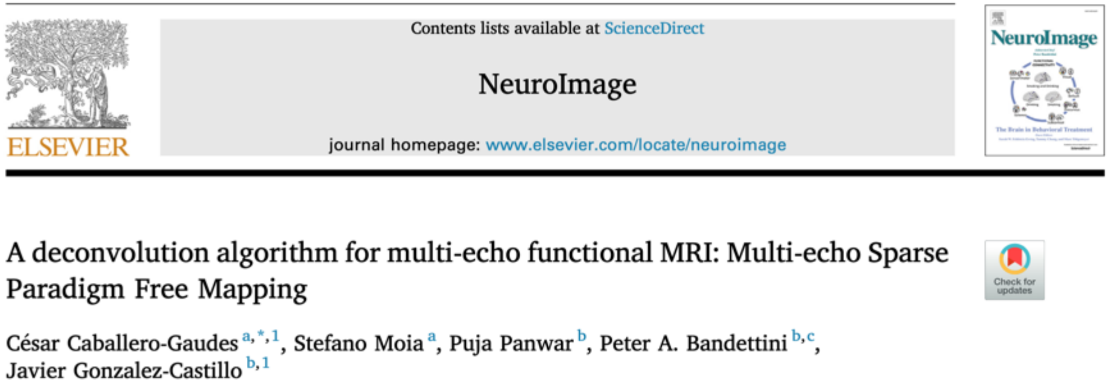

Contents lists available at ScienceDirect

NeuroImage

journal homepage: www.elsevier.com/locate/neuroimage

A deconvolution algorithm for multi-echo functional MRI: Multi-echo Sparse Paradigm Free Mapping

César Caballero-Gaudes[a,*,1], Stefano Moia[a], Puja Panwar[b], Peter A. Bandettini[b,c], Javier Gonzalez-Castillo[b,1]

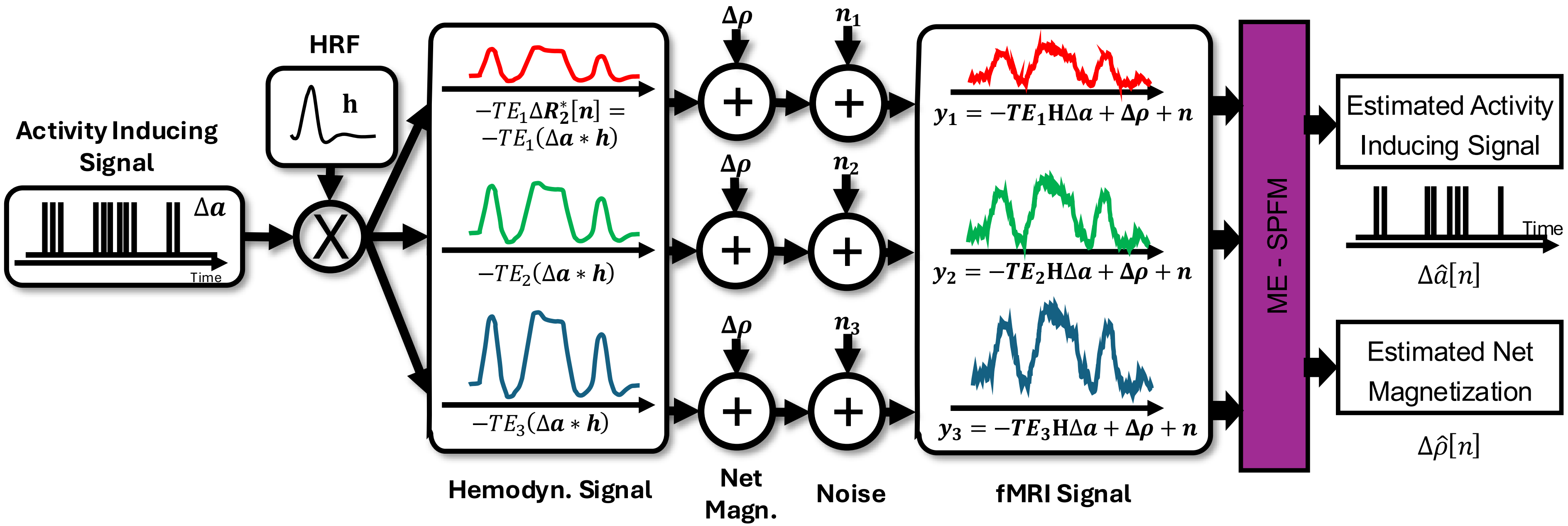

$$\bar{\boldsymbol{y}} \overset{\text{def}}{=} \begin{bmatrix} \boldsymbol{y}_1 \\ \vdots \\ \boldsymbol{y}_K \end{bmatrix} = \underbrace{\boxed{\begin{bmatrix} \mathbf{I} \\ \vdots \\ \mathbf{I} \end{bmatrix}}}_{\bar{\mathbf{I}}} \boldsymbol{\Delta\rho} - \underbrace{\boxed{\begin{bmatrix} TE_1\mathbf{H} \\ \vdots \\ TE_K\mathbf{H} \end{bmatrix}}}_{\bar{\mathbf{H}}} \boldsymbol{\Delta a}$$

Assuming sparsity in both unknowns, we can solve using LASSO regularization

$$\Delta\hat{\boldsymbol{a}}, \Delta\hat{\boldsymbol{\rho}} = \arg\min_{\Delta\boldsymbol{a},\Delta\boldsymbol{\rho}} \frac{1}{2}\|\bar{\boldsymbol{y}} - \bar{\mathbf{H}}\Delta\boldsymbol{a} - \bar{\mathbf{I}}\Delta\boldsymbol{\rho}\|_2^2 + \lambda_1\|\Delta\boldsymbol{a}\|_1 + \lambda_2\|\Delta\boldsymbol{\rho}\|_1$$

ME-based Hemodynamic Deconvolution

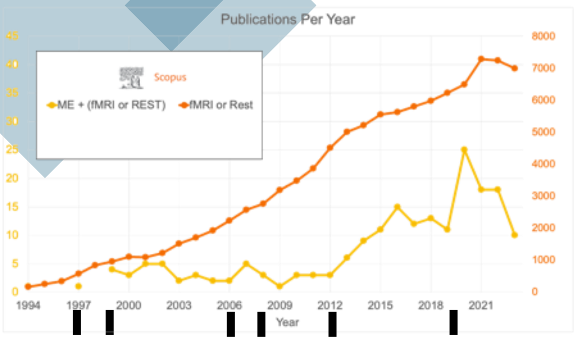

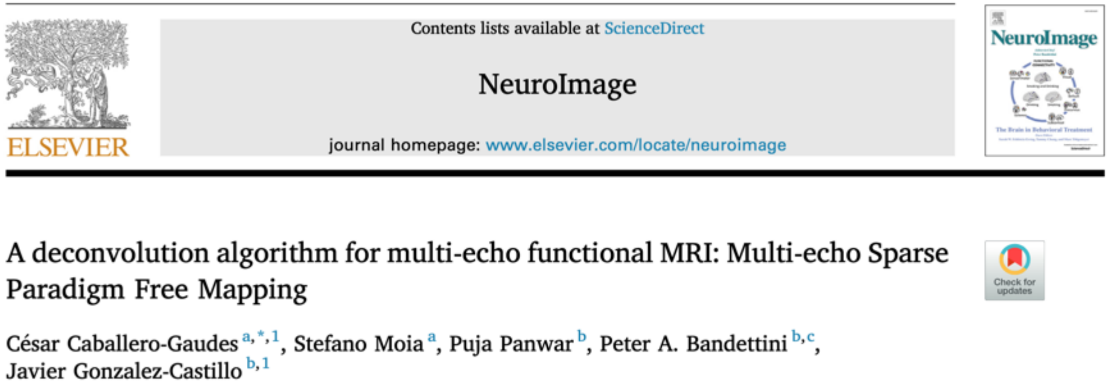
Contents lists available at ScienceDirect

NeuroImage

journal homepage: www.elsevier.com/locate/neuroimage

ELSEVIER

A deconvolution algorithm for multi-echo functional MRI: Multi-echo Sparse Paradigm Free Mapping

César Caballero-Gaudes [a,*,1], Stefano Moia [a], Puja Panwar [b], Peter A. Bandettini [b,c], Javier Gonzalez-Castillo [b,1]

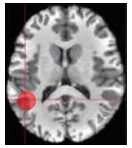

READ THIS

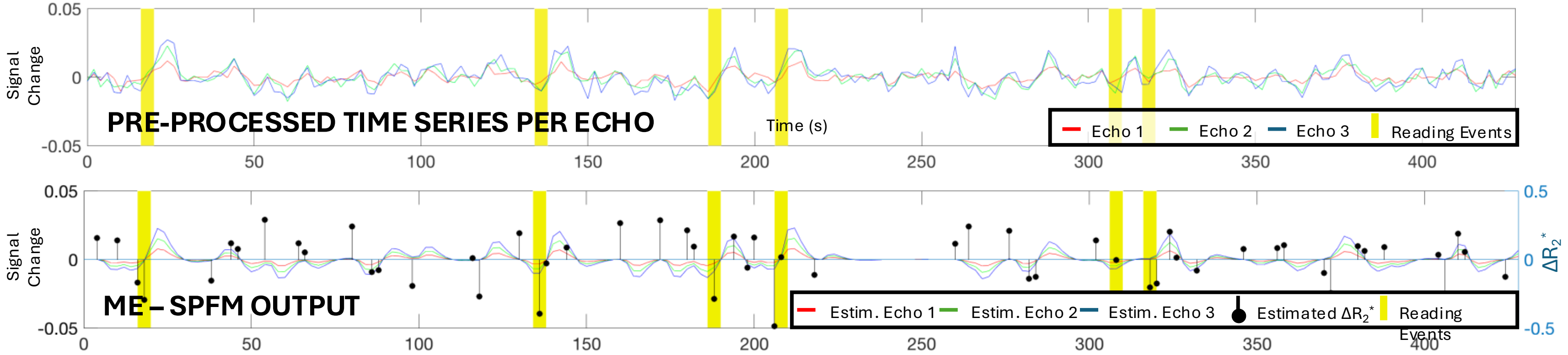

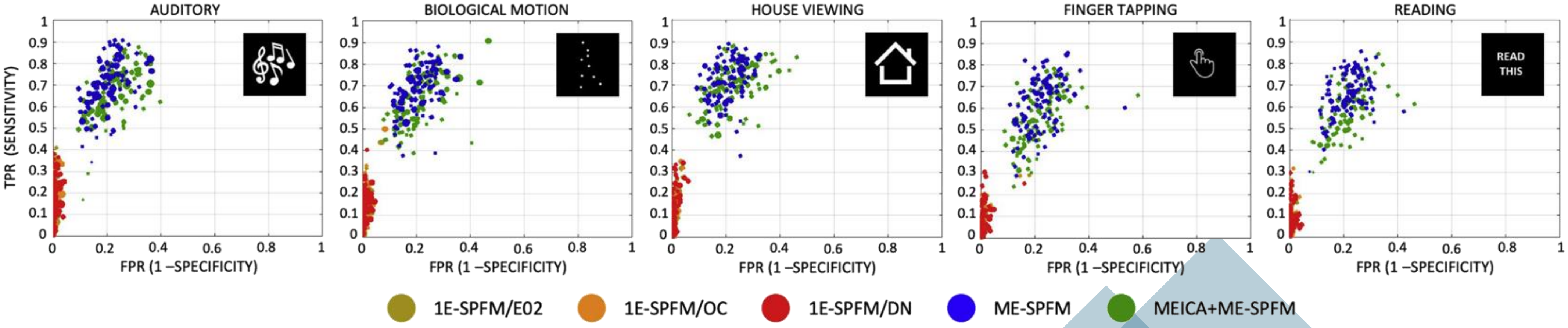

Agenda

- ❑ Why should we consider Multi-Echo acquisitions when doing fMRI experiments?

- ❑ Proposed analytical approaches for Multi-Echo fMRI Data? (timeline)

    - ❑ T2* Fit
    - ❑ Dual Echo
    - ❑ Weighted Combination of Echoes
    - ❑ Multi-Echo ICA-based Denoising
    - ❑ Multi-Echo Deconvolution

- ❑ **Success stories**

- ❑ Status of Multi-Echo fMRI Adoption

- ❑ What can faster gradients do for ME-fMRI?

- ❑ Conclusions

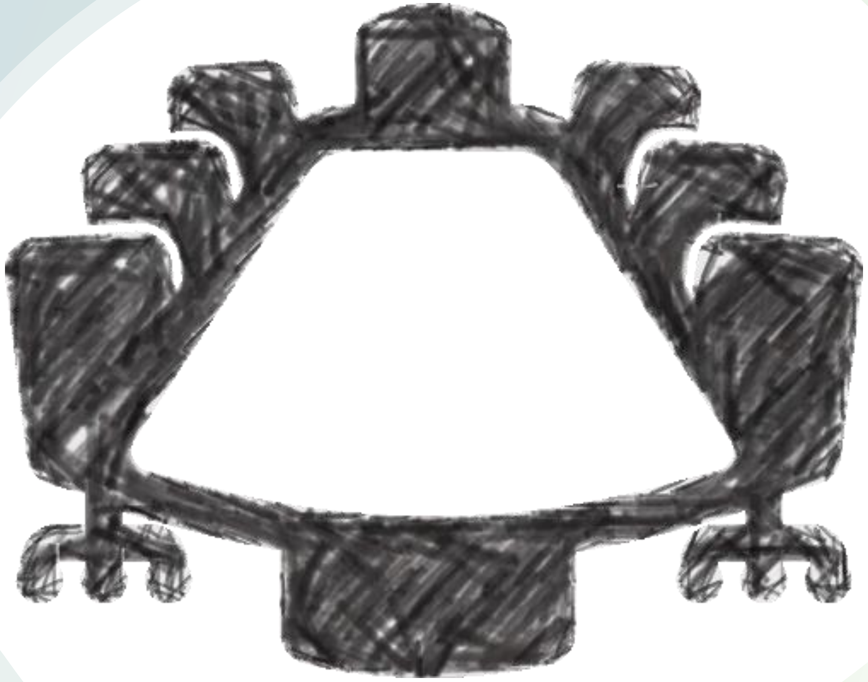

ME-ICA/tedana can: also be applied to animal models at ultra high field

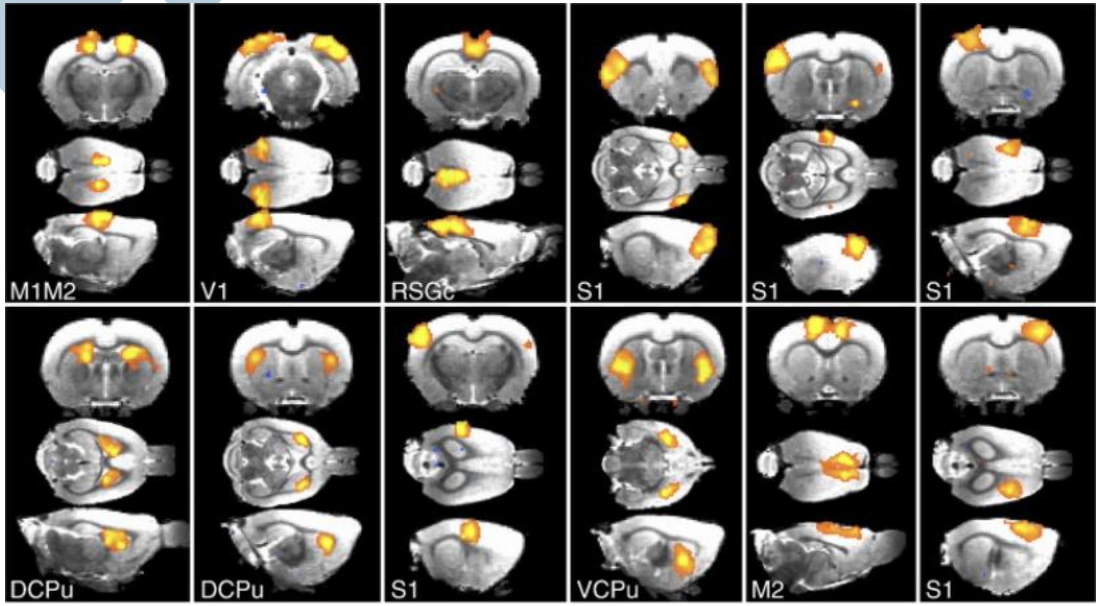

Top 12 κ components

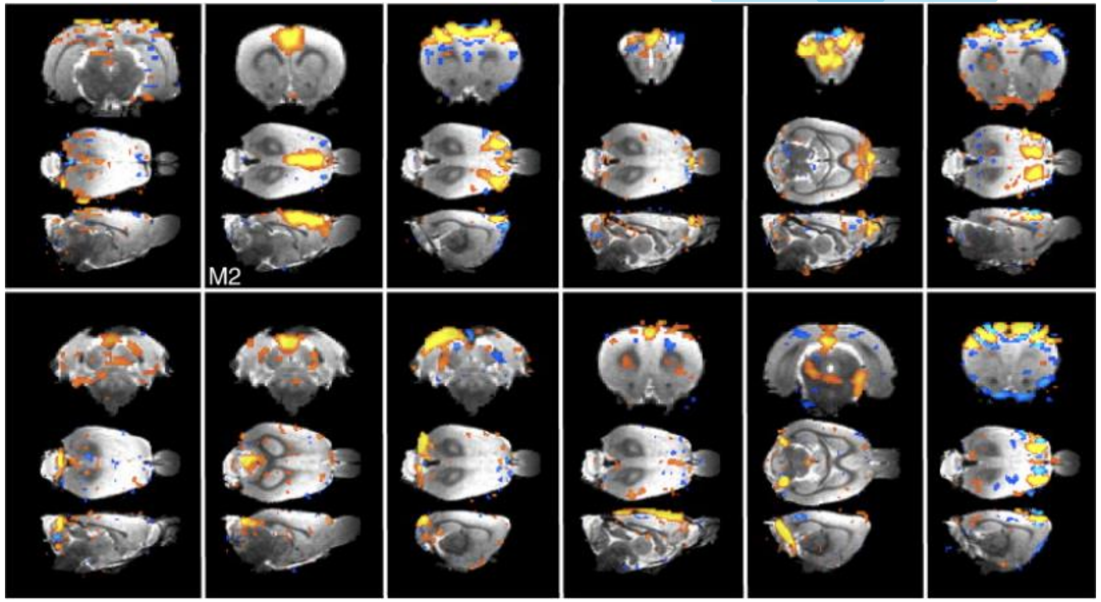

Top 12 Variance-Explained components

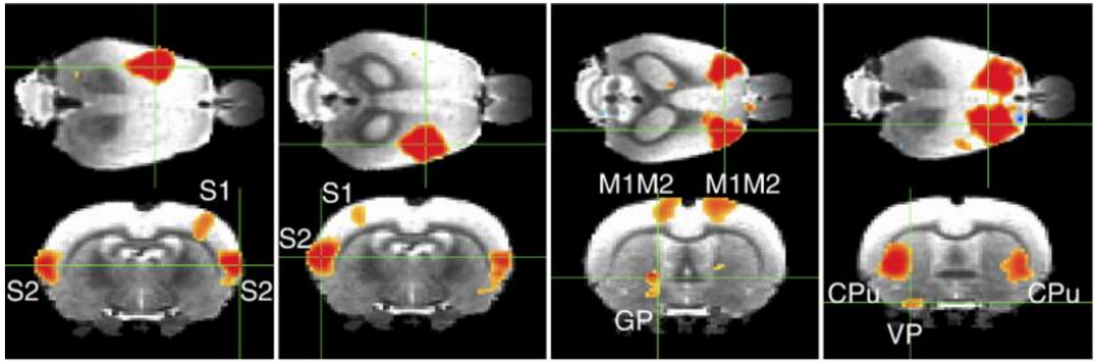

Individual Rat Seed Based Connectivity Maps

Kundu et al. “Differentiating BOLD and non-BOLD signals in fMRI time series from anesthetized rats using multi-echo EPI at 11.7T” NeuroImage (2014)

ME-ICA/tedana can: reliably map subject-level functional connectomes with less scan time

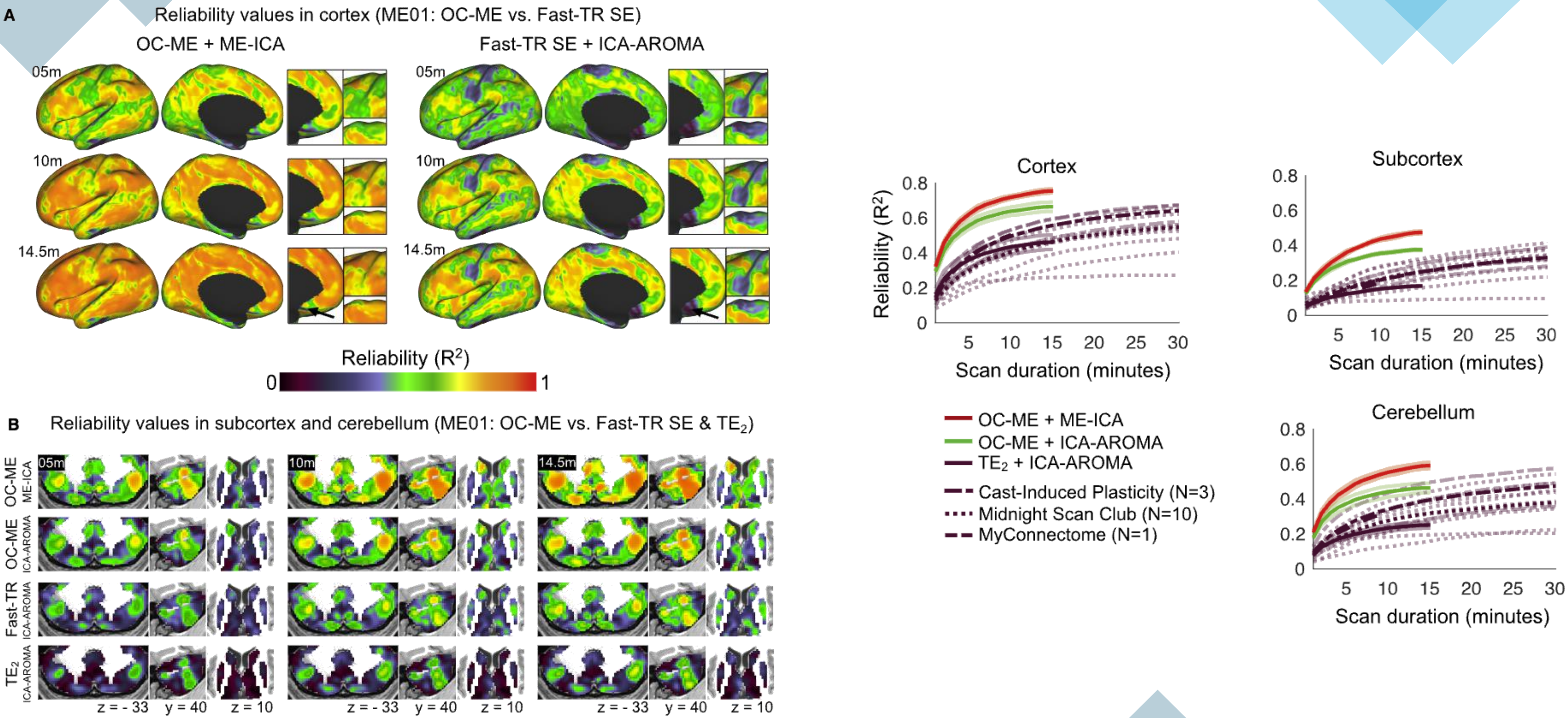

Lynch et al. "Rapid Precision Functional Mapping of Individuals using multi-echo fMRI" Cell Reports (2020)

ME-ICA/tedana can: help study the basal forebrain

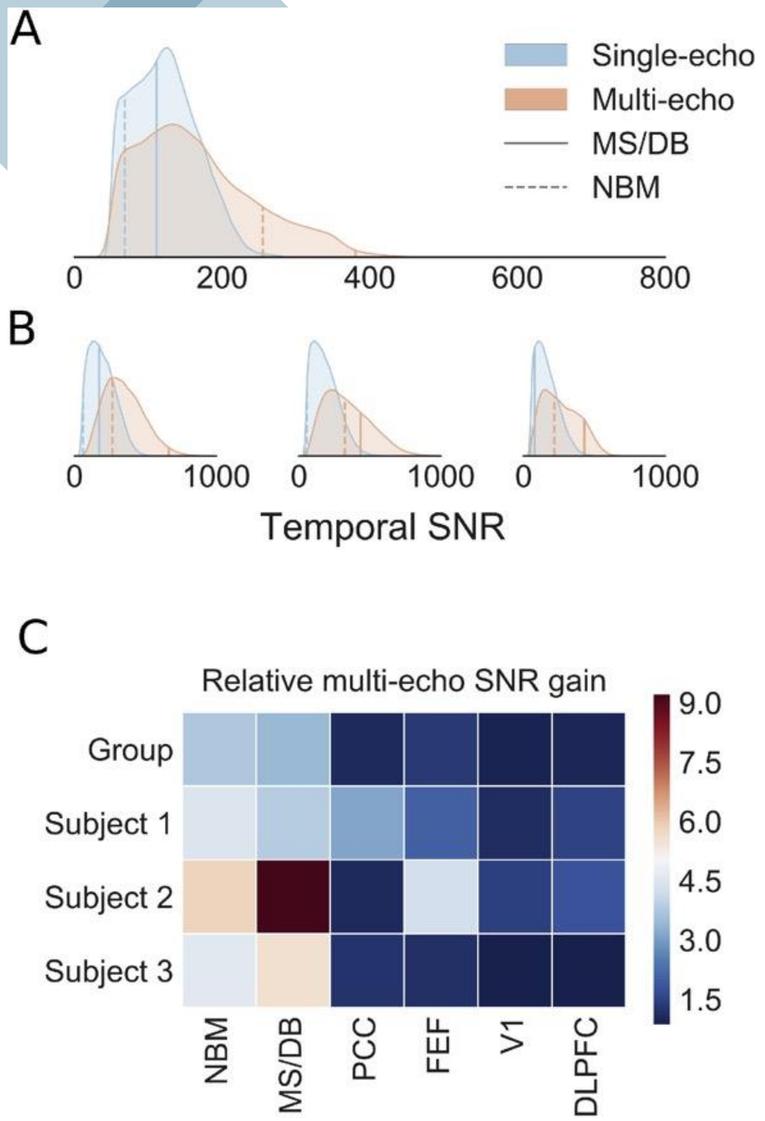

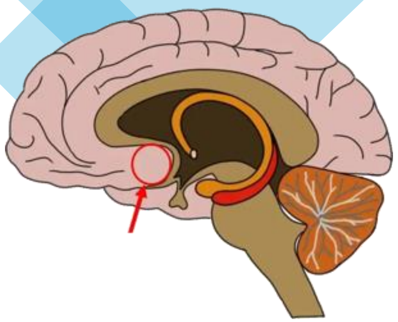

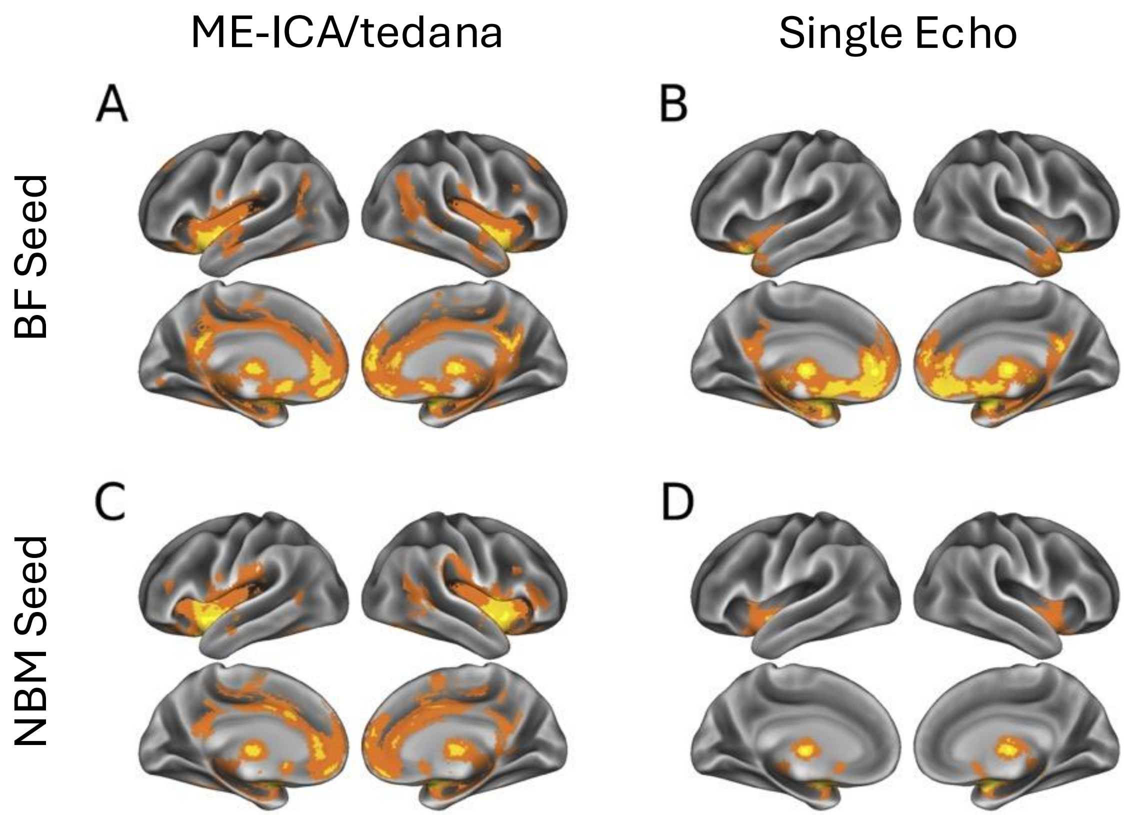

Nucleus Basalis of Meynert (NBM) | Ch 4
Medial Septum/Diagonal band of Broca (MS/DB) | Ch1-3

Markello et al. "Segregation of the human basal forebrain using resting-state functional MRI" NeuroImage (2018)

ME-ICA/tedana can: help study olfactory responses

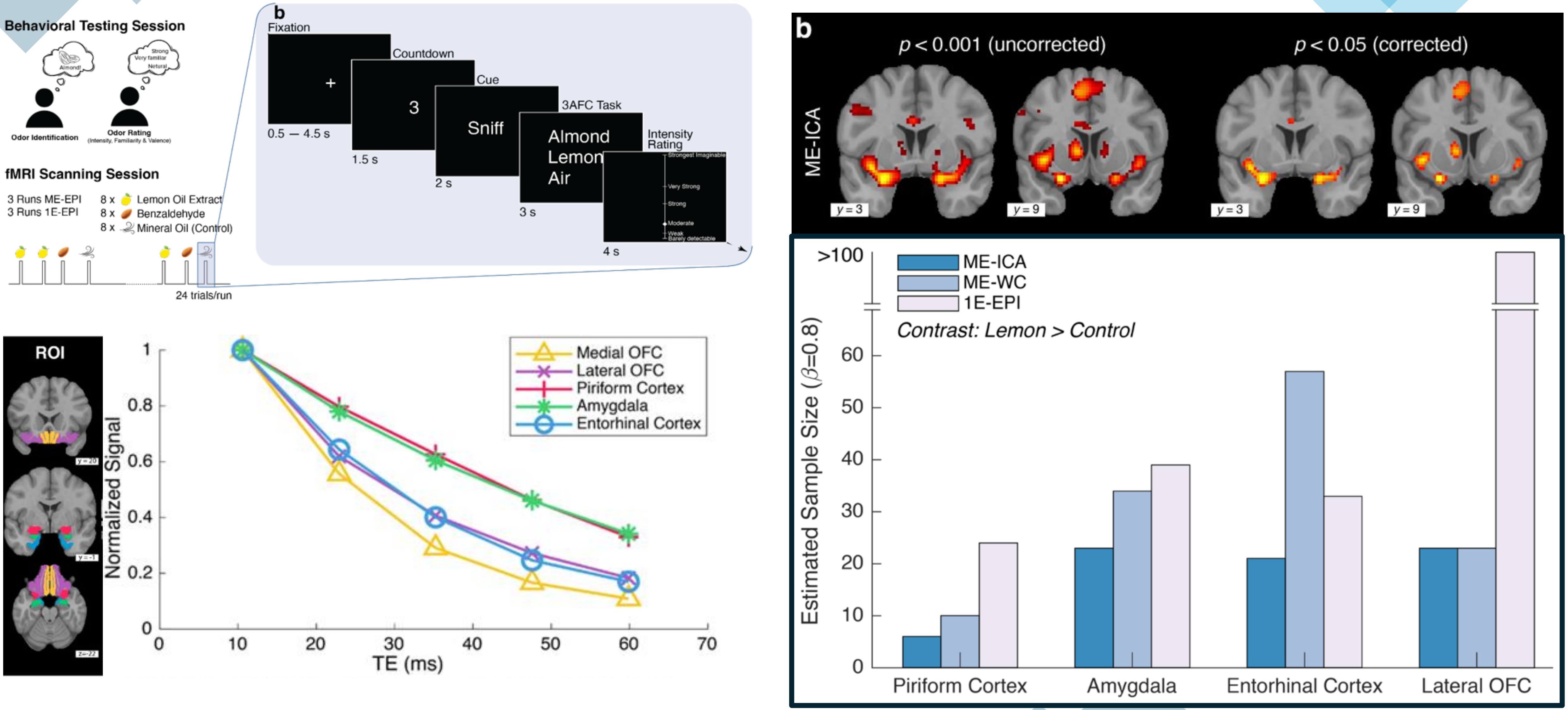

Zhao et al. "Leveraging Multi-Echo EPI to Enhance BOLD Sensitivity in Task-based Olfactory fMRI" BioRxiv (2024)

ME-ICA/tedana can: improve brain association studies

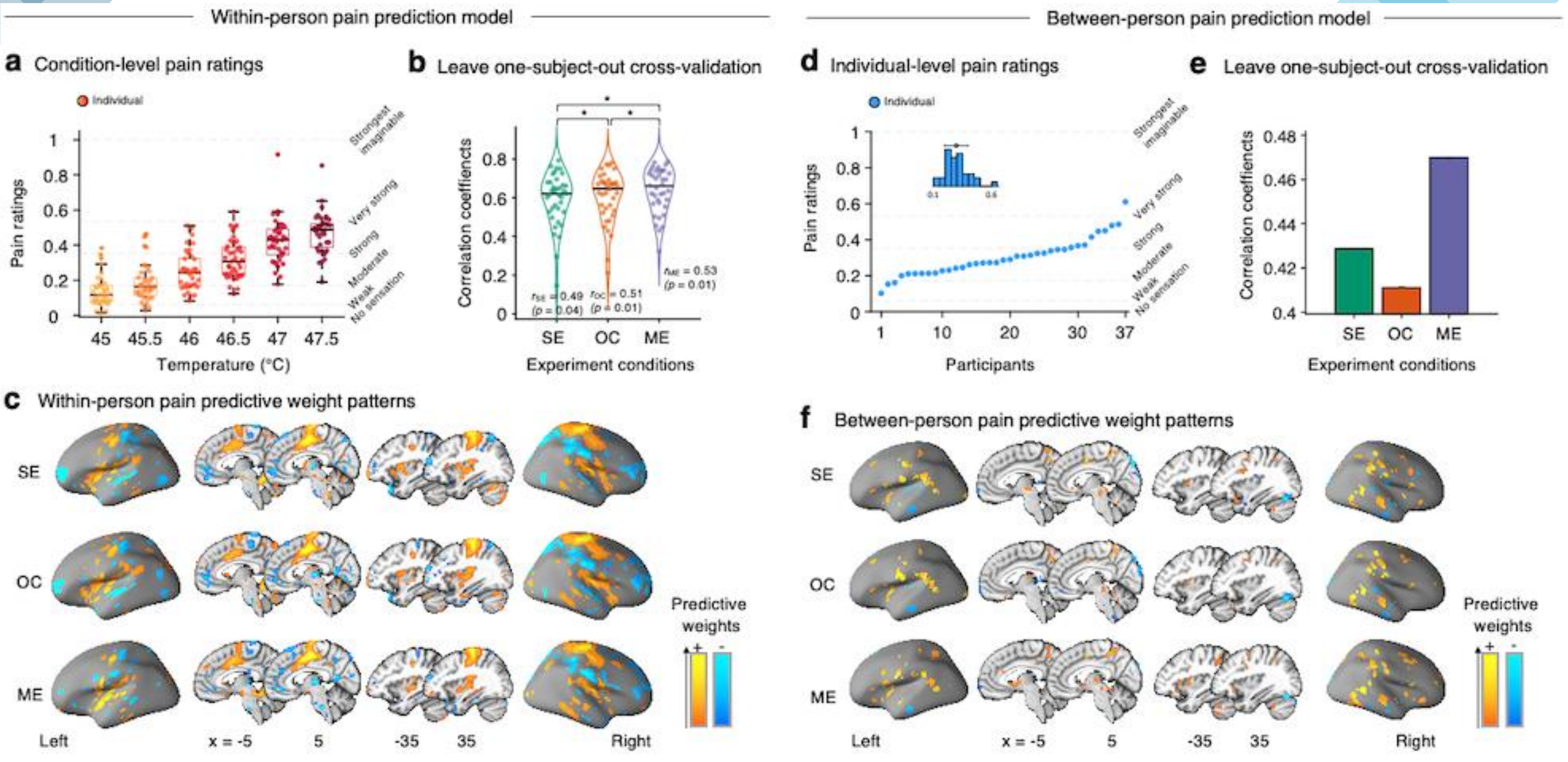

Jung et al. “Improved performance of within- and between-individual pain prediction using multi-echo fMRI” OHBM (2024)

ME-ICA/tedana can: improve reliability of population perceptive field mapping

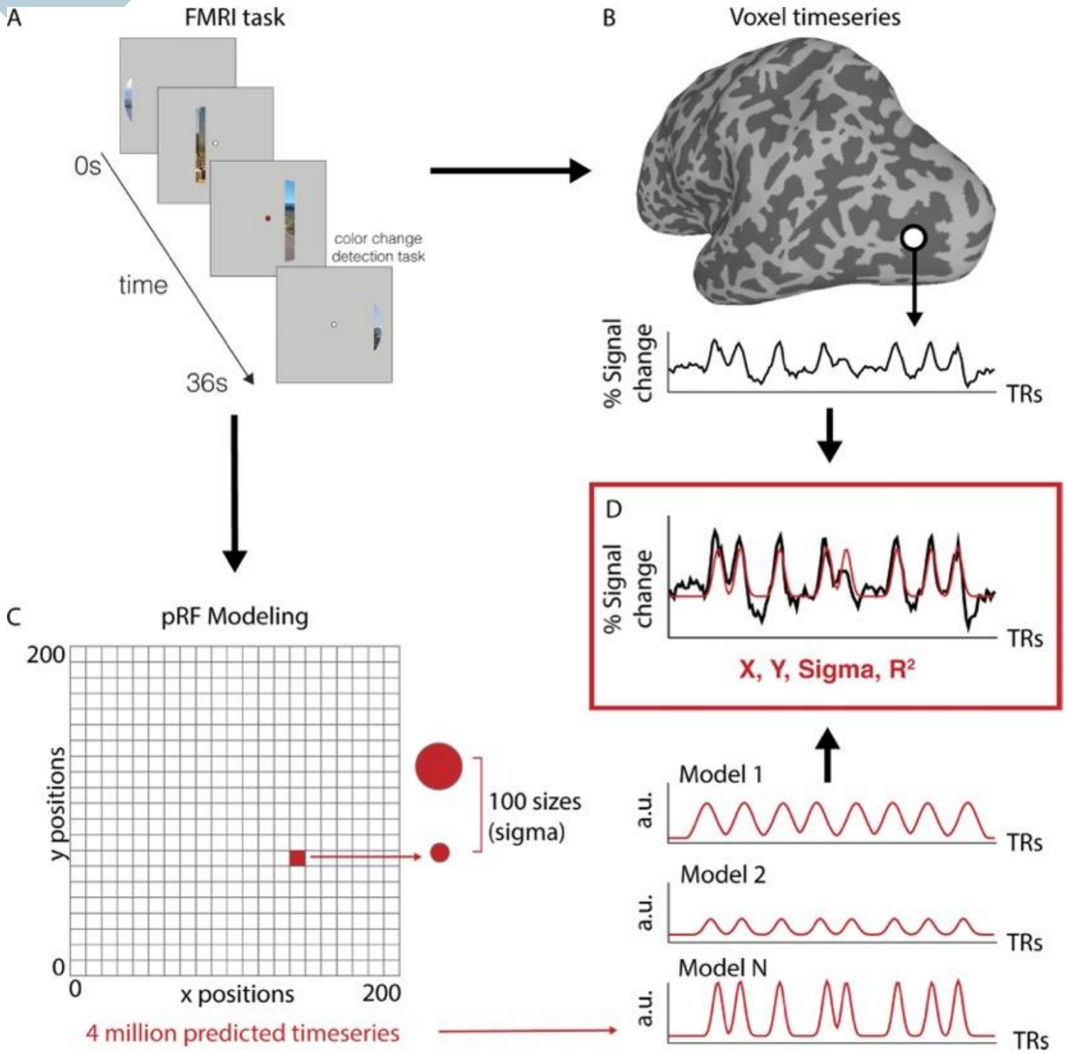

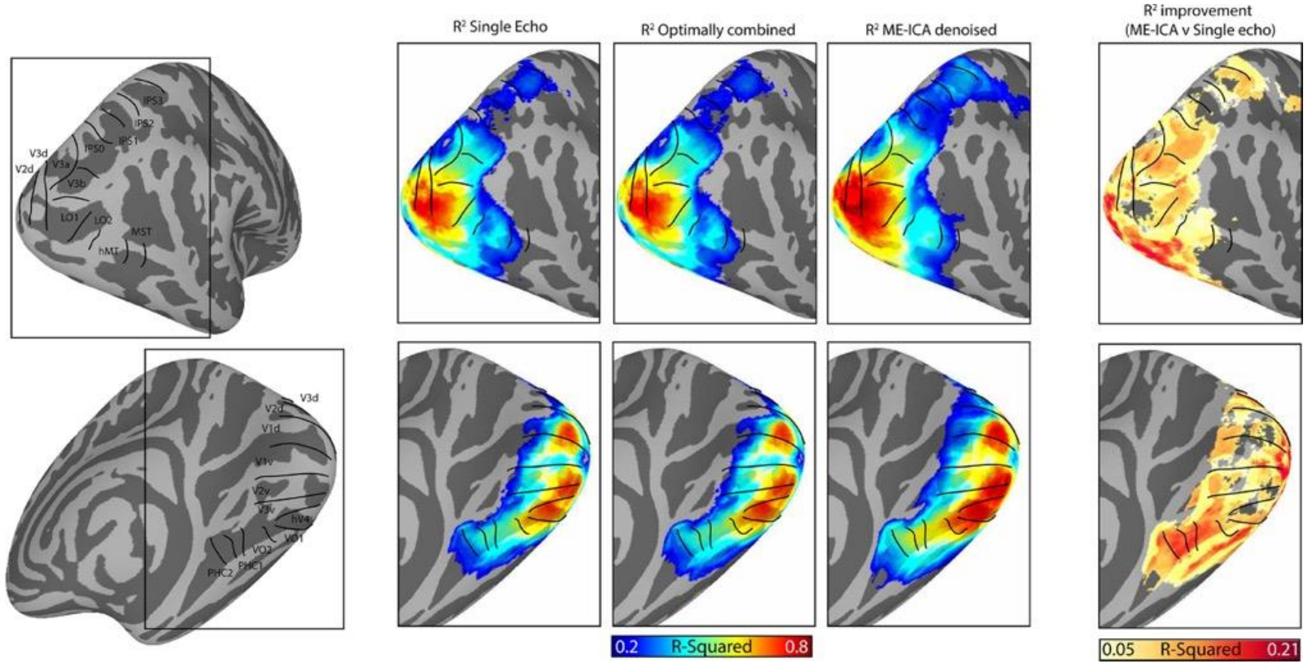

Up to 21% Improvement in model fit

Steel A. et al. "Evaluating the efficacy of multi-echo ICA denoising on model-based fMRI" NeuroImage (2022)

ME-ICA/tedana can: improve reliability of population receptive field mapping

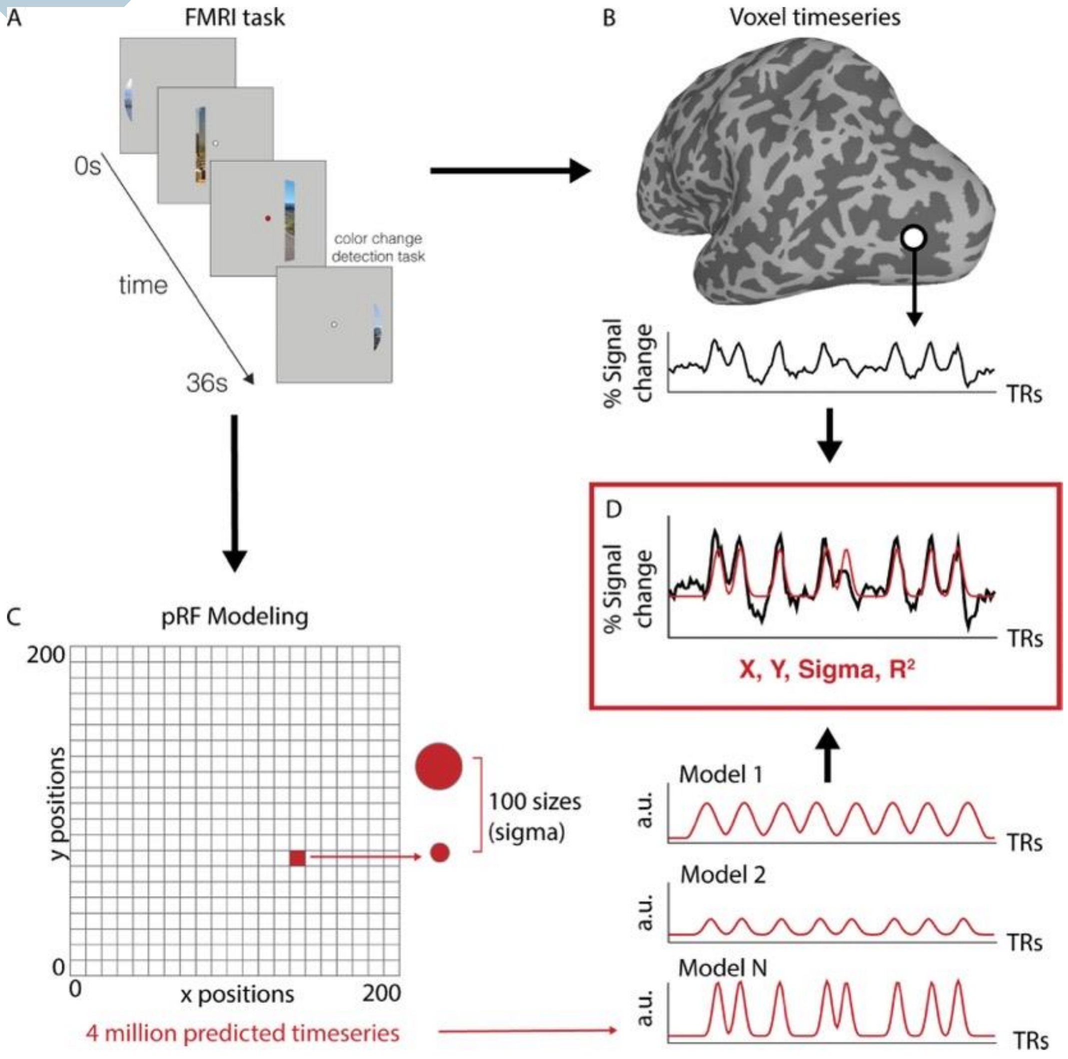

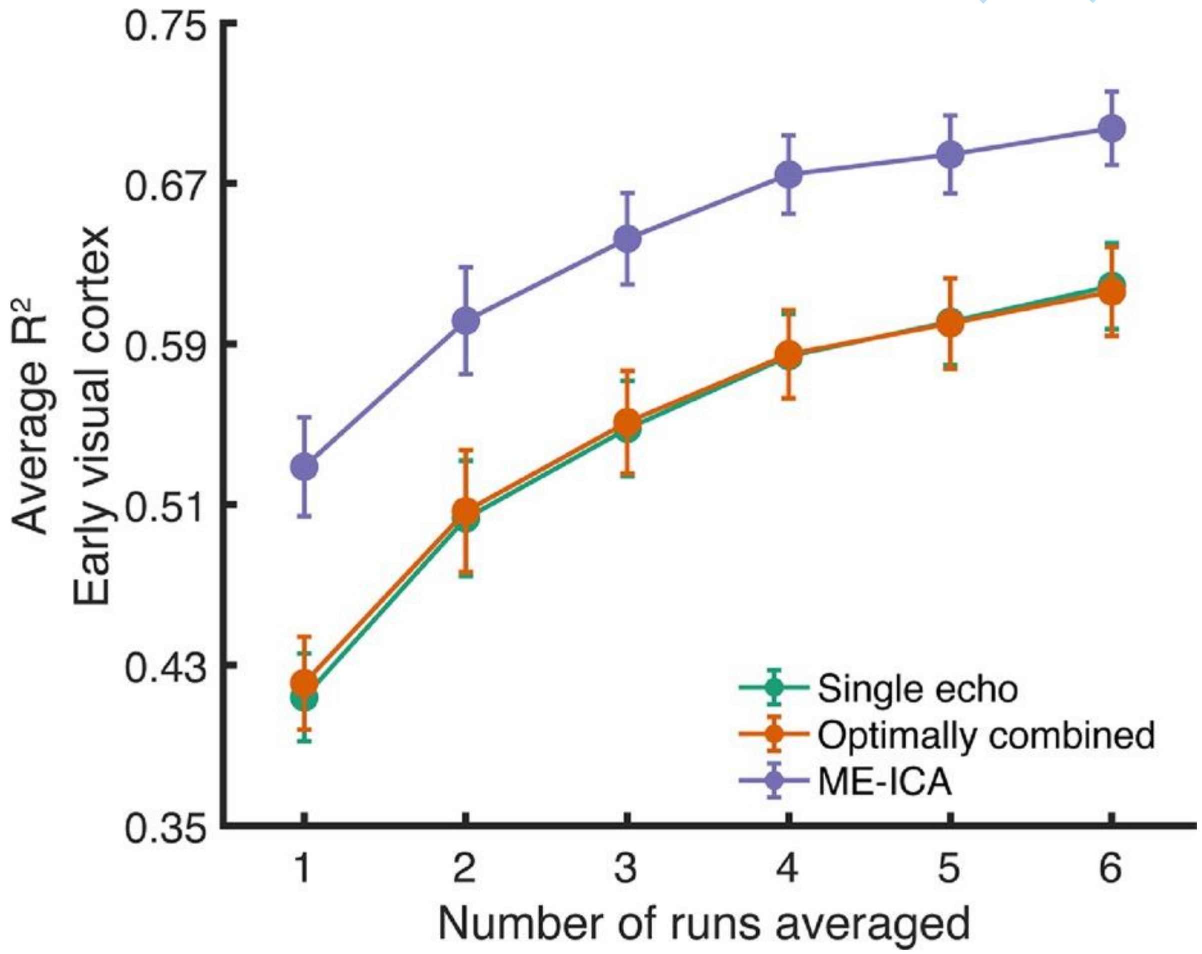

Steel A. et al. "Evaluating the efficacy of multi-echo ICA denoising on model-based fMRI" NeuroImage (2022)

ME-ICA/tedana can: help study slow-changing processes

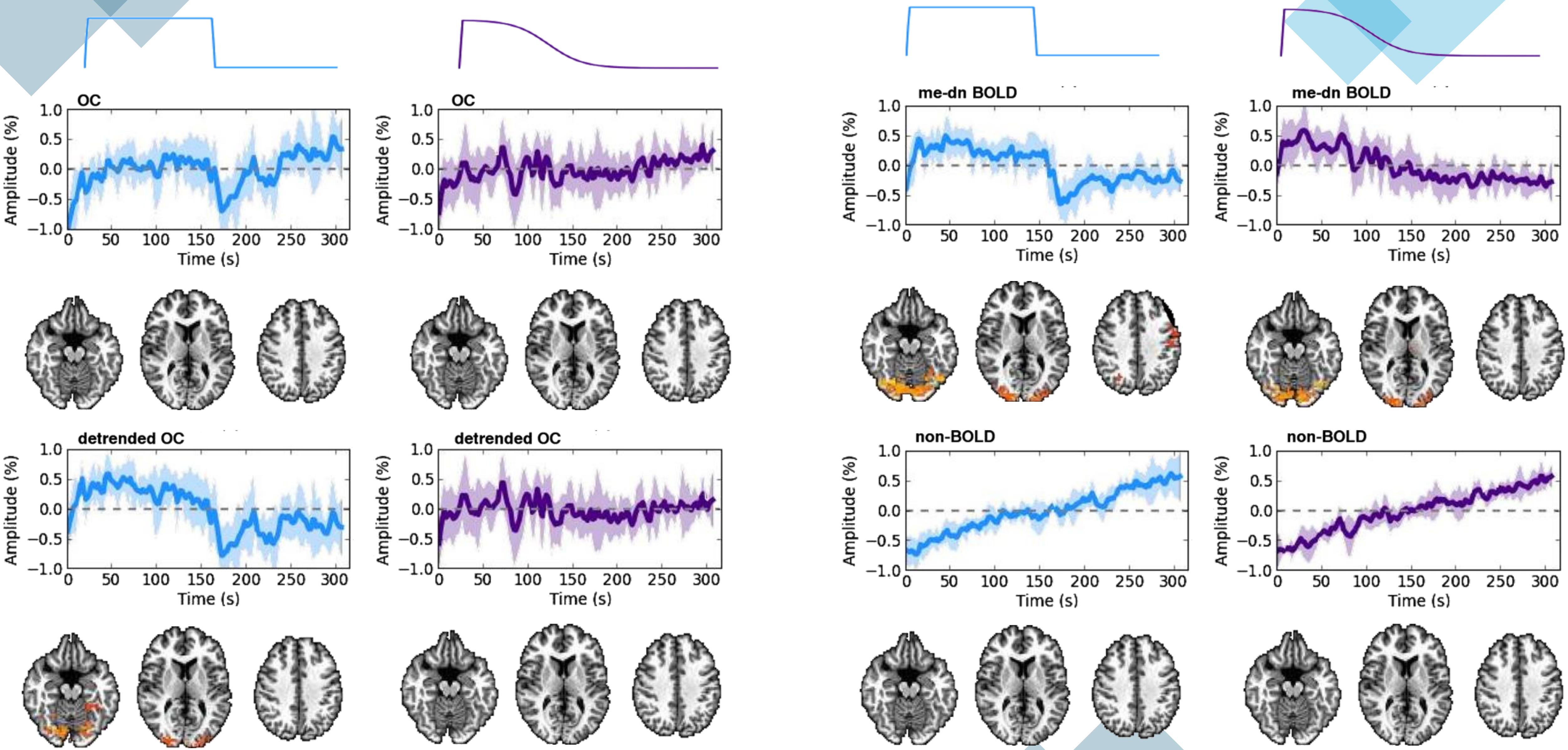

Evans et al. “Separating Slow BOLD from non-BOLD baseline using multi-echo fMRI” NeuroImage (2015)

ME-ICA/tedana can: help image the brainstem with cardiac gating imaging

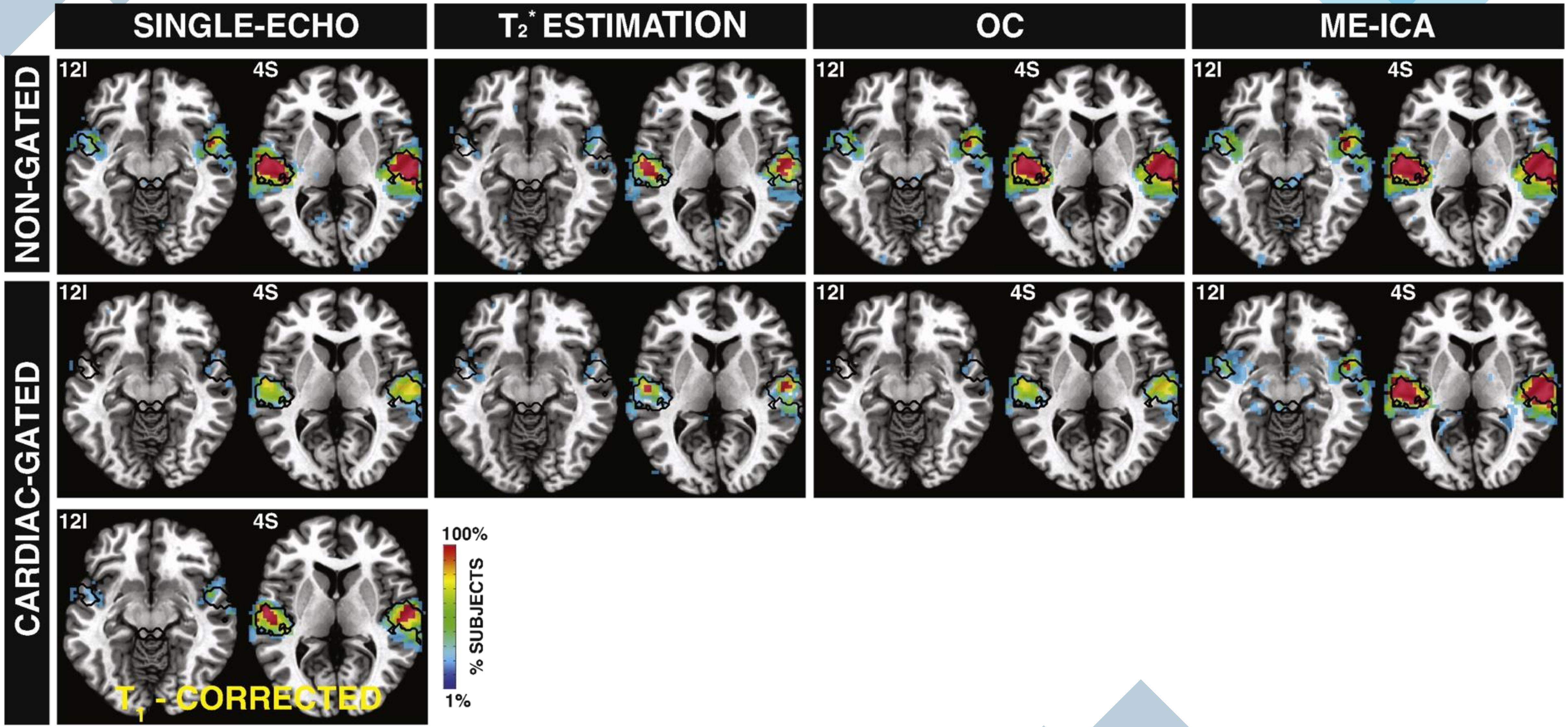

Gonzalez-Castillo et al. "Evaluation of multi-echo ICA denoising for task based fMRI studies: Block designs, rapid event-related designs and cardiac-gaited fMRI" NeuroImage (2016)

ME-ICA/tedana can: help image the brainstem with cardiac gating imaging

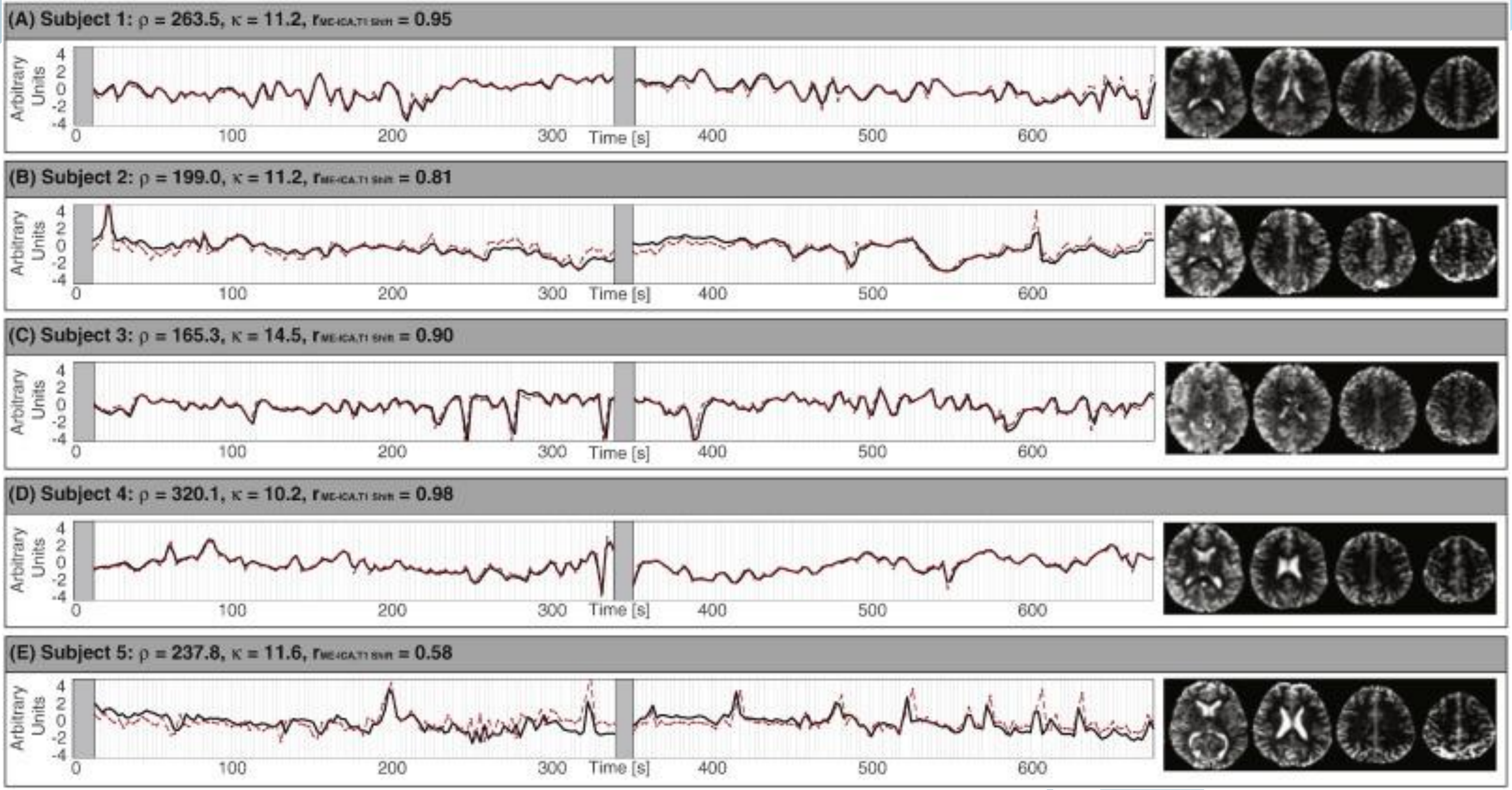

Gonzalez-Castillo et al. “Evaluation of multi-echo ICA denoising for task based fMRI studies: Block designs, rapid event-related designs and cardiac-gated fMRI” NeuroImage (2016)

ME-ICA/tedana can: improve quality of overt speech studies

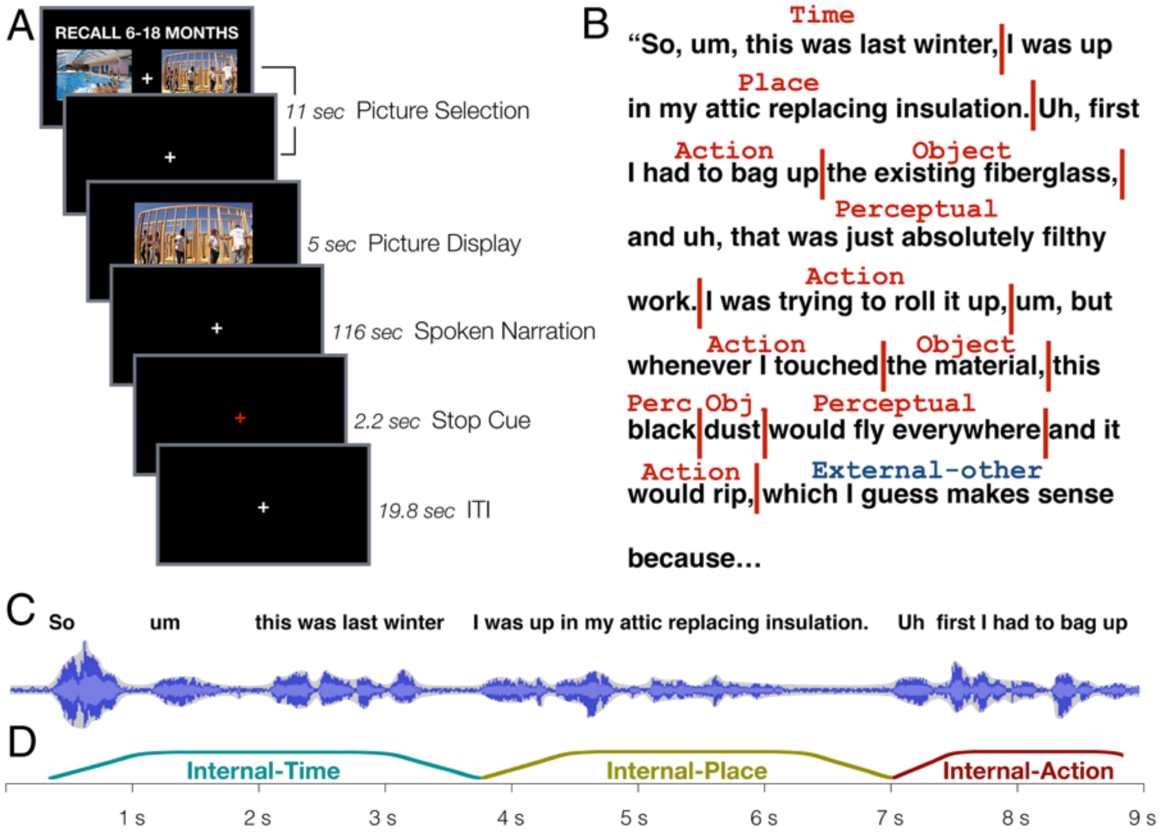

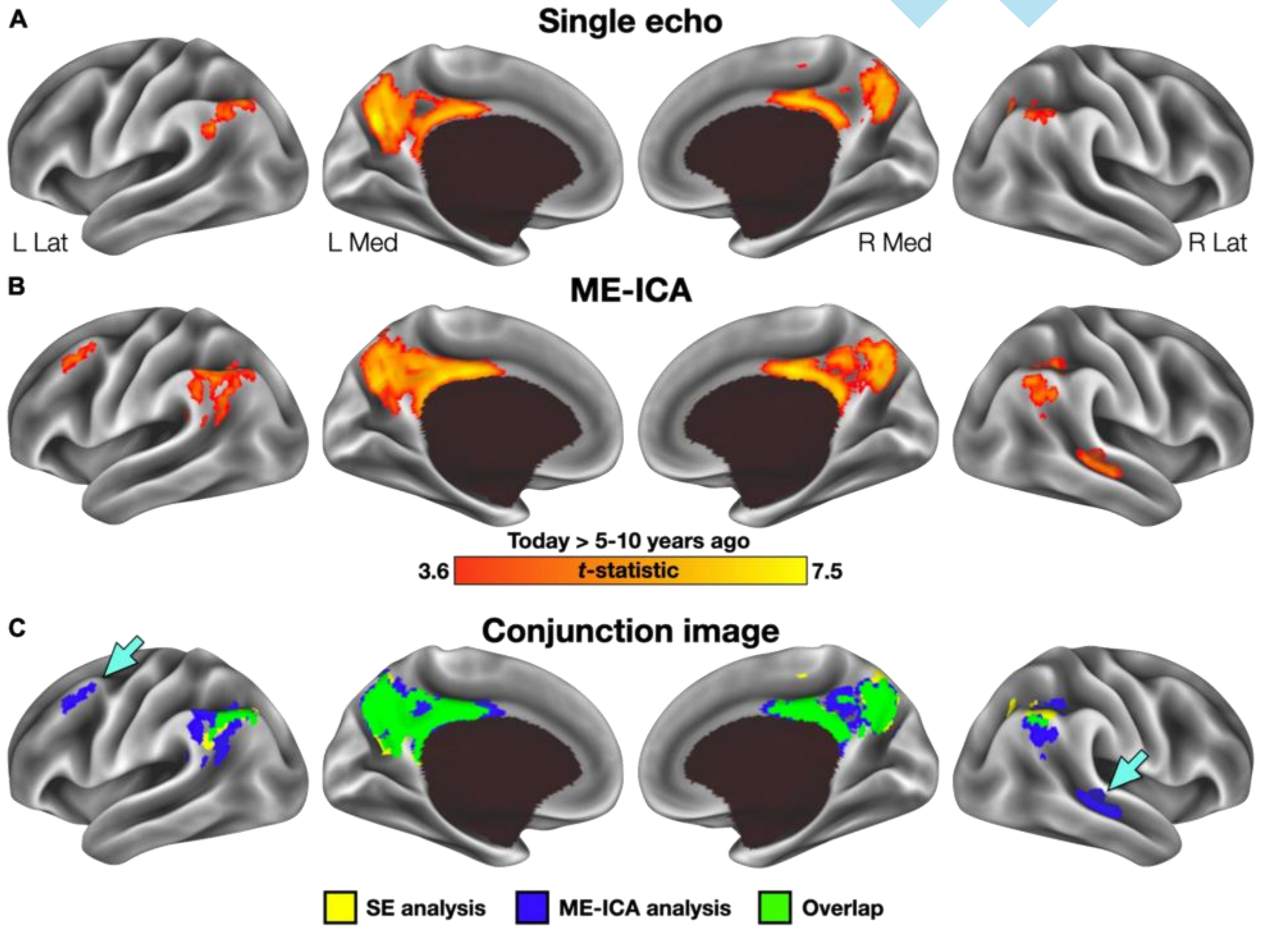

Gilmore et al. "A comparison of single- and multi-echo processing of fMRI Data during autobiographical recall" Front. Neurosc. (2022)

Agenda

- ❑ Why should we consider Multi-Echo acquisitions when doing fMRI experiments?
- ❑ Proposed analytical approaches for Multi-Echo fMRI Data? (timeline)
  - ❑ T2* Fit
  - ❑ Dual Echo
  - ❑ Weighted Combination of Echoes
  - ❑ Multi-Echo ICA-based Denoising
  - ❑ Multi-Echo Deconvolution
- ❑ Success stories
- ❑ **<u>Status of Multi-Echo fMRI Adoption</u>**
- ❑ What can faster gradients do for ME-fMRI?
- ❑ Conclusions

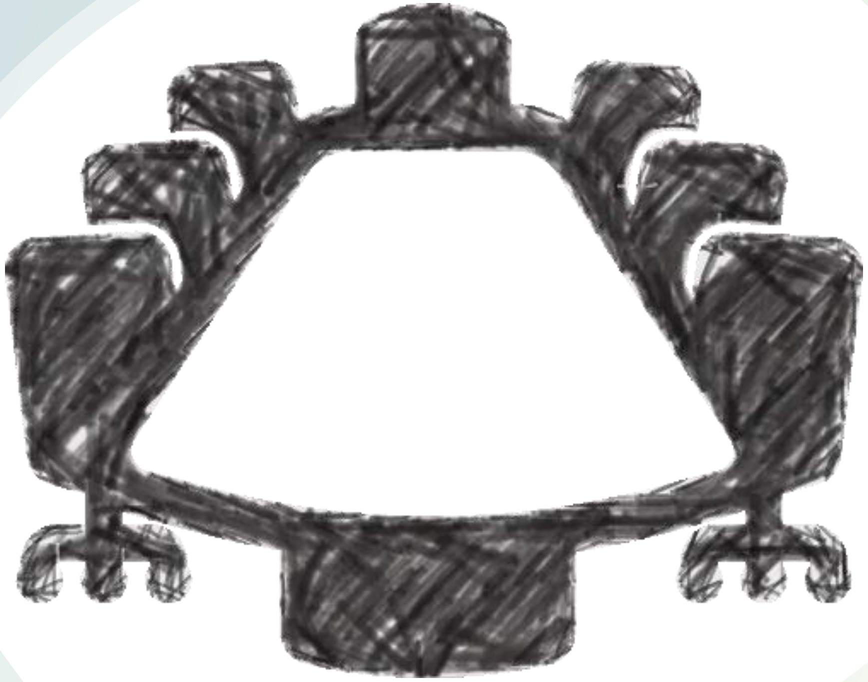

Multi-Echo fMRI: How is used nowadays

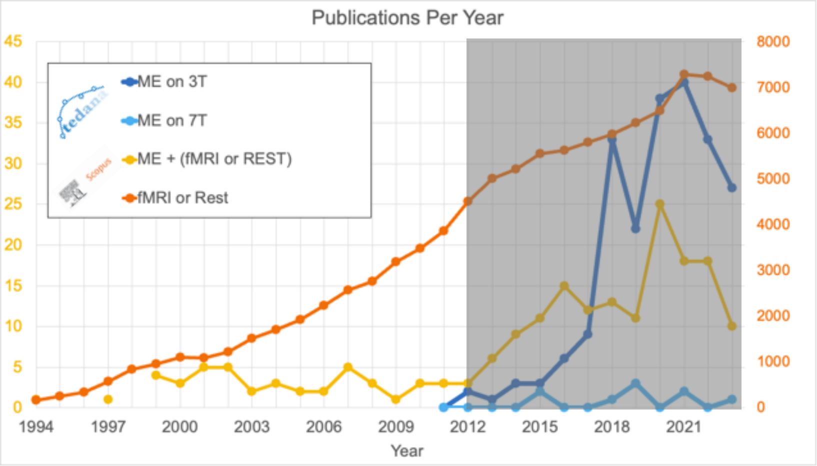

- Increase adoption for Clinical and Basic Science Studies

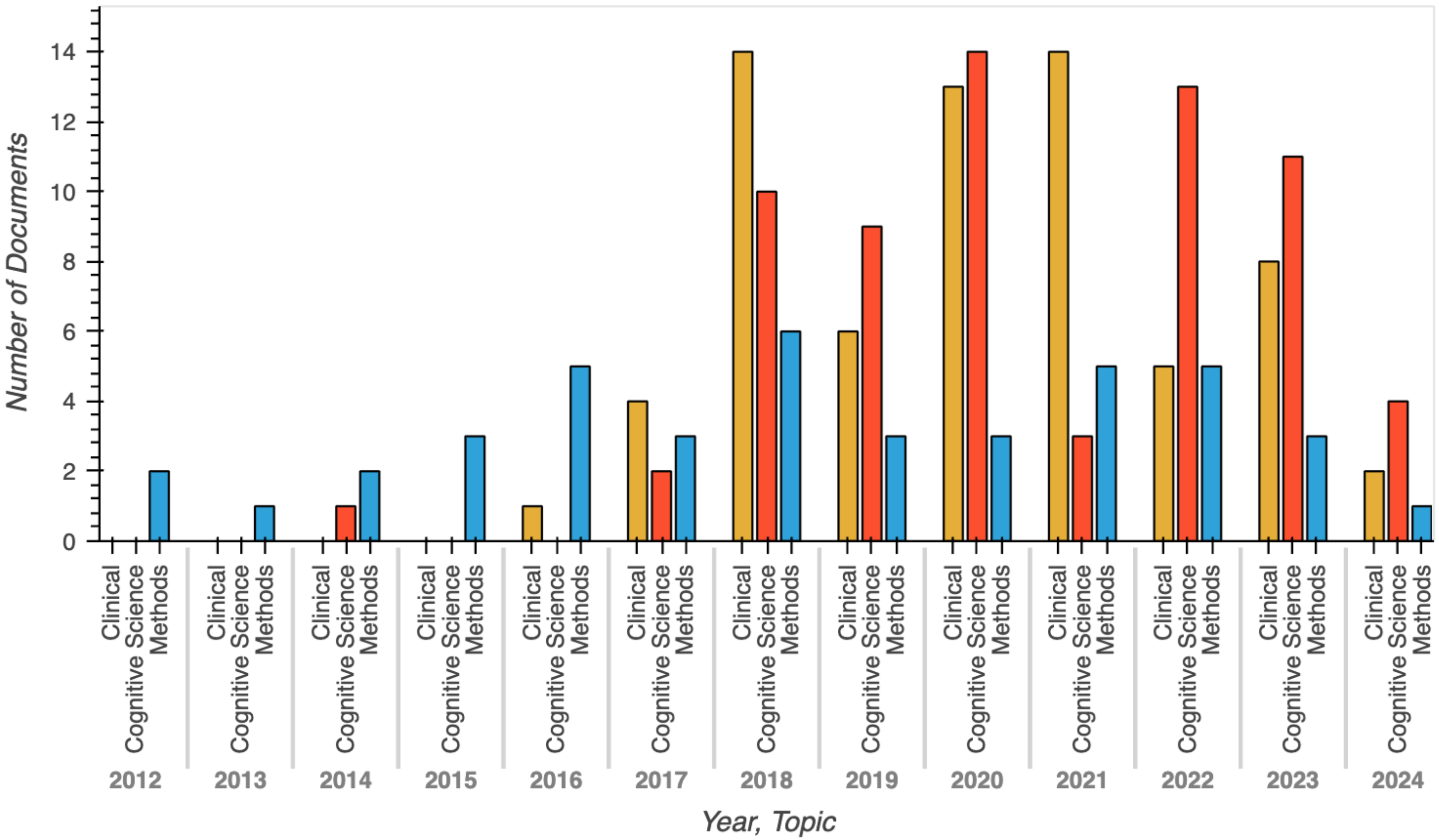

Multi-Echo fMRI: How is used nowadays

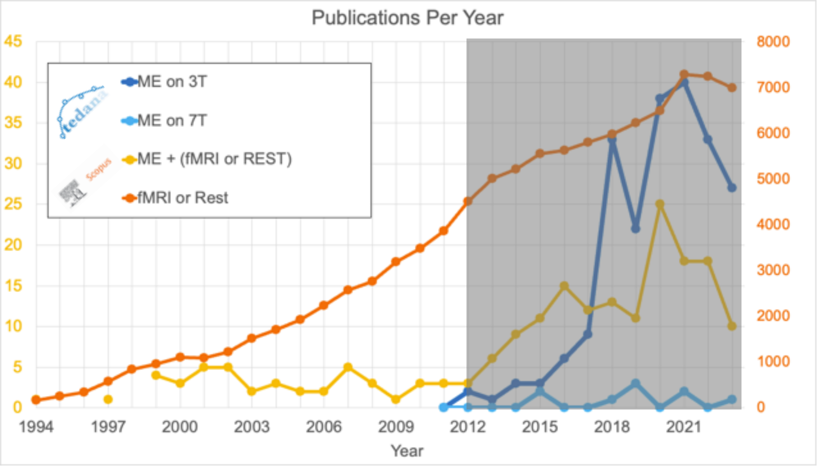

- Increase adoption for Clinical and Basic Science Studies

- Interested in better temporal and spatial resolution

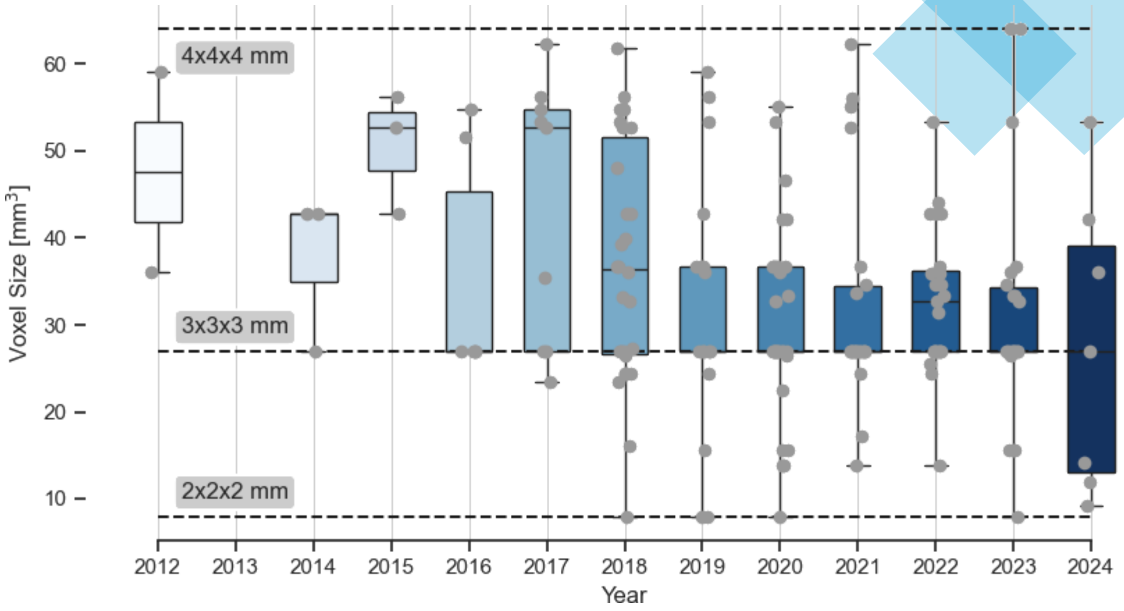

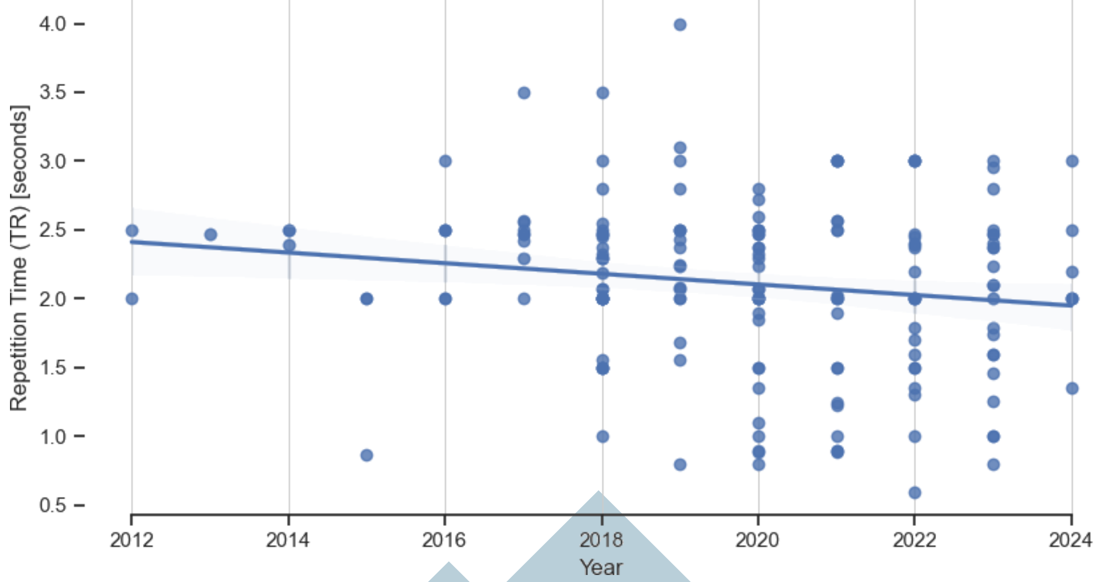

Multi-Echo fMRI: How is used nowadays

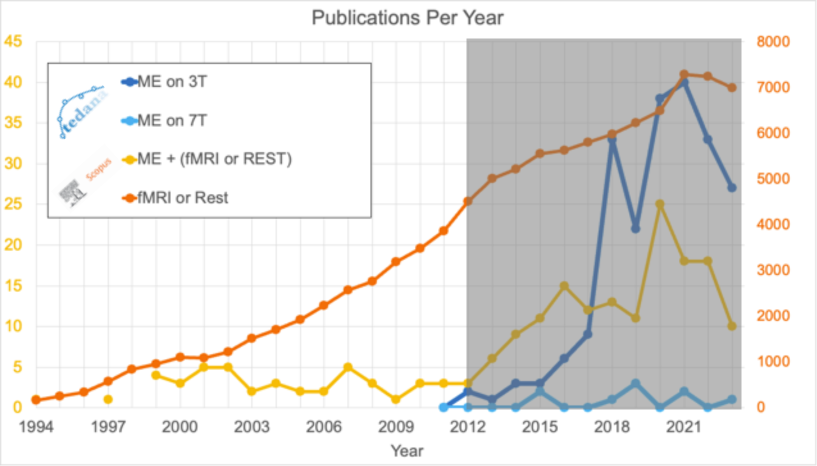

- Increase adoption for Clinical and Basic Science Studies
- Interested in better temporal and spatial resolution
- While increasing the number of acquired echoes

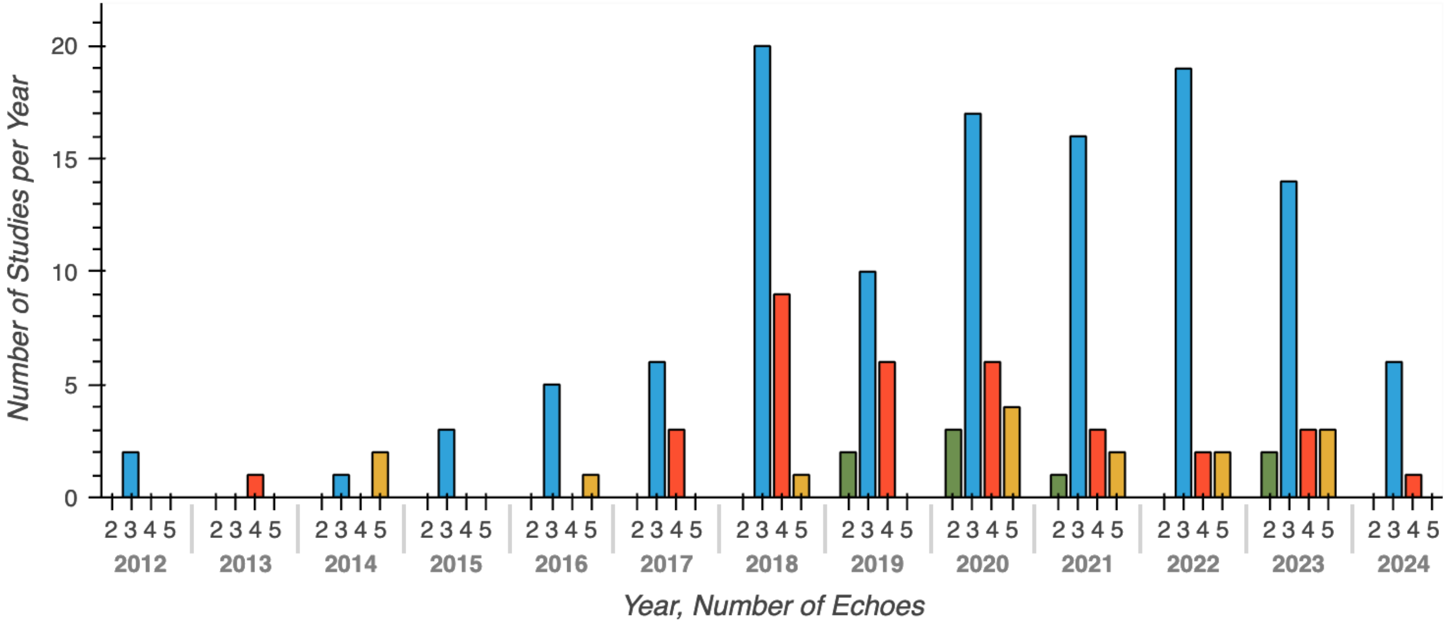

Multi-Echo fMRI: How is used nowadays

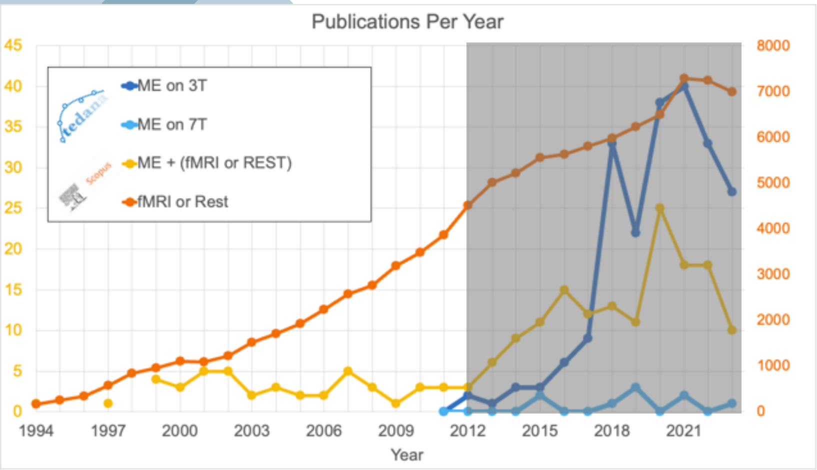

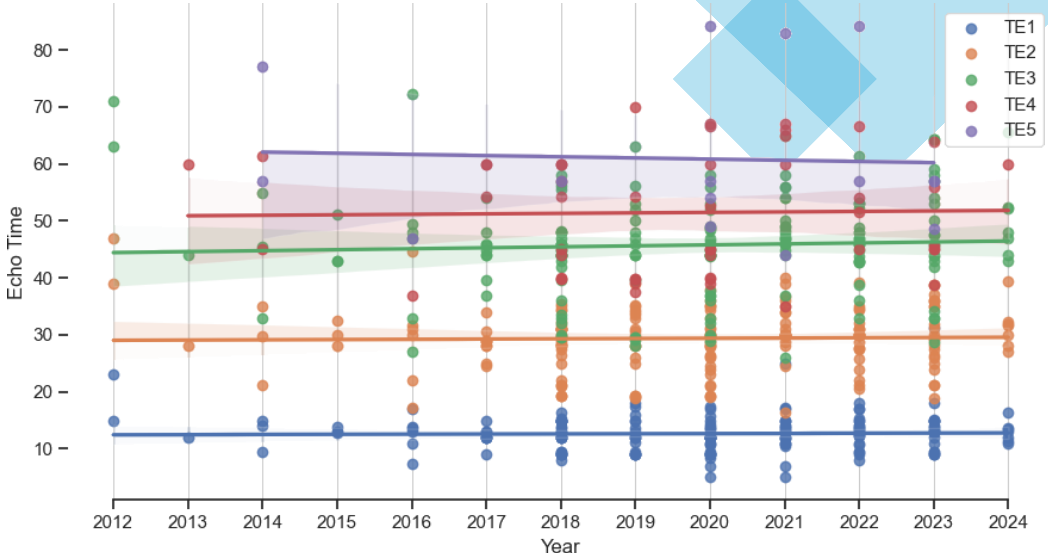

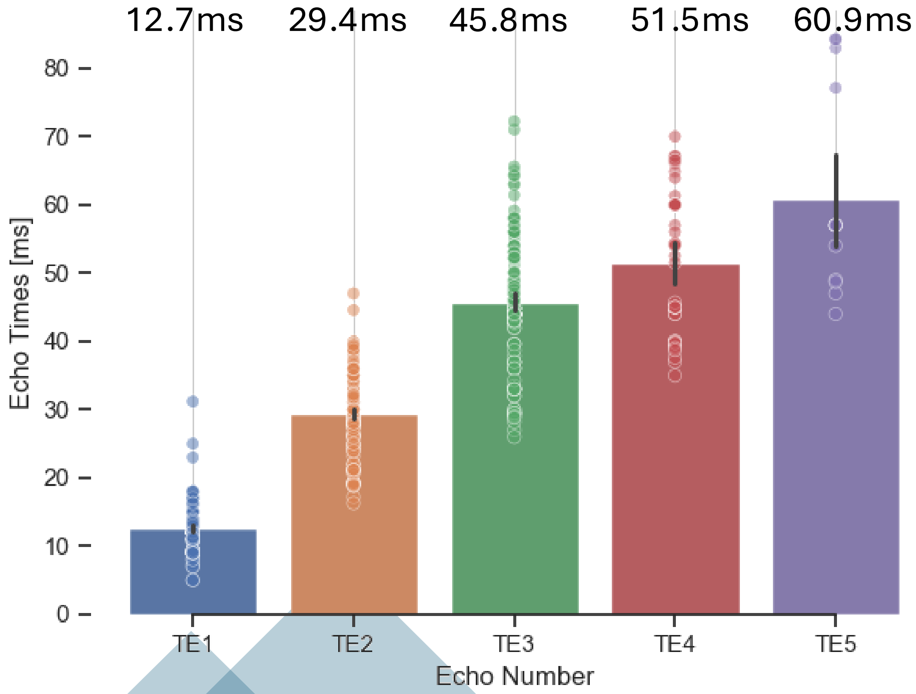

- Increase adoption for Clinical and Basic Science Studies
- Interested in better temporal and spatial resolution
- While increasing the number of acquired echoes
- Shortest echo-times remain the same

Multi-Echo fMRI: How is used nowadays

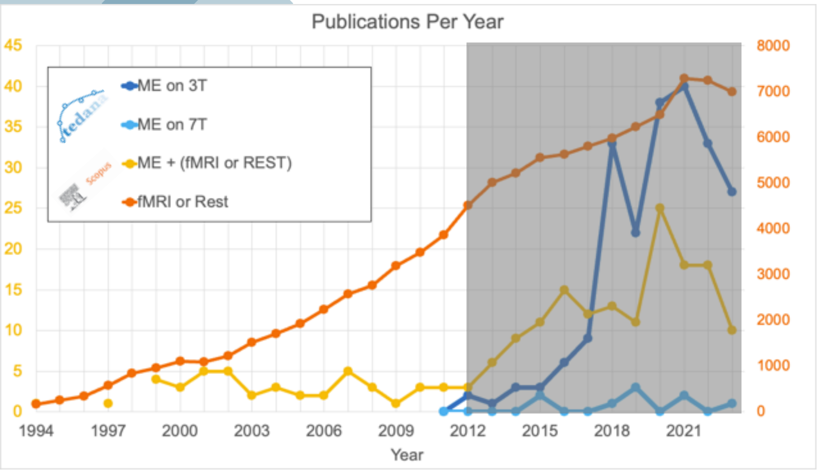

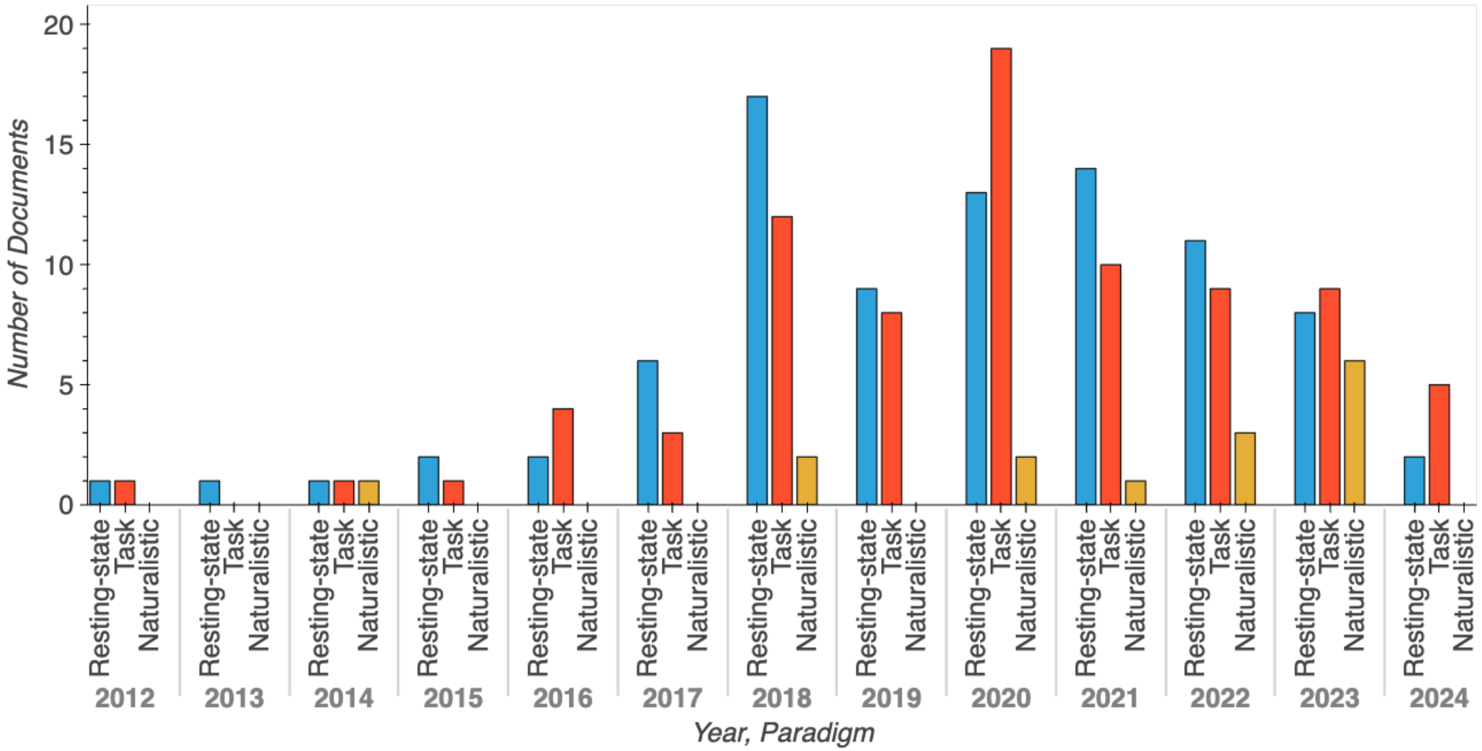

- Increase adoption for Clinical and Basic Science Studies
- Interested in better temporal and spatial resolution
- While increasing the number of acquired echoes
- Shortest echo-times remain the same
- Used in combination with all main experimental paradigms

Multi-Echo fMRI: How is used nowadays

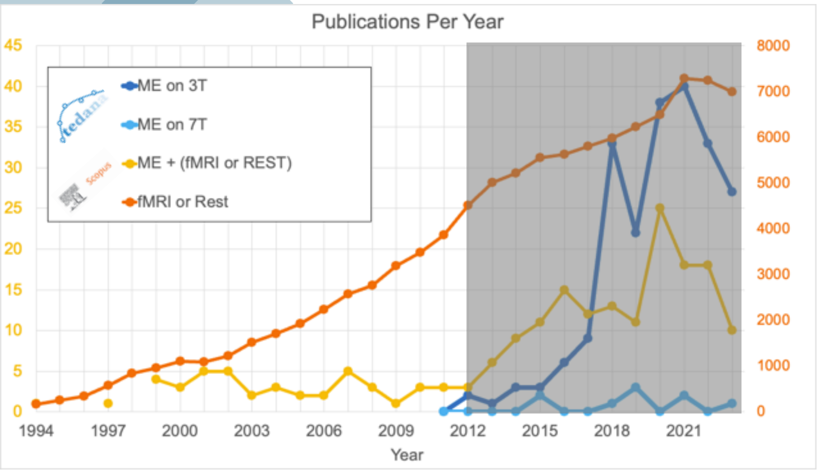

- Increase adoption for Clinical and Basic Science Studies
- Interested in better temporal and spatial resolution
- While increasing the number of acquired echoes
- Shortest echo-times remain the same
- Used in combination with all main experimental paradigms
- Echo Combination & ME-ICA/tedana are the primary analytical approaches

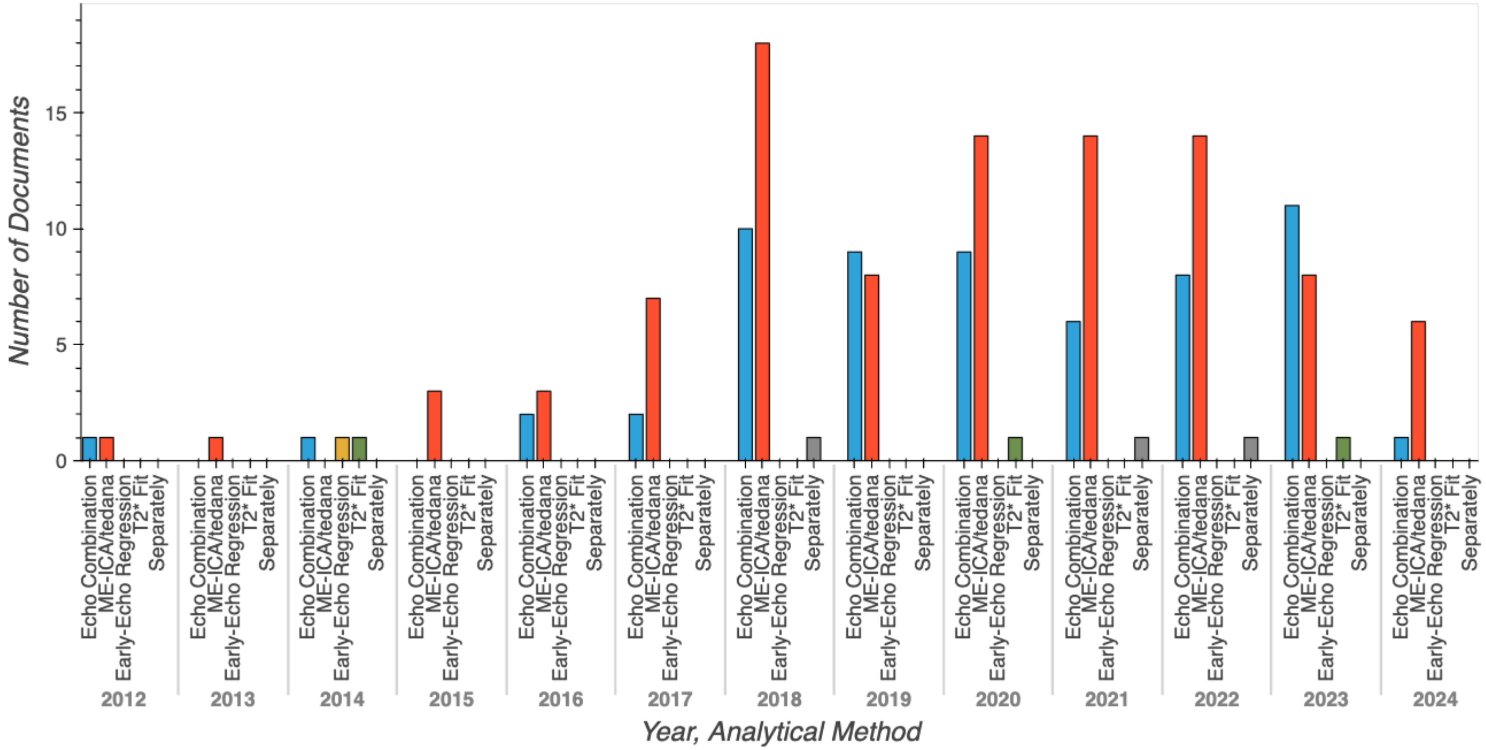

Multi-Echo fMRI: How is used nowadays

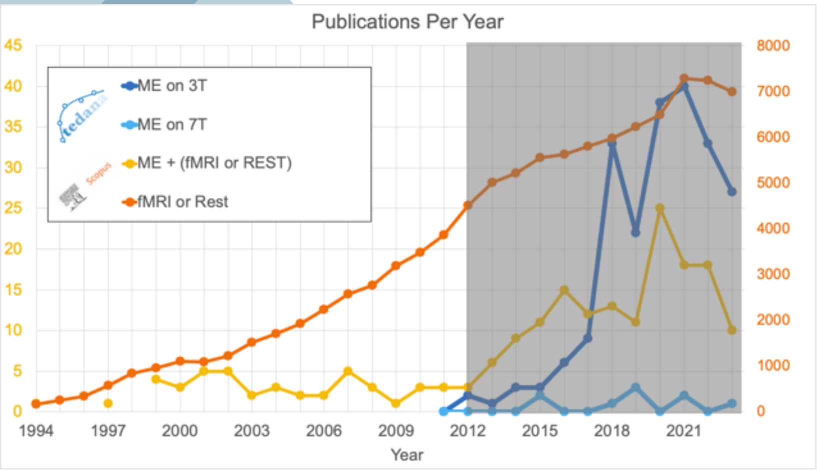

- Increase adoption for Clinical and Basic Science Studies
- Interested in better temporal and spatial resolution
- While increasing the number of acquired echoes
- Shortest echo-times remain the same
- Used in combination with all main experimental paradigms
- Echo Combination & ME-ICA/tedana are the primary analytical approaches
- Increasingly embraced by the open science

Title	URL	Scanner	Number of Echoes		
			3	4	5
MICA-PNI: Precision NeuroImaging and Connectomics	Dataset	7T	X		
SoCal Kinesia and Incentivization for Parkinson's Disease (SKIP): Ultra-High Field Functional Connectivity	Dataset	7T	X		
Single-echo/multi-echo comparison pilot	Dataset	3T			X
Social Reward and Aging: A Preliminary Multi-echo fMRI and Diffusion Dataset	Dataset	3T		X	
Weill Cornell Medicine Multi-echo (WCM-ME) Dataset	Dataset	3T			X
Sequence pilot: multiecho and multiband fMRI	Dataset	3T		X	
Multivariate Assessment of Inhibitory Control in Youth: Links with Psychopathology and Brain Function Dataset	Dataset	3T	X		
NIMH METeR	Dataset	3T		X	
Denoising task-correlated head motion from motor-task fMRI data with multi-echo ICA	Dataset	3T			X
Characterization and Treatment of Adolescent Depression (CAT-D)	Dataset	3T		X	
Multi-echo simultaneous multislice fMRI dataset: Effect of acquisition parameters on fMRI data	Dataset	3T	X		
Heart rate variability biofeedback training and emotion regulation	Dataset	3T	X		
Le Petit Prince	Dataset	3T	X		
Neurocognitive aging data release with behavioral, structural, and multi-echo functional MRI measures	Dataset	3T	X		
EuskalIBUR	Dataset	3T			X
Dense Investigation of Variability of Affect (DIVA)	Dataset	3T		X	
Multi-echo masking test dataset	Dataset	3T		X	
Valence processing differs across stimulus modalities	Dataset	3T	X		
Multi-echo Cambridge	Dataset	3T		X	
Multiband Multi-Echo Simultaneous ASL/BOLD for task-induced functional MRI	Dataset	3T		X	
Multiband Multi-Echo Imaging of Simultaneous Oxygenation and Flow Timeseries for Resting State Connectivity	Dataset	3T		X	
Multi-echo fMRI replication sample of autobiographical memory, prospection and theory of mind reasoning tasks	Dataset	3T	X		

Agenda

- ❑ Why should we consider Multi-Echo acquisitions when doing fMRI experiments?
- ❑ Proposed analytical approaches for Multi-Echo fMRI Data? (timeline)
  - ❑ T2* Fit
  - ❑ Dual Echo
  - ❑ Weighted Combination of Echoes
  - ❑ Multi-Echo ICA-based Denoising
  - ❑ Multi-Echo Deconvolution
- ❑ Success stories
- ❑ Status of Multi-Echo fMRI Adoption
- ❑ **<u>What can faster gradients do for ME-fMRI?</u>**
- ❑ Conclusions

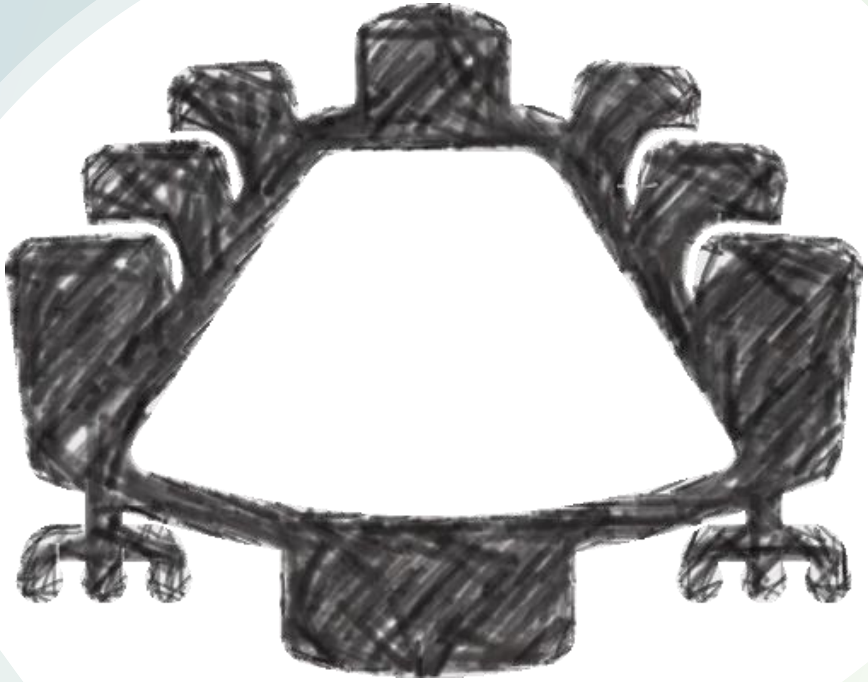

How can ME-fMRI benefit from faster gradients

More Echoes | Better Spatial Resolution | Better Temporal Resolution | Maintain Full Brain Coverage

- To achieve this, we often rely on increasing in-plane and multiband acceleration factors

Signal Dropout

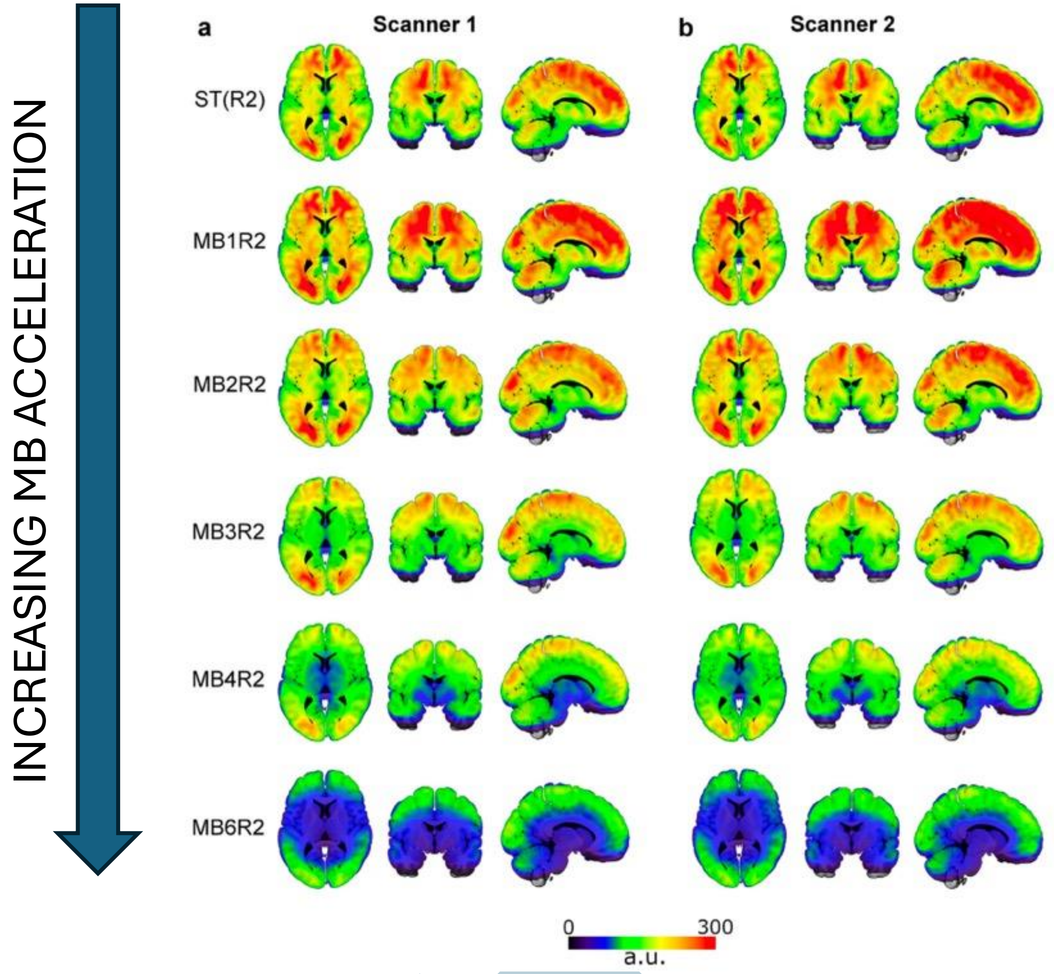

Wall MR “Multiband acquisition sequences for fMRI: proceed with caution” Aperture Neuro (2023)

How can ME-fMRI benefit from faster gradients

More Echoes | Better Spatial Resolution | Better Temporal Resolution | Maintain Full Brain Coverage

- To achieve this, we often rely on increasing in-plane and multiband acceleration factors

- T2* Fitting approaches require improved sampling of the TE-decay curve.

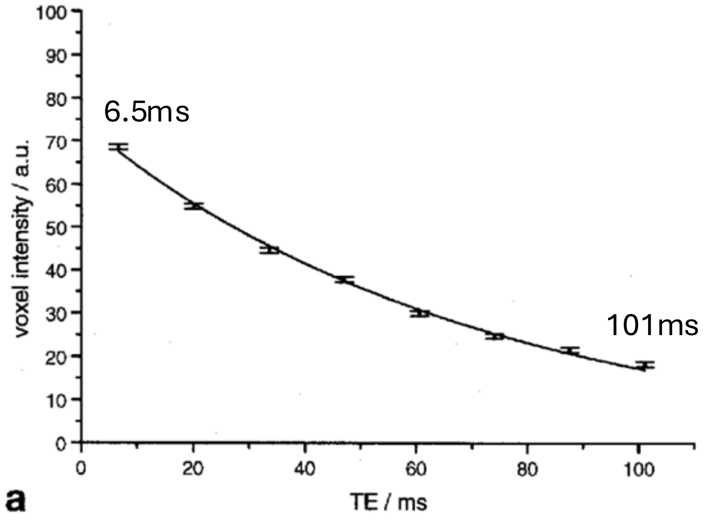

2T Magnet | 3 Slices | TR = 3s

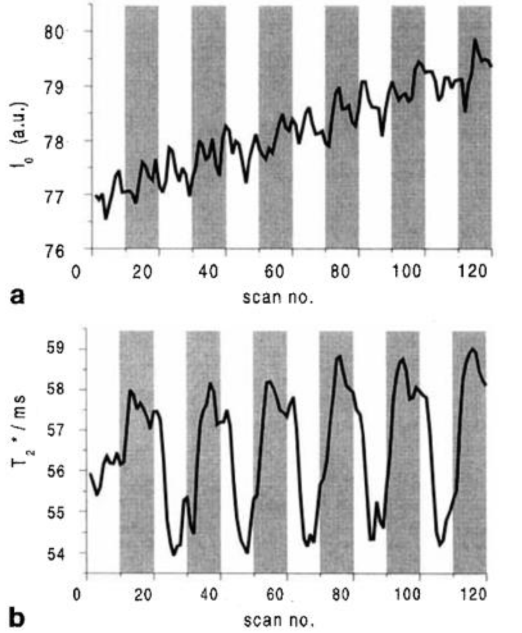

FIG. 5. Time course of I_0 (top) and T_2^* (bottom). Values within the areas with a correlation coefficient >0.3 were averaged for a single subject. The gray shaded areas correspond to the time the visual stimulus was turned on. It is clearly visible that the signal drift in the data is due to an I_0 drift only.

How can ME-fMRI benefit from faster gradients

More Echoes | Better Spatial Resolution | Better Temporal Resolution | Maintain Full Brain Coverage

- To achieve this, we often rely on increasing in-plane and multiband acceleration factors
- T2* Fitting approaches require improved sampling of the TE-decay curve.
- Dual-echo approaches require first echo to be as short as possible to minimize BOLD contamination

Subject	TE1 = 3.3 ms			TE1 = 10 ms		
	Traditional preprocessing	TE1 regression	% Change	Traditional preprocessing	TE1 regression	% Change
No. of activated voxels						
1	1103	882	−20.0%	988	566	−42.7%
2	1187	1002	−15.6%	1366	900	−34.1%
4	1181	1051	−11.0%	987	731	−25.9%
5	1031	851	−17.5%	1970	1293	−34.4%
6	1568	1354	−13.6%	2108	1563	−25.9%
8	1535	1167	−24.0%	2646	1813	−31.5%
9	1697	1360	−19.9%	2288	1629	−28.8%
10	2439	2193	−10.1%	2228	1438	−35.5%
Average	1468	1233	−16.5%	1823	1242	−32.3%*
Mean t-statistic						
1	15.2	13.5	−11.0%	16.4	11.8	−28.1%
2	16.2	14.4	−11.1%	21.9	14.9	−31.9%
4	25.4	21.7	−14.7%	18.2	14.4	−20.6%
5	15.5	13.7	−11.2%	31.9	18.2	−43.0%
6	20.6	16.6	−19.5%	28.3	18.6	−34.2%
8	18.8	15.0	−20.1%	35.2	19.9	−43.4%
9	16.0	13.7	−14.0%	25.3	16.3	−35.6%
10	24.9	19.9	−19.9%	19.4	13.2	−32.2%
Average:	19.1	16.1	−15.2%	24.6	15.9	−33.6% *

Bright & Murphy "Removing motion and physiological artifacts from intrinsic BOLD fluctuations using short echo data" NeuroImage (2013)

How can ME-fMRI benefit from faster gradients

More Echoes | Better Spatial Resolution | Better Temporal Resolution | Maintain Full Brain Coverage

- To achieve this, we often rely on increasing in-plane and multiband acceleration factors
- T2* Fitting approaches require improved sampling of the TE-decay curve.
- Dual-echo approaches require first echo to be as short as possible to minimize BOLD contamination
- Estimating κ and ρ based on more than 3 echoes should benefit ME-ICA/tedana component characterization (as long as echoes as not too long)

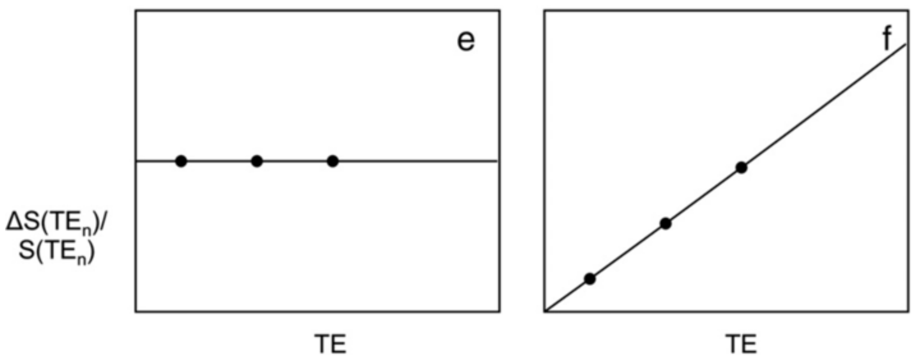

How can ME-fMRI benefit from faster gradients

More Echoes | Better Spatial Resolution | Better Temporal Resolution | Maintain Full Brain Coverage

- To achieve this, we often rely on increasing in-plane and multiband acceleration factors

- T2* Fitting approaches require improved sampling of the TE-decay curve.

- Dual-echo approaches require first echo to be as short as possible to minimize BOLD contamination

- Estimating κ and ρ based on more than 3 echoes should benefit ME-ICA/tedana component characterization (as long as echoes as not too long)

- Lower Distortions derived from shorter readout windows would be welcome.

Conclusions

- ME is a powerful tool to test the properties of different fMRI signal components.

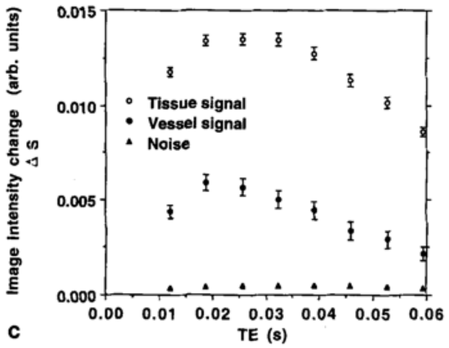

Conclusions

- ME is a powerful tool to test the properties of different fMRI signal components.

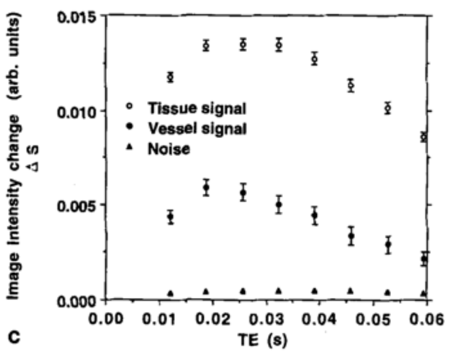

- ME helps recover signal in dropout regions.

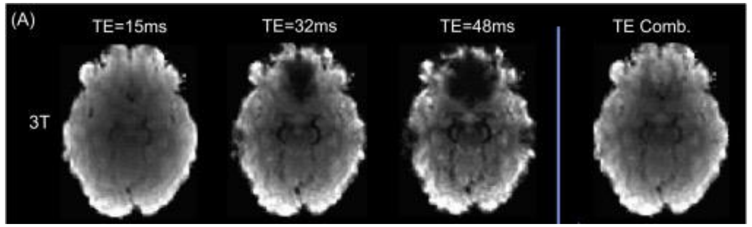

Conclusions

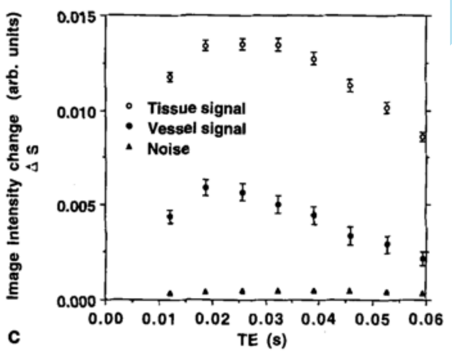

- ME is a powerful tool to test the properties of different fMRI signal components.

- ME helps recover signal in dropout regions.

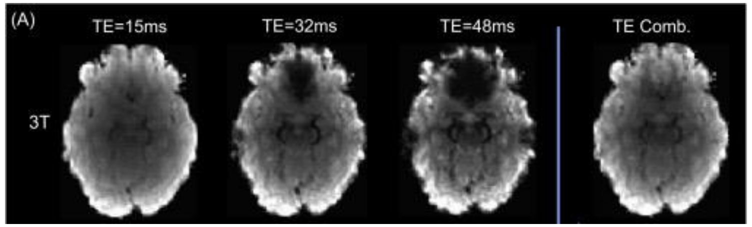

- ME results in improved TSNR.

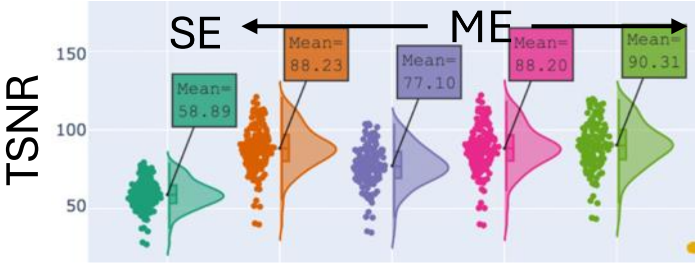

Conclusions

- ME is a powerful tool to test the properties of different fMRI signal components.

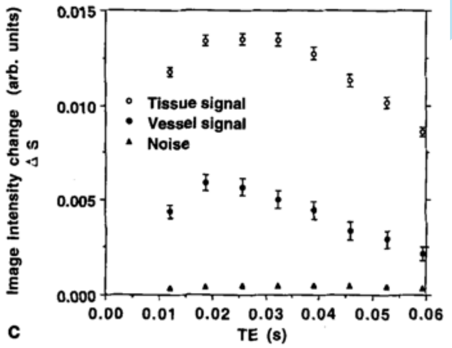

- ME helps recover signal in dropout regions.

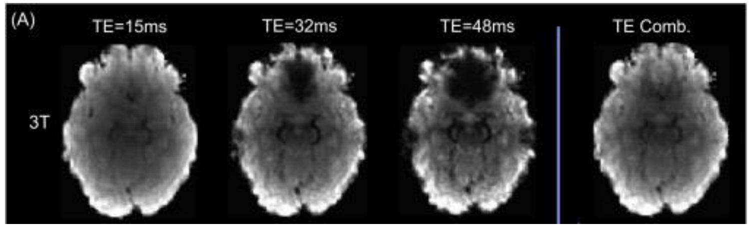

- ME results in improved TSNR.

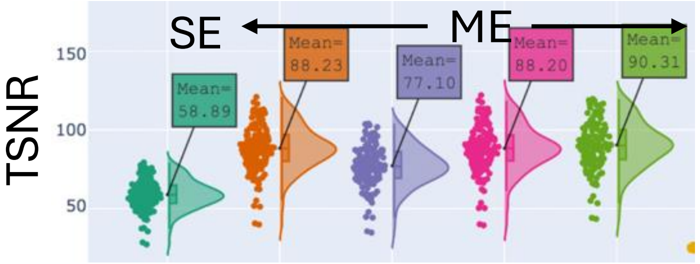

- Allows more advance denoise approaches which translate into gains in sensitivity and reliability.

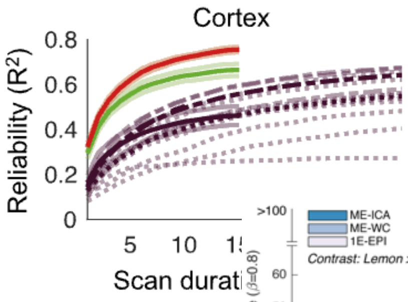

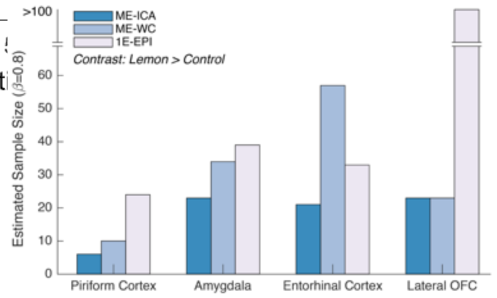

Conclusions

- ME is a powerful tool to test the properties of different fMRI signal components.

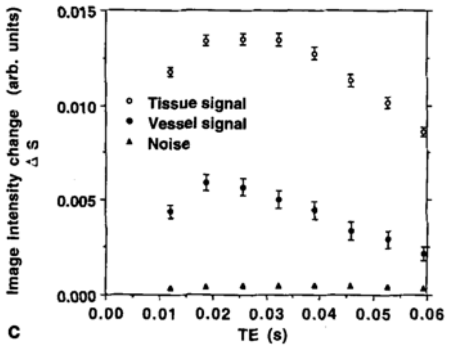

- ME helps recover signal in dropout regions.

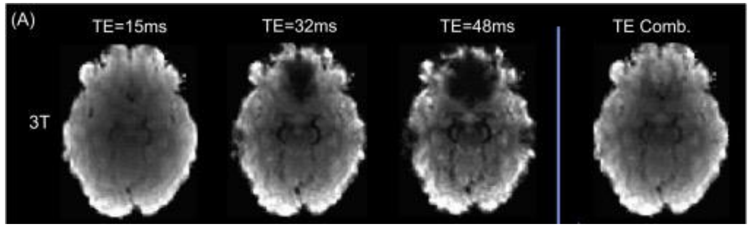

- ME results in improved TSNR.

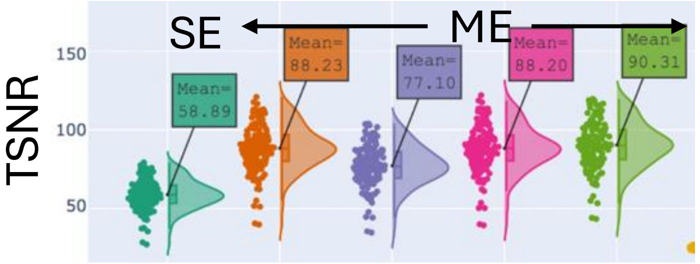

- Allows more advance denoise approaches which translate into gains in sensitivity and reliability.

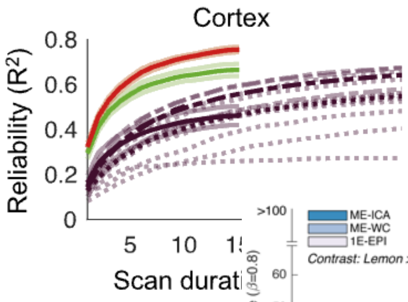

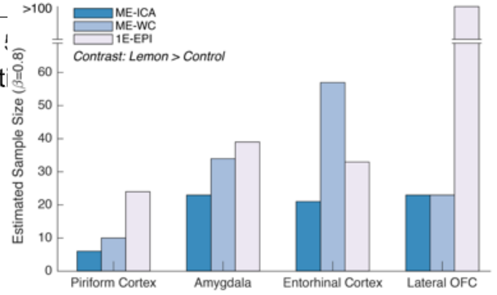

- Faster gradients should further improve all these ME-related gains.

- ME is well suited to play a key role in clinical and real-time applications

Thank you & Questions

National Institute of Mental Health

Sharif Kronemer
Fernando Ramirez
Burak Akin
Joshua Faskowitz
Somayeh Shashavarani
Tyler Morgan
Marly Rubin

Peter A. Bandettini

Daniel Handwerker

National Institute of Mental Health

FMRIF

Peter A Bandettini
Andy Derbyshire
Renzo Huber

Linqing Li
A. Tyler Morgan
Vinai Roopchansingh

BASQUE CENTER ON COGNITION, BRAIN AND LANGUAGE

Cesar Caballero-Gaudes

Eneko Uruñuela